VEGETATION FEEDBACK ON THE BOUNDARY LAYER CLIMATE OF SOUTHERN AFRICA

Hector Chikoore

Thesis for the Master of Science degree

Department of Geography and Environmental Studies,
University of Zululand
SOUTH AFRICA

November 2005

ABSTRACT

Upward feedbacks from the land surface and vegetation to the atmospheric boundary layer over southern Africa are investigated. Satellite derived rainfall and vegetation data and model evaporative fluxes for the period 1981-2000 are used to reveal spatial and temporal inter-relationships via Principal Components Analysis.

Seasonal rainfall and NDVI exhibit distinct unimodal seasonal cycles maximizing during the austral summer over the Zambezi valley and interior plateau. Spectral analysis indicates major cycles of intraseasonal rainfall events at approximately 40 and 20 days. The 40-day oscillation reflects the Madden-Julian Oscillation and is partially phase-locked to the seasonal cycle. The spatial loadings are focused on a region along the eastern edge of the Kalahari (± 23°E), extending from the western Zambezi toward central South Africa, spanning 20° of latitude. The loading pattern is consistent with tropical-temperate troughs and associated northwest (NW) cloud bands. This 40-day mode connects two 20-day modes over the Agulhas current and Angola, hence NW cloud bands are a slower terrestrial harmonic of the faster modes at either end.

NDVI also exhibits intraseasonal cycles operating at approximately 40 days with spatial loadings co-located with the rainfall mode except in the south. Vegetation has a 1-2 dekad lagged correspondence with rainfall. It is hypothesised that an earlier rainfall event and subsequent 'greening' results in an evapo-transpiration flux that affects the next rainfall event. Boundary layer structure is studied along west-east transects and compared with vertical and horizontal fluxes of moisture. The sensitivity of vegetation to rainfall is most pronounced over the eastern Kalahari due to high evaporative losses during the intervening dry spells.

Since vegetation-rainfall interactions can be a result of moisture convergence, surface evapotranspiration, or convection, this study focuses on the vertical moisture flux from the land surface and attempts to separate this from the

dominant large-scale horizontal moisture convergence through a budget analysis. The boundary layer deepens but does not diminish even in the absence of external forcing. A most significant finding is the agreement between vegetation and low level velocity potential. A sharp increase in vegetation appears to draw airflow towards itself, in a self sustaining way.

Results of this study contribute to the understanding of land-atmosphere interactions and their role in the climate system of southern Africa.

To my parents, Barnabas and Lyness Chikoore

The rain pours down from the clouds, and everyone benefits from it.
Can anyone really understand the spreading of the clouds and the thunder that rolls forth from heaven?

Job 36: 28-29 (The Holy Bible, New Living Translation)

PREFACE

Southern Africa is a semi-arid region with high interannual and intraseasonal variability of rainfall. The region is highly vulnerable to extreme events such as droughts and floods with profound implications on rain-fed agriculture which contributes significantly to employment and livelihoods in most countries of the subcontinent. Considerable research attention has therefore been given to rainfall variability and predictability over southern Africa on a variety of time scales.

Advances in numerical weather prediction models have improved short-term (1-10 day lead) rainfall forecasts especially for the subtropical latitudes where their skill is greatest. The large-scale forcing mechanisms on rainfall have been studied and increased understanding of teleconnections between the oceans and atmosphere has enabled prediction of seasonal rainfall for application to agricultural management and proactive disaster preparedness.

Despite these advances, much remains to be understood about the local forcings of the rainfall of southern Africa. Upward feedbacks from the land surface and vegetation are an important source of climate variability. Vegetation is linked to heat and moisture exchanges between the underlying surface and the lower troposphere. It has also been demonstrated that the presence of vegetation can substantially alter the atmospheric boundary layer structure and rainfall through additional moisture provided via transpiration.

Vegetation occupies the interface between the atmosphere and the continental crust as it extends upward into the atmospheric boundary layer and downward into the soil. It provides a link between soil water and the atmosphere above through a process that is five to seven times more efficient than evaporation from the ocean. However, the extent to which vegetation affects climate is less certain (Hoffman and Jackson, 2000).

The principal goal of this research study is to establish vegetation feedback on the atmospheric boundary layer over southern Africa at intraseasonal time-scales. This is achieved through analysis of twenty years (1981-2000) of data for rainfall, vegetation, surface moisture fluxes and horizontal circulation patterns.

The thesis outline is as follows: -

- Chapter 1 presents the background and relevant literature on rainfall variability over southern Africa. A review of research on vegetation and relationships with rainfall and climate is also given. Hypotheses, key research questions and specific objectives are formulated.
- Chapter 2 describes the data employed in this study, their sources and methods of analysis. A theoretical framework for this study is offered.
- Rainfall variability over southern Africa in space and time at seasonal and intraseasonal time scales is discussed in Chapter 3.
- Vegetation characteristics over the subcontinent are presented in Chapter 4. The seasonal variation, interannual variability and intra-seasonal oscillations are analysed and discussed.
- Chapter 5 presents the variability of evapotranspiration-related surface fluxes at seasonal and intraseasonal timescales.
- Vegetation feedback on rainfall events over southern Africa is investigated and discussed in Chapter 6 using intra-seasonal composites of events with large amplitude changes of NDVI. The sensitivity of the regional climate to local forcings is also established.
- A synthesis of the major findings and fundamental conclusions of this study is given in Chapter 7. Land use influences on the climate are discussed qualitatively. Limitations in the interpretation of results are also given whilst the scientific objectives are evaluated. Recommendations for future research are made at the end.

CONTENTS

LIST OF FIGURES

Figure

LIST OF TABLES

ACKNOWLEDGEMENTS

This research project was co-sponsored by the Department of Arts, Culture, Science and Technology, the Agriculture Research Council and the National Research Foundation. Professor Mark R. Jury provided resources to conduct this research at the Department of Geography and Environmental Studies, University of Zululand. His guidance and direction throughout the duration of the study was beyond measure.

I acknowledge Anna Kozakiewicz for her invaluable assistance with computer applications particularly the acquisition and processing of satellite NDVI and radiosonde data. Lukiya Tazalika (Uganda Meteorological Services) is thanked for assistance with signal processing.

I recognize several data sources for making this study possible. Climatological data was obtained from the National Centers for Environmental Prediction (NCEP) and satellite vegetation data from the archives of the United States Geological Survey's (USGS) African Data Disseminating System (ADDS). The South African Weather Service provided radiosonde data for Bloemfontein.

Many thanks to the Government of Zimbabwe for granting Manpower Development Leave enabling me to pursue graduate studies in South Africa. Finally, a debt of gratitude goes to my family for their unwavering support whilst I pursued further education.

Chapter 1

BACKGROUND AND LITERATURE REVIEW

1.0 Introduction

While significant research effort has focused on climate variability and predictability in many regions of Africa, the role of the African land surface in the climate system is not well established. Key variables on the land surface include vegetation, surface albedo, soil moisture, and surface fluxes of heat and moisture. The impact of vegetation variability is receiving increasing attention and earlier studies to relate vegetation to climate were initially based on satellite-derived, large-scale vegetation response patterns to rainfall (e.g. Justice *et al.*, 1986; Malo and Nicholson 1990; Davenport and Nicholson, 1993; Nicholson, 1993; Gondwe and Jury, 1997).

Satellite-derived biophysical parameters such as the Normalized Difference Vegetation Index (NDVI) are used in vegetation studies. NDVI is a measure of vegetation reflectance to a visible band satellite sensor indicating vegetation 'colour'. High reflectances are linked to 'green' and vibrant vegetation whilst lower reflectances refer to 'brown' vegetation or bare surfaces. The NDVI has proven a robust indicator of biomass production and photosynthetic activity and has been related to evapotranspiration and rainfall. Interannual rainfall variability is well represented by NDVI in most areas of Africa, especially over the semi arid regions (Davenport and Nicholson, 1993), but NDVI is less variable in the more humid forest regions. Other uses for NDVI include land cover classification, agricultural crop monitoring, drought monitoring and desertification studies.

Relevant work on vegetation-rainfall dynamics has been done mostly in semi-arid and agricultural regions of the world such as the Sahel and the Great Plains of the United States. Many studies have also targeted East Africa whilst some

modelling groups have focused on modelling vegetation change at long time scales evaluating response patterns to climate variability.

The objective of this chapter is to present the background of this study and relevant literature on the variability of vegetation 'colour' and rainfall and their feedback mechanisms. The study hypotheses, key research questions and objectives are formulated.

1.1 The vegetation of southern Africa

The regional landscape consists of spatially varying vegetation cover, high topography and hydrological gradients which have strong influences on the climate (Fig 1.1). The seasonal and intra-seasonal growth and development of vegetation are largely determined by water availability. Hence, the satellite-observed large-scale spatial distribution of vegetation over southern Africa is significantly related to rainfall patterns over the subcontinent (Fig. 1.2).

The regional vegetation south of 15°S is dominated by grassland savanna (Jury *et al.*, 1997a; Dube, 2002) but forests and woodlands occur in the east with dry and thorny savannas in the central desert. In the west, the soil is nearly bare. The vegetation biomes of southern Africa are shown in Fig. 1.3 and have been detailed by Rutherford and Westfall (1986). Miombo woodlands characterise the savanna regions but the largest of the savannas is the Kalahari which comprises of grasslands and small groups of trees covering most of Botswana, Namibia and part of South Africa. The trees and shrubs of the arid savannas in southern Africa are distinctly deciduous.

Spatial gradients exist between the dense vegetation cover to the northeast (Zambezi and the Drakensberg) and the arid southwestern desert (Gondwe and Jury, 1997). Satellite derived vegetation images show a distinct boundary between the 'green' northeast and the 'brown' western areas (Fig. 1.2a). Similar

west-east gradients exist in regions of the world such as the central Great Plains of the United States (Wang *et al.*, 2001) and in the north-south axis from the Guinea Coast to the Sahara desert (Zeng *et al.*, 2002). These regional vegetation patterns are further differentiated seasonally and interannually (Hulme *et al.*, 1996).

Previous studies have demonstrated that the NDVI maximum over southern Africa occurs during January-February lagging the rainfall maximum by 1-2 months (Anyamba *et al.*, 2002). Justice et al. (1986) and Nicholson (1993) also noted a similar lag in studies over East Africa. Time lags for vegetation response to rainfall vary depending on environmental factors such as soil type (Richard and Poccard, 1998) which largely determine the water holding capacity of soils. The temporal manner in which the precipitation is received also influences the NDVI lag.

Gondwe and Jury (1997) investigated the sensitivity of vegetation to the summer climate over southern Africa using relationships between NDVI and satellite OLR as a measure of convective rainfall. As expected, they determined a significant inverse relationship between OLR and NDVI. Their study found that the Zambezi Valley is less sensitive to climate impacts than the southern plateau, whilst the late summer is more sensitive than the early summer. NDVI reaches a minimum over southern Africa in September and rises sharply during October but is less variable during the austral summer. Jury *et al.* (1997a) also established that vegetation-climate relationships are strongest during the late summer.

Jury *et al.* (1997a) used NDVI data as an indicator of climate variability over southern Africa. Their study justified the use of NDVI as a measure of food production and obtained a time series analysis of area-averaged NDVI for crop-growing districts of four countries in southern Africa: Namibia, Zimbabwe, Botswana and South Africa. The NDVI values were at their lowest corresponding

to the worst droughts of 1982/83 and 1991/92. Correlations with maize yields were as high as 85% over a 13-year period.

Anyamba *et al.* (2002) studied El Nino and La Nina events via NDVI anomalies over east and southern Africa during the period 1997-2000. They detected a distinct contrast in vegetation anomalies during the warm 1997/98 and cold 1999/2000 ENSO events. Their study determined an inverse relationship between SSTs of the central Pacific and NDVI anomalies over southern Africa. A similar inverse relationship between southern African rainfall and Pacific SSTs has long been established. NDVI anomalies were used in Anyamba *et al.* (2002) to show that the drought of 1997/98 over southern Africa was not as severe as previous droughts associated with warm ENSO events. Anyamba and Eastman (1996) determined that vegetation variability over southern Africa is largely modulated by the ENSO phenomenon at time scales ranging from 4-7 years.

Elsewhere, in a study of the central Great Plains of the United States, Wang *et al.* (2001) studied spatial response patterns of NDVI to rainfall and temperature, for example between spatial patterns of NDVI and annual rainfall. The intraseasonal analysis of bi-weekly NDVI is of particular relevance to this study. Wang *et al.* (2001) established that precipitation is a useful predictor of NDVI and productivity and that temperature was not strongly correlated with NDVI in the central Great Plains.

Davenport and Nicholson (1993) studied the relationship between rainfall and NDVI for East Africa and determined that the NDVI-rainfall relationship is strongest over the semi-arid bushland/thicket or shrubland zones but the wetter woodlands exhibit little correlation. The strongest correlation occurs for monthly NDVI and three-month mean rainfall for the current and two preceding months. They suggested that a point of saturation is reached after which NDVI does not increase even with increasing rainfall.

It is recorgnised that NDVI data has only been available since the 1980s and hence previous studies used a limited set of data e.g. 1982-1985 in Davenport and Nicholson (1993), 1982-1987 in Farrar *et al.* (1994) and 1997-2000 in Anyamba *et al.* (2002). The data series used in these studies are too short to obtain conclusive results as regards interannual variability. Most studies over southern Africa have used monthly NDVI data (e.g. Anyamba *et al.*, 2002; Gondwe and Jury, 1997, Jury *et al.*, 1997) which is a coarse resolution to obtain useful responses at intraseasonal time scales.

Twenty years of NDVI data obtained at dekadal (ten-day) time resolution are used in this study. It is hoped this work will pioneer research on intraseasonal variability of vegetation over southern Africa and that research findings will advance the state of knowledge.

1.2 Climate variability over southern Africa

Southern Africa experiences a variety of climatic regimes which are largely semi-arid with significant variability on several time scales (Tyson *et al.*, 2002). Climatic regimes of southern Africa are largely delimited by the regional topography and ocean currents (Landman and Tennant, 2000). The landscape is distinguished by an interior plateau and a sharp escarpment to a narrow coastal belt (Vogel, 2000).

Ocean currents enhance west-east gradients of rainfall over southern Africa (Fig. 1.2b; Landman and Tennant, 2000) from less than 50 mm of annual rainfall to more than 900 mm in the east (Bartman *et al.*, 2003). Heat and moisture fluxes into the atmosphere above the warm Agulhas Current have a significant influence on the regional climate (Jury *et al.*, 1993; Rouault *et al.*, 2003). Variability in the Agulhas current region has also been linked to climate variability over South Africa (e.g. Walker, 1990; Jury *et al.*, 1993). Enhanced cumulus convection occurs above the Agulhas (Lutjeharms and van Ballegooyen, 1988)

and significant coastal rainfall is influenced by proximity of the current (Jury *et al.*, 1993). By contrast, the cool Benguela current on the west coast is linked to upwelling and aridity (Jury *et al.*, 1996).

Rainfall is by far the most important climate factor over the subcontinent and is highly seasonal, mostly received during the austral summer from October to March. The mean annual spatial pattern shows higher rainfall in the tropical latitudes with distinct west-east gradients over the southern plateau (Fig. 1.2b). North-south gradients are also evident in the mean pattern south of the Zambezi River (~ 15°S).

The Inter-Tropical Convergence Zone (ITCZ) provides good rainfall to the Zambezi River basin and is the main rain bearing system over the subcontinent largely modulated by the movement of the sun and the Hadley circulation. Re-curved south Atlantic southeast trade air (Congo Air) advects moisture from above the forests of the Congo basin and converges with the northeast Monsoon and southeast trade winds in the Near-Equatorial Trough. This trough links the Angola low to a low in the Mozambique Channel and is the zonal axis of the ITCZ. The farther south the ITCZ moves, the higher the likelihood for good rains over the more arid subtropics during that season. North-south oscillations of the ITCZ during summer are mostly influenced by pressure changes south of Africa (Unganai and Mason, 2002) whilst the establishment of a mid-tropospheric anticyclone over Botswana pushes the ITCZ away.

NW cloud bands on the eastern edge of the Kalahari are a major feature of the summer climate of southern Africa. They provide a significant proportion of annual rainfall for regions of the subcontinent south of the Zambezi River (Harrison, 1984; Jury and Nkosi, 2000; Vogel, 2000). The cloud bands are forced by tropical-temperate troughs which link tropical easterly lows to mid-latitude westerly waves. Heavy rainfall is often associated with slow eastward propagation of these troughs (Crimp *et al.*, 1998). During drier summers,

tropical-temperate troughs are pulsed east of the subcontinent (Jury, 1993) and convection is thus displaced to the Indian Ocean east of Madagascar (Jury and Pathack, 1991; Jury *et al.*, 1993b).

The southern coastal margins of the subcontinent are influenced by subtropical and mid-latitude weather systems. The south Atlantic high-pressure system is the forcing mechanism for large-scale subsidence and aridity over the west coast (Jury and Reason, 1989). Rainfall seasonality along the narrow coastal belt varies from strong winter rainfall in the southwest through an all year rainfall region in the south to a summer rainfall region in the east (Vogel, 2000). Ridging subtropical anticyclones and the associated cold fronts provide the bulk of the rainfall over the southeast coast and the adjacent interior (Jury and Levey, 1993; Landman and Tennant, 2000; Vogel, 2000). They also account for 16-25% of total rainfall variance over the subregion (Preston-Whyte and Tyson, 1988).

1.2.1 Intraseasonal rainfall characteristics

The summer rainfall season of southern Africa is not entirely unimodal, it is characterised by alternating sequence of wet and dry weather at near monthly intervals (Makarau, 1995). The timing and duration of wet and dry spells exhibit high variability and have profound effects on rain-fed agriculture. Wet spells of the summer are often caused by many different weather systems whilst dry spells are largely associated with the mid-tropospheric anticyclone centered over Botswana (Botswana upper high). Mid-season droughts are frequently the result of the persistence of the Botswana upper high affecting nearly the entire subcontinent.

Intraseasonal oscillations are cycles of rainfall and other meteorological parameters operating at time scales shorter than the annual cycle. The best known intraseasonal oscillation (ISO) is the Madden-Julian Oscillation (MJO) which is a tropical phenomenon of the coupled ocean-atmosphere system with oscillations in zonal winds and surface pressure in tropical regions. These

oscillations are linked to fluctuations in cloud and rainfall propagating eastward every 30-60 days near the equator. Meteorologists monitor distinct circulation patterns associated with the MJO to predict regions of ascending or descending motion within monsoon systems. It is known that the MJO is weakest over the tropical Atlantic, hence incoming wave energy is somewhat disorganised over Africa. Apart from the MJO, other shorter intraseasonal oscillations occur (Levey, 1993).

A number of previous studies found major cycles of intraseasonal oscillations of rainfall over southern Africa operating between 20-60 days.

In the mean, Makarau (1995) found five main wet spells and two main dry spells during the summer with each lasting up to 3 pentads (15 days). He determined rainfall cycles operating between 10-25 days and 40-50 days with a mean frequency of approximately 3-4 pentads (15-20 days). He also investigated mean onset and cessation dates and duration of wet and dry spells in an 'ideal' season. He studied wet spell phases of the southern African summer and found two troughs located over the subcontinent, one zonal trough extending from Angola to the Mozambique Channel and another meridional trough over the west coast. Makarau (1995) also determined that the midsummer dry spell is largely a result of large-scale subsidence induced by the Botswana upper high.

OLR is commonly used as a proxy for rainfall data in tropical regions. Since clouds are near perfect absorbers of OLR, regions of low OLR are associated with deep convection and frequent cloudiness (Gondwe and Jury, 1997). Levey (1993) found a combination of the 40-60 day MJO and a 20-30 day OLR oscillation operating over southern Africa. The study established that the MJO is the dominant oscillation during wetter years whilst the 20-30 day ISO dominates the dryer years. The oscillations propagate eastward but of particular interest to this study, he found 25-40% stationary modes, which he suggests, are linked to

tropical-temperate troughs. Levey (1993) also suggested that two 20-30 day ISOs occur within a MJO.

In a study of intraseasonal convection over southern Africa, Levey and Jury (1996) found a 20-35 day cycle of OLR to be the primary mode of weather variability over southern Africa. They determined that uplift is widespread over southern Africa during wet spells with compensating subsidence in the tropics and mid-latitudes. Levey and Jury (1996) also established that nearly one third of all ISOs propagate eastward in concert with mid-latitude and equatorial disturbances.

Anyamba (1992) determined a 40-50 day oscillation and a 20-35 day oscillation in tropical OLR over the western Indian Ocean. She determined that the 40-50 day oscillation is the dominant ISO and linked it to the MJO. She also established that the 20-35 day oscillation exhibits weaker eastward propagation. It is not the scope of this study to analyse the propagation of intraseasonal oscillations but rather the impact with respect to the land surface.

Other intraseasonal oscillations determined include a 20-25 day oscillation that is distinct from the MJO (Michelson and Klein, 1991) whilst Ghil and Mo (1991) detected a 23-day oscillation and a 40-day mode in 500 hPa geopotential heights. A 26-day oscillation has also been determined for SSTs of the western Indian Ocean from 52°E to 60°E in low latitudes (Tsai *et al.*, 1992).

Jury and Levey (1997) determined synoptic conditions favourable for wet spells over southern Africa using a vertical analysis of composite sequences of mid-latitude Rossby waves. They found that Rossby waves facilitate the poleward flow of tropical moist unstable air whilst a deep-ridging anticyclone provides the dynamical trigger. Similar synoptic features were described earlier by Lyons (1991) and Jury *et al.* (1996) whilst Tyson (1981) observed that wet spells are associated with deepening pressure over the subcontinent. Wet spells have also

been associated with reduced upper westerlies south of Africa (Jury and Levey, 1997).

Tennant and Hewitson (2002) studied intraseasonal rainfall characteristics in South Africa using Self Organising Maps (SOMs) on daily station data. They calculated nine different rainfall characteristics such as seasonal totals, lengths of wet and dry spells, correlations between different stations in a region and variances. They argued that rainfall characteristics such as the lengths of wet and dry spells should be given in addition to seasonal rainfall totals when analysing rainfall. Tenant and Hewitson (2002) also determined that northern South Africa is influenced by tropical rain bearing systems whilst the south is more dependent on mid-latitude synoptic scale disturbances.

1.2.2 Rainfall extremes

Due to high intraseasonal and interannual variability, droughts and floods are distinct features of the climate of southern Africa (Tyson, 1986), and are becoming more frequent (Mason, 1996), and severe (Mason and Jury, 1997). One of the most severe droughts on record was that of 1991/92 whilst notable floods occurred in 1975/76 and 1999/2000 affecting mainly the eastern regions.

Flood events over southern Africa are consistently related to tropical cyclones and occasionally to cut-off lows of the mid-troposphere and associated severe thunderstorms. Cut-off lows are an early or late summer phenomenon which form in the mid-troposphere when closed lows are 'cut-off' from the westerlies. Widespread heavy rainfall often results when cut-off lows are accompanied by a surface ridging anticyclone (Dube, 2002).

Tropical cyclone Demoina of January 1984 dumped more than 800 mm of rainfall north of Durban in one day in the midst of a widespread drought (Poolman and Terblanche, 1984). Cyclone Eline of February 2000 affected more than 150 000 families with losses of up to US$600 million in Mozambique (Mozambique

National News Agency, 2000). Disease epidemics and malaria incidences peaked in flood hit areas.

Tropical cyclones can also cause enhanced subsidence and prolonged dry periods over the subcontinent when they are quasi-stationary over the Mozambique Channel (Matarira, 1990; Jury and Pathack, 1991). Dry spells also result from the persistence of the Botswana upper high which often pushes the ITCZ away inhibiting uplift over the subcontinent. Extended mid-season dry spells frequently culminate in droughts (Makarau, 1995) and during drought years, rainfall often increases over the warm ocean east of Madagascar (~60°E).

1.2.3 Remote forcings of the regional rainfall

Rainfall oscillations longer than the annual cycle have been observed over southern Africa. A 2.3 year rainfall cycle has been attributed to the stratospheric Quasi-Biennial Oscillation (Jury *et al.*, 1992; Mulenga, 1998) whilst cycles operating between 3-7 years, 10-12 years, 18-20 years have also been determined and largely attributed to forcing from the remote oceans and ENSO. Several studies have demonstrated the influence of SSTs on the climate of southern Africa (e.g. Nicholson and Entekhabi, 1987; Walker, 1990; Jury and Pathack, 1991; Mason *et al.*, 1994; Makarau and Jury, 1997; Mason and Jury, 1997; Rocha and Simmonds, 1997; Reason and Lutjeharms, 1998) and warm ENSO events have been linked to dry conditions over the eastern sector of the sub continent (Ropelewski and Halpert, 1987; Janowiak, 1988; Jury *et al.*, 1994; Hastenrath *et al.*, 1995; Shinoda and Kawamura, 1996; Rocha and Simmonds, 1997; Vogel, 2000). In Africa, teleconnections between ENSO and rainfall are strongest in East and southern Africa (Anyamba *et al.*, 2002) where above normal rainfall over East Africa often precedes below normal rains over southern Africa (Ogallo, 1988).

Recent work suggests that ocean Rossby waves are at work to produce these cycles in climate (Jury *et al.*, 2004). Thus, ocean temperatures and the Southern

Oscillation are the major forcings of the regional climate at interannual and multiyear time scales. They are also the main predictors for seasonal rainfall over southern Africa (Palmer and Anderson, 1994).

1.3 Vegetation-climate dynamics

Whereas, vegetation growth and distribution is largely determined by climate (Woodward, 1987; Wang, 2004), vegetation and landuse characteristics can feedback on the climate (Zeng and Neelin, 2000; Wang, 2004). Feedbacks from the land surface affect boundary layer fluxes of moisture, energy and atmospheric dynamics. Vegetation-climate interactions occur through various thermal, hydrological and biogeochemical processes (Wang, 2004) involving such variables as soil moisture, surface albedo, evapotranspiration (hence precipitation), surface roughness and atmospheric dynamics.

Charney (1975) pioneered research on vegetation-rainfall dynamics in a study of Sahel drought. He suggested that positive feedback mechanisms between vegetation cover and surface albedo could be used to explain a trend toward drought in the Sahel. He argued that high albedo from non-vegetated surfaces causes a cooling of surface temperatures, inducing subsidence and surface moisture divergence thus suppressing convection and precipitation. Charney's (1975) hypothesis has been criticised for only considering moisture divergence and not surface moisture fluxes (e.g. Dickinson, 1992). However, in some regions, effects of evapotranspiration may be enhanced or cancelled by changes in moisture divergence (Claussen, 1997). Some studies have argued by contradiction that, although vegetation removal increases surface albedo, sensible heat fluxes also increase at the expense of latent heat (e.g. Schlesinger *et al.*, 1987).

Since Charney's (1975) work, several studies have observed or modelled effects of a changed land-surface, including changes in available moisture from the land-

surface, changes in land-surface roughness and changes in aerosol properties of the atmosphere (e.g. Carleton *et al.*, 1994). The NDVI has been a robust indicator for vegetation health and has thus been used in these studies as a measure of vegetation. Several studies have also shown that rainfall and vegetation are best related in semi-arid regions (e.g. Davenport and Nicholson, 1993; Zeng *et al.*, 2002) because of high evaporative losses during dry spells.

Climate variability has an internal component that is largely determined by energy exchanges at the land-atmosphere interface (Chahine, 1992) whilst variability in regional temperature and moisture is often associated with heat exchange between the boundary layer and the underlying surface (Jury and Reason, 1989). Recent studies have not only considered the energy budget but also the hydrological cycle due to vegetation influence on evapotranspiration (Wang, 2004). However, few studies have quantified the vegetation-climate relationship (Zhou, *et al.*, 2003).

Since vegetation-climate feedbacks involve many 'difficult-to-measure' parameters, this discussion will now consider the role of the principal variables in turn.

1.3.1 Soil Moisture

A noticeable relationship is that vegetation responds to rainfall events. However, it is relevant to note that vegetation has no direct response to rainfall, but rather to soil moisture - an integral of rainfall (Malo and Nicholson, 1990). Soil moisture exhibits a longer memory than most atmospheric variables (as do SSTs) and thus has potential to influence atmospheric variability and predictability (Entin *et al*, 1999). In the short term, besides providing moisture for evaporation, near-surface soil moisture controls the partitioning of available energy at the ground surface into sensible and latent heat exchange with the boundary layer. Over longer periods, soil moisture also modulates droughts and floods (Pan *et al.*, 1999). Thus, an understanding of the distribution and linkages of soil moisture to

evapotranspiration is essential to predict upward feedbacks of land surface processes on weather and climate. Davenport and Nicholson (1993) determined that NDVI reflects soil moisture better than rainfall and numerical modellers have recognized the need for soil moisture inclusion in model simulations of climate.

In a study on NDVI response to soil moisture in semi-arid Botswana, Nicholson and Farrar (1994) suggested that NDVI temporal variability and response patterns to rainfall might be largely a function of soil type and they concluded that there was uncertainty in how much NDVI reflects photosynthetic activity. Tinley (1982) determined that soil moisture balance is a dominant factor in the distribution of forest, savanna and grassland. The more clayey soils tend to hold more soil water than sandy soils. Topographic factors, soil texture, vegetation and atmospheric forcing also influence soil moisture. However, Douville *et al.* (2001) concluded that the soil moisture - precipitation feedback varies according to region, suggesting stronger positive feedback in regions where moisture convergence is weak. A limiting constraint is that soil moisture has largely been obtained from models rather than field data (Wang *et al.*, 2003).

1.3.2 Evapotranspiration

Evapotranspiration is a key element in the surface water budget that helps determine the humidity of the lower atmosphere (Tyson and Preston-Whyte, 2000). Up to 91% of the rainfall of southern Africa returns to the atmosphere through evapotranspiration (Martyn, 1992), significantly greater than the global average of 65-70% (Gondwe and Jury, 1997).

Evapotranspiration involves moisture transfer away from the earth's surface into the atmosphere often resulting in a build up of atmospheric water vapor. This process involves mass and energy transfer as latent heat used for change of state during evaporation is transferred into the atmosphere along with water vapour. The positive feedback of evapotranspiration on cloud formation and precipitation also affects incoming radiation (Bounoua *et al.*, 2000).

Using scale analysis, averaged over long periods and over large areas, a classical equation of hydrology is given by: -

$$E - P = \nabla \cdot Q \qquad (1.1)$$

where E is evaporation, P is precipitation and $\nabla \cdot Q$ is moisture divergence, the net flux of water vapour out of a region. Evaporation and precipitation are unevenly distributed over the earth's surface and regions of moisture convergence such as the deep tropics and ITCZ, are regions of excess precipitation. Frequently, evaporative losses exceed precipitation rate in semi-arid regions and constitute regions of moisture divergence (Peixoto, 1993). The Kalahari desert is characterised by reduced evapotranspiration and cloud cover but high sensible heat fluxes (Jury *et al.*, 2002).

Evapotranspiration and rainfall are significantly correlated with the NDVI in a wide range of conditions (Gray and Tapley, 1985; Justice *et al.*, 1986; Nicholson *et al.*, 1990; Cihlar *et al.*, 1991). Szilagyi *et al.* (1998) demonstrated that NDVI has a stronger correlation with lagged evapotranspiration than lagged rainfall. However, reliable measurements for area-averaged evapotranspiration are not readily available.

Bowen Ratio

Sensible heat is the heat flux transferred into the atmosphere by thermal conduction with the ground whilst latent heat is the heat used or released during phase changes of water from liquid to vapour. A comparison between sensible and latent heat fluxes is important when determining energy balance. The Bowen ratio was developed as a quick method to do that and is expressed as a ratio of latent heat flux to sensible heat flux. It is significantly affected by the presence of transpiring vegetation and has been used in many studies as a proxy to estimate evapotranspiration. However, in situ measurements of sensible and latent heat fluxes are not readily available for the period of climatological record.

1.3.3 Surface albedo

Vegetation removal alters the reflective capacity (albedo) and the heat fraction used to evaporate and transpire water into the atmosphere. A number of studies (e.g., Charney, 1975; Gondwe and Jury, 1997; Zeng *et al.*, 1999) have shown that vegetation removal results in higher albedo and reduced evapotranspiration. Low net short-wave radiation absorbed at the surface results in suppressed convection and rainfall through a series of feedback mechanisms. Conversely, increased vegetation density results in higher humidity and reduced albedo due to strong absorptance in the Photosynthetically Active Radiation (PAR) band of the solar spectrum (Bounoua *et al.*, 2000).

Processes for vegetation removal are largely anthropogenic and include overgrazing, agricultural extension and fuel wood extraction (Taylor *et al.*, 2002). Vegetation loss is likely to continue given the patterns of population and economic growth and urbanization in southern Africa. There are potential regional and global impacts associated with landscape changes.

1.3.4 Surface roughness

The size and phenology of vegetation affect the amount of solar radiation and rainwater captured by the surface, and the depth to which soil water may be transmitted to the atmosphere via roots. Changes in vegetation density affect surface roughness thereby altering the exchanges of moisture, energy and momentum at the land-atmosphere interface (Bounoua *et al.*, 2000). Surface roughness refers to the influence of obstacles on the wind. For example, a landscape with bushes and dense forest will have higher roughness length than grasslands. In general, forests or mountain ranges slow the wind down considerably (causing wind convergence) more than grasslands. Apart from altering the divergence field, surface roughness also determines the intensity of mechanical turbulence.

It is essential to note that this study will not analyse specific aspects of the complex feedback mechanisms using all variables stated above, but will assess the correspondence between vegetation, related moisture fluxes and rainfall at intraseasonal (or event) time scales. A theoretical framework is offered in Chapter 2 following on a conceptual model of Wang (2004).

1.4 Modelling vegetation impacts

General circulation models (GCMs) have difficulty resolving regional effects such as orography, land/sea contrasts, surface albedo and fluxes of heat and moisture between the surface and the boundary layer. Climate modelling is also hindered by land-biosphere-atmosphere interactions which are still not well understood (Bounoua *et al.*, 2000).

Vegetation modelling began more than twenty years ago and many studies have focused on the physiological impacts of vegetation on the climate particularly in deforestation and desertification studies. Advances in numerical modelling have not only included simulating vegetation response to climate variability, but also atmospheric response to vegetation change (Wang, 2004). The coupling of dynamic vegetation (biosphere) models to atmospheric models in climate studies has increased in recent years (e.g. Levis *et al.*, 1999; Delire *et al.*, 2003).

The sensitivity of global and regional climates to projected changes in vegetation density was tested using the Simple Biosphere Model (SiB2) coupled to a GCM (Bounoua *et al.*, 2000). The major findings of the simulations are that increases in vegetation density cause corresponding increases in evapotranspiration and precipitation. Increased vegetation causes an annual mean cooling of up to 0.8 K in tropical regions. The Bowen ratio is lower, reflecting a cooler and moister boundary layer climate. Furthermore, precipitation was modeled to increase more than evapotranspiration reflecting more water stored in the atmosphere, as transferred from soil moisture.

Using a simplified coupled atmosphere-vegetation model, Zeng *et al.* (2002) found that rainfall and vegetation are reduced by climate variability in high rainfall regions but increased in low rainfall regions. The study revealed that positive upward feedbacks of vegetation on rainfall are more distinct in intermediate precipitation regions although climate variability reduces this gradient in the semi-arid regions (Zeng *et al.*, 2002).

In a modeling study of the African Savanna, Zeng and Neelin (2000) suggested that without external climate variability, positive feedbacks from vegetation would enhance the gradient between desert and forest regions at the expense of the savanna, but in drier regions climate variability would act to weaken this gradient.

Bonan (1997) investigated the effects of land use change on the climate of the United States and showed that the climate with modern vegetation is significantly different from climate with natural vegetation. He found a cooling of 1 K over the eastern United States and a warming of 1 K over the west during spring and suggested that climate change due to land use change may be comparable to that caused by well known anthropogenic forcings.

More recently, Drew (2004) ran a Dynamical Global Vegetation Model (the Sheffield Dynamic Global Vegetation Model or SDGVM) to simulate vegetation change over Africa south of 20°N, obtaining data from 2 GCMs and 2 climate change scenarios up to 2099. The model simulates vegetation change and likely variability in the possible vegetation changes until the turn of the century. Experiments were undertaken to test the climate response to increases in surface roughness length and albedo which represent significant changes in vegetation distribution and structure.

The experiments by Drew (2004) simulated increases in surface roughness length and albedo by 20% each resulting in reduced moisture transport into the interior of the sub-region. This caused reduced cloudiness, higher insolation

reaching the surface and a corresponding increase in surface air temperatures. However, her study did little to establish how the atmosphere responds to changes in vegetation. Drew (2004) recommended consideration of soil moisture in land-atmosphere interactions over southern Africa. She also suggested that sparse vegetation in the arid zones might not have significant feedback to the atmosphere.

It must be noted that vegetation modelling studies have focused on a particular aspect of land surface processes and have not accounted for coupling among the different parameters (Bounoua *et al.*, 2000). This is necessitated by the complexity of the feedback mechanism especially considering the multiple spatio-temporal scales involved and the 'difficult-to-measure' surface parameters.

1.5 The boundary layer

Feedbacks of the land surface and overlying vegetation are strongest in the atmospheric boundary layer. The boundary layer is the lowest layer of the earth's atmosphere usually below 1000 m where effects of frictional drag are most significant (Fig.1.4a). Above the boundary layer is the free atmosphere.

Fluctuations in boundary layer height reflect surface influences in terms of heat and moisture fluxes and turbulence. Boundary layer height is a useful concept for studies on air pollution, atmospheric chemistry and meteorological modelling. However, it is difficult to quantify and has been defined in many ways due to its high variability in space and time. It may shrink to less than 100 m at night, but extend to about 2 km above the earth's surface due to rigorous thermal mixing by day (Oke, 1987).

Research studies define boundary layer height according to some surface forcing such as turbulence, evapotranspiration or heat transfer. Yin and Albrecht (2000) define the marine atmospheric boundary layer as extending from the surface to

the top of the trade wind inversion over the eastern Pacific. Frictional drag (hence turbulence) has also been used to demarcate the boundary layer height.

The flux Richardson's number is a ratio of buoyant to shear turbulent kinetic energy (TKE). It may be written as :-

$$Ri_f = \frac{\frac{g}{\theta_v} w'\theta'_v}{u'w'\frac{\partial U}{\partial z} + v'w'\frac{\partial V}{\partial z}} \qquad (1.1)$$

where $\frac{g}{\theta_v} w'\theta'_v$ is the thermal component and $u'w'\frac{\partial U}{\partial z} + v'w'\frac{\partial V}{\partial z}$ is the shear component. The Coupled Ocean/Atmosphere Mesoscale Prediction System (COAMPS^{tm}) defines the height at which $Ri_f \leq 0.25$ as the depth of the boundary layer. Many mesoscale meteorological models such as the MM5, ETA, RAMS, ARPS use the bulk Richardson number and TKE schemes in resolving boundary layer height. Grimsdell and Angevine (1998) compared calculations from the Richardson's number against profile measurements and determined that the calculations overestimate the depth of the boundary layer. Surface turbulence generated mixing results in a mixed layer whose thickness has been used as a proxy for boundary layer height. However, models using turbulence fail when stable conditions prevail.

The availability of radiosonde data is crucial in determining boundary layer height, (e.g. potential temperature and specific humidity profiles). An abrupt decrease in specific humidity or abrupt increase in potential temperature occurs at the top of the boundary layer. However, radiosonde data are expensive, discontinuous and sparse in many regions of the world.

This research study prefers a boundary layer height determined by the height of the moist layer. An increase in moisture fluxes from local evapotranspiration results in a deepening of the boundary layer. A vertical section on 27°S latitude

shows the height of the moist layer (~10 g kg^{-1}) over southern Africa peaking around 28-30°E and capped at 1 km due to a combination of surface vegetation, sensible heat fluxes and horizontal moisture convergence (Fig. 1.4b). Fluctuations in moisture fluxes can also be used as proxies for boundary layer height.

1.6 Hypotheses

It is hypothesized in this study that: -

1. Vegetation is directly related to rainfall in a lagged manner
2. Spatial modes of variability for rainfall and vegetation are co-located.
3. An earlier rainfall event and subsequent 'greening' results in an evapo-transpiration flux that affects the next rainfall event.
4. The position of the NW cloud band on the eastern edge of the Kalahari Desert is related to surface moisture fluxes.
5. Fluctuations in specific humidity and latent heat flux from local evapotranspiration are key determinants of boundary layer height and hence land surface influences.

Key research questions are:

- What proportion of the vertical water vapor flux is locally forced by evapotranspiration relative to horizontal moisture advection?
- To what extent is the position of the NW cloud band affected by surface moisture fluxes? and therefore,
- How sensitive is the regional climate to vegetation cover?

1.7 Objectives

Specific objectives of this study are:

1. To establish the intra-seasonal variability and distribution of rainfall over southern Africa

2. To characterize the temporal and spatial variability of satellite-derived vegetation (NDVI) over southern Africa
3. To demonstrate interannual and event-scale variability of evapotranspiration-driven moisture fluxes over southern Africa
4. To investigate the influence of vegetation and related moisture fluxes on rainfall events over southern Africa
5. To test the sensitivity of the regional boundary layer climate to local surface forcing

Southern Africa is defined in this study to include the immediately adjacent southeast Atlantic and southwest Indian oceans extending from 10°S to 40°S and bounded by longitudes 10°E and 50°E. The region covers ten Southern African Development Community (SADC) countries stretching from the Democratic Republic of Congo to South Africa.

1.8 Summary

This chapter has defined the background, vegetation and climate of the study area. Relevant literature on existing knowledge on land-atmosphere interactions has also been presented. The hypotheses to be tested, key research questions and objectives of the study have been formulated.

It has been determined from the literature that vegetation feeds back on the climate through soil moisture, albedo, evapotranspiration and surface roughness via a number of complex feedback mechanisms. This study will analyse specific aspects of this feedback and evaluate the correspondence between vegetation, related moisture fluxes and rainfall events. Details of the data used in this study, analysis methods and a theoretical framework are given in Chapter 2.

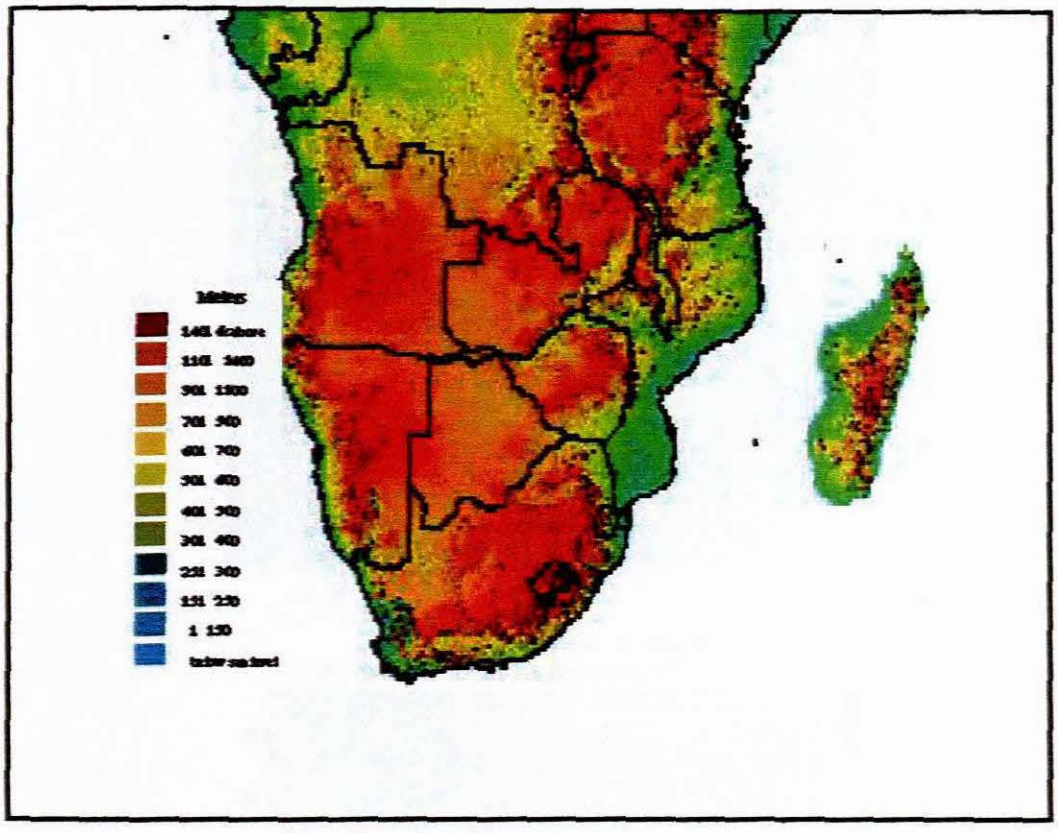

Fig. 1.1 Topographical map of southern Africa showing the elevation.

(a)

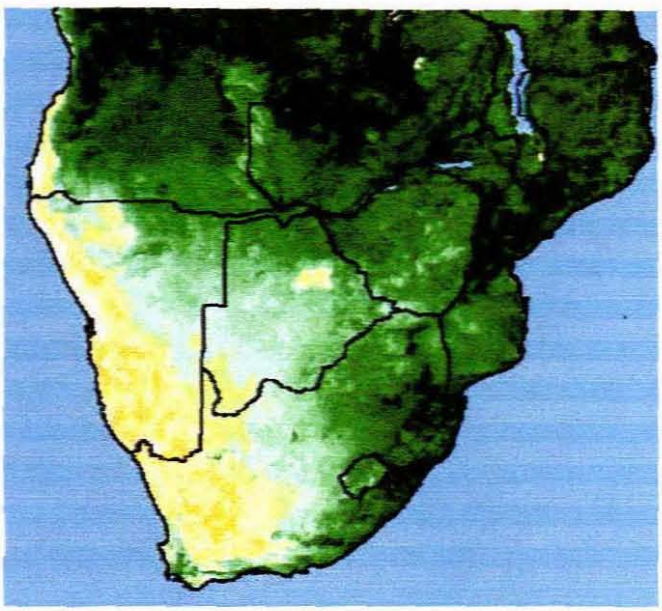

(b)

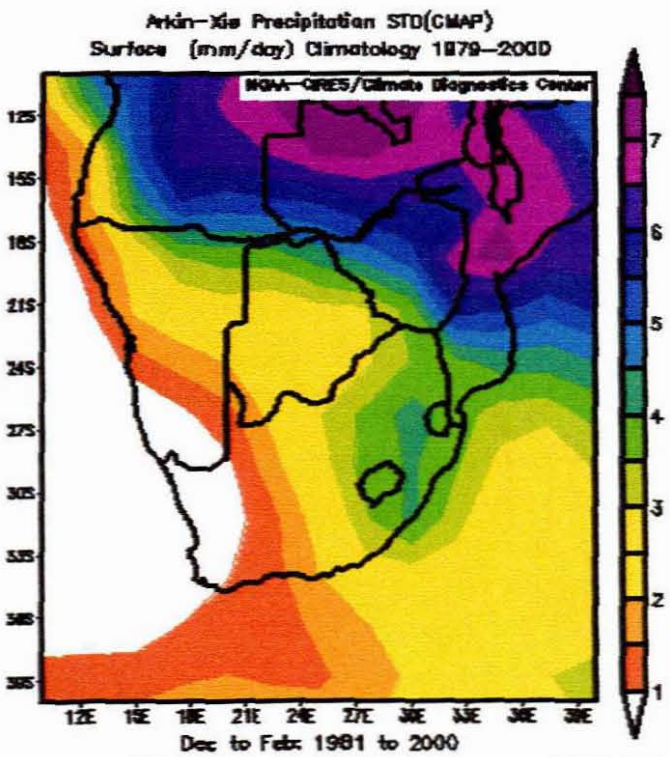

Fig. 1.2 (a) January mean NDVI over southern Africa and (b) Climate prediction center Merged Analysis of Precipitation (CMAP) Dec-Feb climatology. The mean rainfall largely determines the spatial distribution of vegetation.

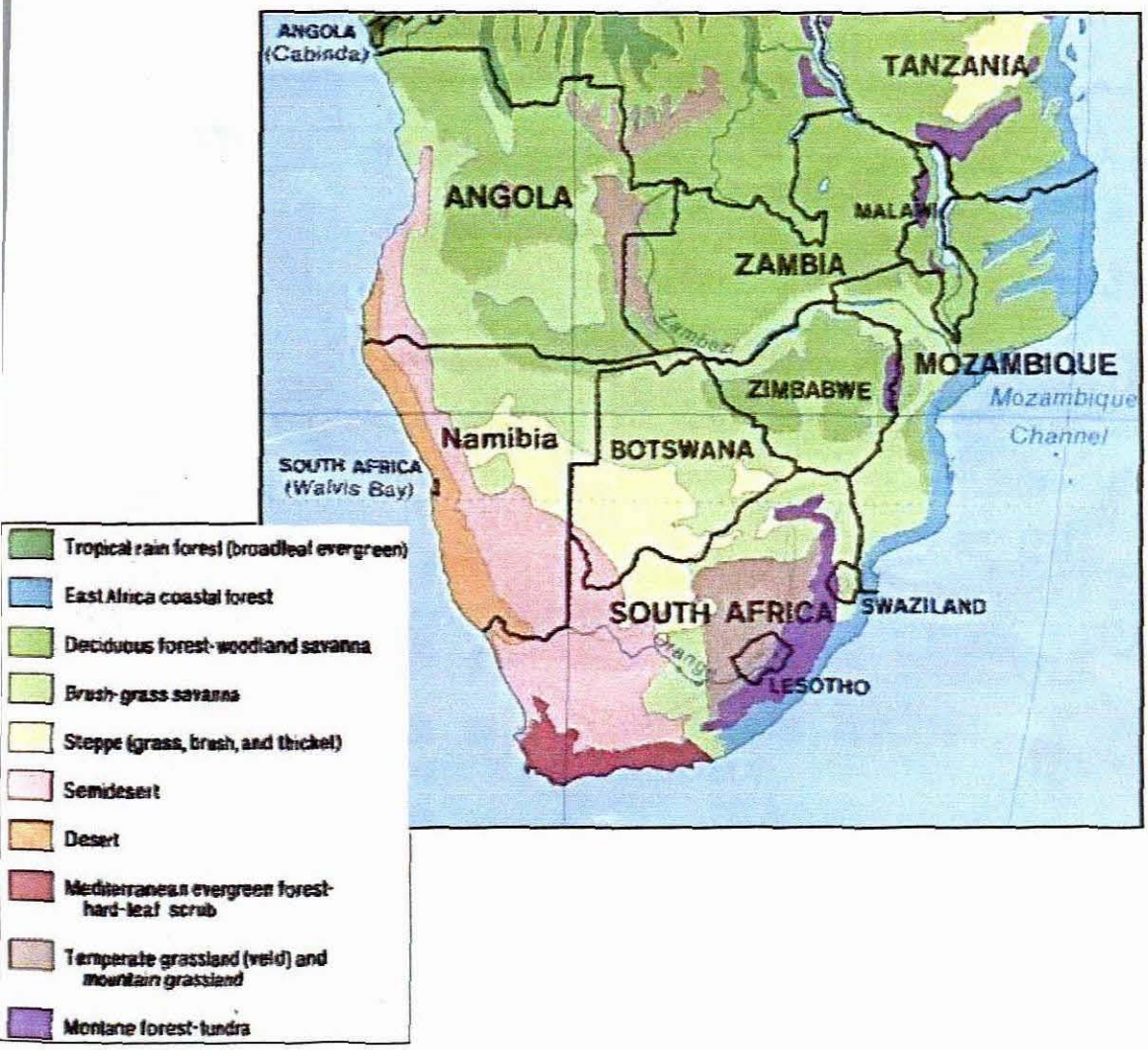

Fig. 1.3. Natural vegetation of southern Africa. A gradual change is observed from the western desert to forests on the eastern seaboard. (source: Azimuth Equal Area Projection)

(a)

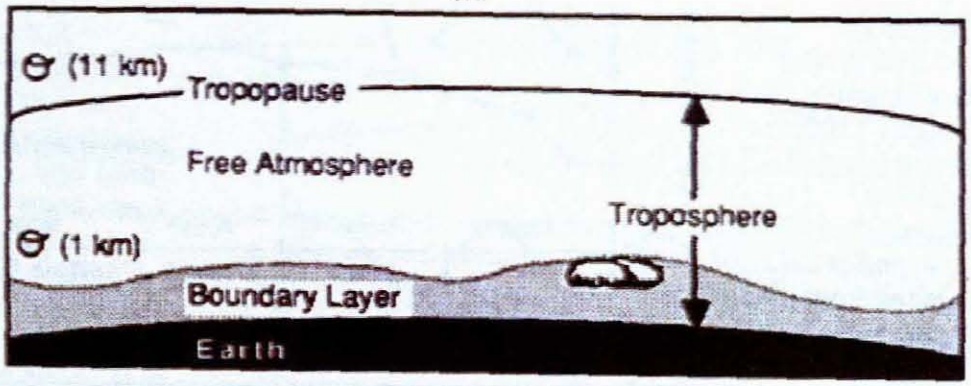

(b)

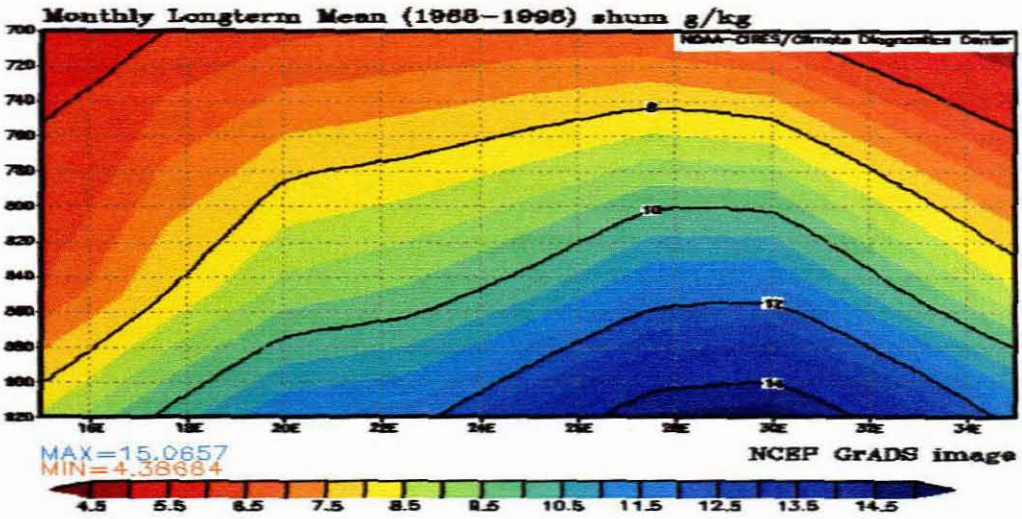

Fig. 1.4. (a) Vertical profile of the planetary boundary layer (after Stull, 1988) (b) Long term mean distribution of specific humidity over southern Africa plotted as an east-west cross section from the plateau upward to 3 km elevation, averaged for latitude 27°S.

Chapter 2

DATA AND ANALYSIS METHODS

2.0 Introduction

To achieve the objectives of this study, regional vegetation characteristics, rainfall patterns and horizontal and vertical moisture fluxes over southern Africa are studied using satellite data, station observations and model reanalyses.

The objective of this chapter is to present the datasets and analysis techniques employed in this study. A theoretical framework is also offered. Major datasets includes satellite estimated vegetation and rainfall data, analysed to establish spatial and temporal variability and the associated responses and impacts. The influence of the land surface on the climate over southern Africa is examined using an analysis of moist boundary layer structure and response to vegetation forcing.

2.1 Data and Sources

2.1.1 Vegetation NDVI

NDVI data (1982-2000) are acquired by the Advanced Very High Resolution Radiometer (AVHRR) aboard the National Oceanic and Atmospheric Administration (NOAA) polar orbiting environmental satellites. The data are extracted from the United States Geological Survey (USGS)/African Data Dissemination Service (ADDS) Internet websites. The NDVI data have been detailed by Tucker *et al* (2005).

NDVI is a normalized ratio evaluated using satellite observations of vegetation reflectance at two wavelengths or bands - one band in the visible region (VIS; 0.58 μm to 0.68 μm) and another in the near infrared (NIR; 0.725 μm to 1.1 μm).

Vegetation reflectance maximises at about 0.8 μm, making the NIR channel moresensitive to vegetation 'colour' (Tucker, 1979; Tucker *et al.*, 1991; Jury *et al.*, 1997a). Since the NDVI is a non-destructive measurement of the intercepted or absorbed photosynthetically active radiation (Myneni *et al,* 1995), a sum of the NDVI results in a quantity highly related to net primary production (Tucker *et al,* 2005). Vegetation reflects a greater proportion of near-infrared light than visible (red) light but bare soils or little vegetation will have similar reflectances in both bands. Water and ice reflect more visible light than near-infrared light.

The NDVI is derived using the following relation: -

$$NDVI = \frac{NIR - VIS}{NIR + VIS} \qquad (2.1)$$

Mathematically, NDVI is a non-linear function ranging from -1 to +1, but typical values on the earth's surface vary between -0.1 to 0.7 with negative values indicating water bodies, snow surfaces and clouds (Wang *et al.*, 2003). NDVI values below 0.3 indicate scant vegetation and water stress conditions (Jury *et al.*, 1997b) whilst values above 0.5 reflect dense and vibrant vegetation.

Quality control and spatial sub-sampling

The ADDS NDVI are obtained at dekadal (10-day) time resolution because dekads give enough over-passes of the satellite to produce cloud-free images. Once 10 days of daily data are accumulated, dekadal NDVI are derived based on the maximum value in each pixel or gridpoint.

NDVI values are often reduced in the presence of water vapor, clouds, snow and aerosols. In regions of agricultural activity, types of crops, soil types and irrigation may influence observed changes in NDVI (Gondwe and Jury, 1997). The soil background also affects NDVI magnitudes with dark coloured soils such as vertisols and fluvisols increasing NDVI whilst light colored soils reduce it (Nicholson and Farrar, 1994). Atmospheric interference tends to reduce NDVI through cloud contamination, Rayleigh scattering and absorption by atmospheric

constituents such as ozone and aerosols. The ADDS data are corrected for these effects.

The NDVI data are obtained with stretched values in the 8-bit range of 0-255 for southern Africa and processed in *Idrisi for Windows*. A *Matlab* program was developed to shrink the values back to a range of 0.0 to 0.75.

NDVI data are available at a high spatial resolution of 8x8 km. For the purposes of this climate-oriented study, the data are reduced to approximately 2.5° through a process of sub-sampling by averaging with neighboring pixels. Low NDVI on the eastern seaboard are due to spatial averaging with ocean pixels (Davenport and Nicholson, 1993). Quality control of unreliable NDVI values found near water bodies and coastlines is done by interpolation using values from adjacent inland pixels. The ADDS data provided for southern Africa are considered in the latitudes of 10°-35°S for this study.

NDVI time series

The data may be viewed as a 'stack' of NDVI images over time. Extracting a value for each geographic point in the 'stack' creates a time series. A *Matlab* program is used to convert the 'stack' into a three dimensional matrix with longitude, latitude and time. A macro is then used to extract each timeseries.

The data are standardized for further analysis with respect to their historical mean and standard deviation using the following relation:

$$z = \frac{(x_i - \bar{x})}{\sigma} \qquad (2.2)$$

Where x_i is an individual data point, $\bar{x}$ is the climatological mean and σ is the standard deviation. Standardization can lead to distorted patterns if the standard deviation is significantly varying in the data. Here the variations are low and standardizing assists intercomparisons.

2.1.2 NCEP-NCAR data

Meteorological reanalysis data are obtained from the National Centers for Environmental Prediction (NCEP)-National Center for Atmospheric Research (NCAR) reanalysis. The reanalysis is a result of a joint project between NCEP and NCAR as an outgrowth from the Climate Data Assimilation System (CDAS) project. It was developed and launched in 1991 primarily to support the needs of the research and climate monitoring communities. The reanalysis data are based on assimilation of surface, ship, rawinsonde, pibal, aircraft, satellite and other data which are quality controlled (Kalnay *et al.*, 1996). The websites enable users to make plots, obtain time series of a box average, and obtain subsets of the GRIB fields and FTP access to many of the GRIB fields at different temporal and spatial resolutions. It is recorgnised that NCEP model reanalyses are not uniformly reliable (Kalnay *et al.*, 1996).

Most of the climate data used in this study are obtained from the NCEP-NCAR reanalysis (CDAS) data sources. Other sources of reanalysis include NCAR, the Climate Prediction Center (CPC) and Climate Diagnostics Center (CDC).

2.1.3 CMAP Rainfall

Five-day averaged (pentad) precipitation data at 2.5° resolution for the period 1981-2000 are analysed. The pentad data are produced by merging rain gauge observations with satellite precipitation estimates inferred from infrared radiation (IR), outgoing longwave radiation (OLR), microwave sounding unit (MSU), and special sensor microwave imager (SSMI). Over oceanic regions, the satellite infrared and microwave data are merged with gauge observations from some islands. Thus, CMAP rainfall data provides accurate data at high spatial and temporal resolution. In the study of Tazalika (2003), seasonal rainfall characteristics including the evolution and propagation of intraseasonal oscillations over central Africa are presented using CMAP rainfall data. Previous studies have used station data (e.g. Makarau, 1995; Mulenga, 1998; Unganai and Mason, 2001; Tennant and Hewitson, 2002) and were mainly confined to

rainfall characteristics for certain regions/countries of the subcontinent. There is still need for more rainfall research over the adjacent Indian and Atlantic oceans.

The data for this study are obtained from the NCEP/CPC Internet websites and used to describe rainfall patterns and trends over southern Africa and the adjacent oceans. CMAP rainfall data provides contiguous coverage at a reasonable resolution, especially considering data scarce regions such as rainforests, deserts, mountainous regions and the vast oceans.

2.1.4 *Evapotranspiration-related flux estimates*

Soil Moisture

Due to the vast extent and heterogeneity of soils on continental surfaces of the earth, ground based measurements using gravimetric techniques cannot provide adequate spatial coverage. Satellite observations of soil moisture are also unavailable for the period of meteorological record. However, aircraft microwave remote sensed data may be used to obtain better spatial coverage, but are unable to provide reliable measurements of the subsurface (Choudhury, 1993). In future, more reliable soil moisture climatologies could be obtained from the Global Soil Wetness Project (GSWP) which aims to produce high-resolution soil moisture using land surface schemes, meteorological observations and analyses (Douville *et al.*, 2001), and microwave satellite imagery.

In this study, NCEP soil moisture derived from mean precipitation and radiation are used to characterize the surface soil moisture climatology. The NCEP soil moisture is expressed as a fraction. For example, 0.2 refers to 2 cm of water in a 10 cm layer of soil. The saturation value of soil moisture is 0.477 and the field capacity is 0.358. A limitation is that the soil depth (layer depth) and field capacity are considered to be horizontally uniform.

Evapotranspiration and latent heat flux

Evaporation losses are often monitored by observation of a Class A-Pan. Evaporation from a natural water body usually proceeds at a slower rate and therefore the pan overestimates the actual evaporation. Besides, errors due to heating of the pan may affect the data usefulness. Typically, evaporation data are adjusted using empirical 'pan coefficients' to correct these effects (Shuttleworth, 1993). A-Pan measurements are commonly made at weather stations but the data are often discontinuous and sparse over much of the study region.

Potential evaporation is widely used as a measure of the amount of water that could be evaporated if it was in unlimited supply. It is a measure of atmospheric demand for water vapour and is estimated using surface and air temperature, insolation and wind. Versions of Penman's equation are often used to calculate potential evaporation. One version may be written as: -

$$E_p = \frac{\Delta}{\Delta+\gamma}(R_n + A_h) + \frac{\gamma}{\Delta+\gamma}\frac{6.43(1+0.53U_2)D}{\lambda} \quad (2.3)$$ (Shuttleworth, 1993)

where R_n is the net radiation exchange, A_h is the energy advected across the water body, U_2 is the wind speed at 2 m, D is the average water vapour deficit.

A bulk dynamical formula for evaporation used by the NCEP model to calculate latent heat flux is given by: -

$$Q_e = \rho C_e L(U)(q_s - q_a)(10^{-3}) \quad (2.4)$$

where ρ is air density, C_e is a dimensionless coefficient at 10^{-3}, L is a temperature-independent latent heat of vaporisation, 2.5 x 10^6 J kg^{-1}, and q_s and q_a are specific humidity from the vegetation surface and air above.

The data are obtained at 6 hourly resolution and reduced to dekadal resolution by time averaging for comparisons with vegetation NDVI. Latent heat flux and potential evaporation are analysed and discussed in this study.

Specific humidity

Specific humidity (q) or moisture content of the air may be defined as the mass of water vapor per unit mass of air. It is a dimensionless ratio usually expressed as grams of water vapor per kilogram of air (g kg^{-1}). Specific humidity may be derived from the following equation:

$$q = \frac{(\varepsilon \times e)}{(p - (1 - \varepsilon) \times e} \quad \textit{(Rogers, 1979)} \quad (2.5)$$

where ε is 0.622 which is the ratio of the molecular mass of water vapor to that of dry air, e is the vapor pressure and p is the total pressure of the system (water vapor + dry air). Equation 2.5 reduces to:

$$q = \frac{0.622e}{(p - 0.378e)} \quad (2.6)$$

Satellite profile measurements of specific humidity have been made only since 1991. NCEP reanalysis specific humidity is used in this study to characterize the moist boundary layer structure along west-east transects over southern Africa where radiosoundings are frequently made and reported for model assimilation. Humidity is the weakest of the primary atmospheric variables in the NCEP model as it is unconstrained. It is produced by a univariate analysis with no dynamical constraint on the gradients.

2.1.5 700 hPa wind vectors and velocity potential

NCEP model assimilated wind vectors at 700 hPa over southern Africa are analysed. Satellite cloud drift data help underpin the model-derived winds especially for the data sparse regions such as the vast oceans and remote regions where radiosonde observations are unavailable. Wind data contains wind speed and direction and is often used to determine wind divergence and transport (advection). As with dew-point depression, the 700 hPa level was selected because of its role in moisture transport over southern Africa. Maximum water vapour flux divergence over South Africa occurs at 700 hPa (D'Abreton and Lindesay, 1993).

The two dimensional velocity wind vector may be written as

$$V = V_\Psi + V\chi \qquad (2.7)$$

where ψ is the streamfunction and χ is the velocity potential. The streamfunction is the rotational component which is non-divergent whilst the velocity potential is divergent and irrotational. Velocity potential and divergence are not directly related but the positive two-dimensional Laplacian of velocity potential equals convergence in the Southern Hemisphere as in the following equation:- $$\nabla^2\chi = -\nabla \bullet V \qquad (2.8)$$

Here, NCEP model velocity potential is evaluated at sigma level $\sigma = 0.8458$ and used as a proxy for divergence. Sigma (σ) levels represent flow over the terrain better than fixed pressure surfaces.

2.1.6 Station radiosonde data

Station radiosonde data for Bloemfontein (68442; 26°E, 29°S) obtained from the South African Weather Service are used in this study. The data are obtained at twice daily resolution at approximately twelve-hour intervals. However, some of the data are available only once a day. This is typical of radiosonde data in many regions largely due to high costs.

Time variations in boundary layer height over Bloemfontein are estimated using the dew-point depression. The dew-point depression is defined as the difference between the ambient air temperature and the dew-point temperature at a certain level. It is written as: -

$$DD = T - T_d \qquad (2.9)$$

where DD is the dew-point depression, T is the ambient air temperature and T_d is the dew-point temperature. Low values of dew-point depression reflect moist conditions and high likelihood for clouds to develop.

In this study the DD is evaluated at 700 hPa which is often a critical level for boundary layer processes and moisture transport over southern Africa. The daily

radiosonde data are averaged to dekadal time scales to allow comparisons with vegetation and other data. However, the data are at a single point and therefore caution must be taken in interpreting relationships with gridded field data.

2.2 Data availability

Most of the climate data required for the study are available readily from NCEP data servers whilst NDVI data are available from the ADDS servers. However, some limitations exist. NDVI data are available for twenty-two years at best and satellite-estimated latent heat flux and soil moisture are available for not longer than ten years. In the absence of in-situ observations, model reanalyses are employed and caution should be taken when interpreting results based on these data for individual events. Here, multiple events are averaged together using specified criteria to improve and generalise the results.

Upper air observations are sparse and discontinuous over much of the study region. This limits the amount of analysis that can be done with radiosonde vertical profiles. There are very few stations in southern Africa that are operating radiosondes throughout the year. Most national weather services operate one or two radiosonde stations and only during summer. The South African Weather Service also obtain aircraft AMDAR data for ascents and descents to Johannesburg International Airport.

2.3 Analysis Methods

The analysis techniques used in this research study can be classified into five categories.

1. Techniques used to analyze a time series e.g. analysis of linear trends, spectrum analysis.
2. Techniques that remove trends and seasonality and other cycles from a time series e.g. wavelet analysis.

3. Techniques that analyze varying patterns in space and time e.g. principal component analysis.
4. Techniques that evaluate relationships between two time series e.g. cross-correlation.
5. Techniques that analyse the relative contribution of one process relative to another occurring simultaneously e.g. budget analysis.

2.3.1 Spectrum Analysis

Spectrum analysis is used to convert a signal from the time domain (amplitude-time) to the frequency domain (amplitude-frequency). A frequency domain display is known as a spectrum. The data is passed through a math algorithm known as a Fast Fourier Transform (FFT) which converts the signal from the time domain to the frequency domain. The spectrum is presented as a two-dimensional plot of frequency in Hertz (Hz) on the horizontal axis and amplitude of each frequency line on the vertical axis. The plot is also known as a Periodogram.

The goal of spectral analysis techniques is to determine how important cycles of different frequencies are in accounting for the behavior of a time series. They provide insight on how much a specific frequency is contributing to variations in the series of interest. Spectral analysis is used in this study to determine the dominant cycles and their wavelengths for vegetation and rainfall over southern Africa.

2.3.2 Wavelet Analysis

Time series of NDVI, CMAP rainfall, and surface latent heat flux are studied using wavelet analysis. Wavelet analysis is a time series analysis method widely used in the geophysical sciences. It was developed as an alternative to Fourier and spectral analysis to determine variance spectra especially when amplitudes of dominant oscillations are time dependant (Tyson *et al.*, 2002). While Fourier expansion has frequency resolution and no time resolution, it presents the

frequencies inherent in the data, but not when they occur. Wavelet analysis maps a one-dimensional timeseries to a two-dimensional image depicting evolution of scales and frequencies with time (Lau and Weng, 1995). It determines dominant timescales of variability and their evolution in time through transforming timeseries data into time-frequency data.

Satellite NDVI, CMAP rainfall and NCEP model latent heat flux are filtered using wavelet analysis to retain cycles between 20-70 days as determined by the vegetation's temporal resolution. It was shown in Chapter 1 that several studies obtained rainfall cycles shorter than 30 days (e.g. Levey, 1993; Makarau, 1995) and since CMAP data are obtained at pentad resolution, they are filtered again to retain cycles between 10-35 days.

2.3.3 *Principal Components Analysis*

Space-time variance of dekadal NDVI, pentad CMAP rainfall, and NCEP latent heat flux is analysed using the principal components analysis technique. Principal components analysis (PCA) or Empirical orthogonal function (EOF) analysis is a classical statistical method that has become standard for data reduction and factor analysis in climate research. It is used to represent spatial and temporal variability of variables such as NDVI and rainfall as a number of empirical modes. Each mode (or principal component) consists of a spatial pattern and a time series derived from eigenvalues of the correlation matrix (Mestas-Nuñez, 2000) which are orthogonal to each other. An eigenvalue is the amount of variance that is accounted for by a given factor.

PCA describes the fundamental modes of variability over space and time (Unganai and Mason, 2001) and seeks to reduce the dimensionality of the data by transforming two or more correlated variables into a smaller number of uncorrelated variables called principal components. Most of the variability in the data is represented by the first principal component (PC1) and it decreases with

ensuing PCs. Temporal scores describe the periodicities of seasonal and intraseasonal trends and their intensity (Jury, 1999).

Rotation

Rotation is applied to simplify the spatial and temporal structure of the modes. The variance maximizing (varimax) rotation technique is most commonly used in principal component analysis to group the variability in geophysical applications (Mestas-Nuñez, 2000). Rotation simplifies the spatial/temporal structure by isolating regions of similar temporal variability or similar spatial patterns (Mestas-Nuñez, 2000). Varimax rotation is also used to enhance the spatial loadings of the dominant modes of variability (Jury, 1999).

Scree test criteria

Ideally, the number of PCs should equal the number of data in a time series (Aldrian and Susanto, 2003) but only a few will represent significant variance in the data. A scree plot is frequently used to determine the number of PCs to retain for discussion. It is a plot of eigenvalue for each factor or PC mode against the mode number (Fig. 2.1).

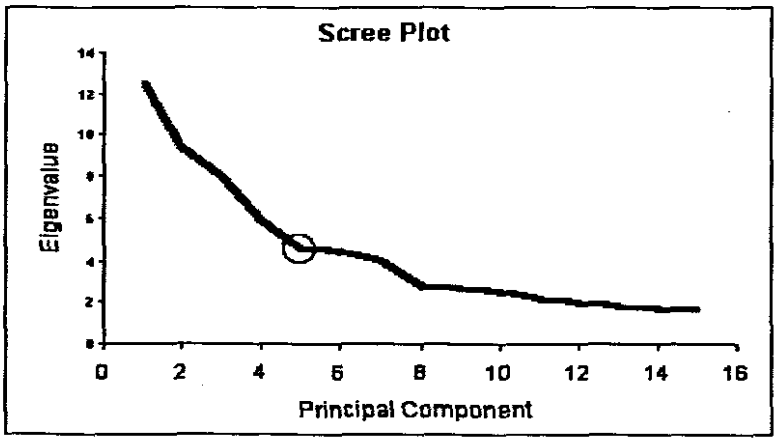

Fig. 2.1 The critical point occurs at PC5. Modes to the right of this point may be discarded as noise.

The larger the eigenvalue the more meaningful the common factor is. Large eigenvalues are linked with the steep slope of the plot whilst the smaller

eigenvalues are associated with the gradual slope (Mulenga, 1998). An abrupt jump in eigenvalue tends to separate groups of factors. To the right of the inflection point on the plot are factors to discard as noise.

A number of studies have used PCA to study seasonal rainfall over southern Africa. Mulenga (1998) applied principal component analysis to study the dominant modes of variability in a study on summer rainfall over southern Africa. Jury (1999) used PCA on pentad OLR to study intra-seasonal convective variability over southern Africa. Unganai and Mason (2001) applied PCA to station rainfall data over Zimbabwe whilst Anyamba and Eastman (1996) used it for studying vegetation patterns as related to ENSO in Africa. In this study, PCA is performed on satellite NDVI, CMAP rainfall and NCEP latent heat flux using consecutive maps over a 20-year period (1981-2000).

2.3.4 Composite Analysis

Composite analysis is a technique commonly used in climate research to detect common climatological features and contrasts. Composites reflect trends and patterns better than individual cases (Levey, 1993). Meteorological contrasts between wet and dry summers or 'green' and 'brown' NDVI events are analysed here using this technique. However, this technique is prone to bias through subjective selection of potentially conflicting events or cases.

Intra-seasonal composites are analysed for selected events with large amplitude changes in NDVI. These events are of critical importance to this study such that intraseasonal composites of rainfall, specific humidity, dew-point depression, latent heat flux, wind vectors and velocity potential are also selected based on them. This allows comparisons with respect to NDVI big 'events' of boundary layer height fluctuations due to moisture fluxes and circulation. Intraseasonal composites are used in this study to assist in a budget analysis to determine the upward feedback - the evapotranspiration flux from vegetation into the boundary layer. Compositing is potentially problematic because events in the composite

may be having intraseasonal cycles with different speeds, different maxima and different amplitudes. The individual events of the composite are plotted to determine coherence or whether a single or few events dominate the composite (Fig. 2.2).

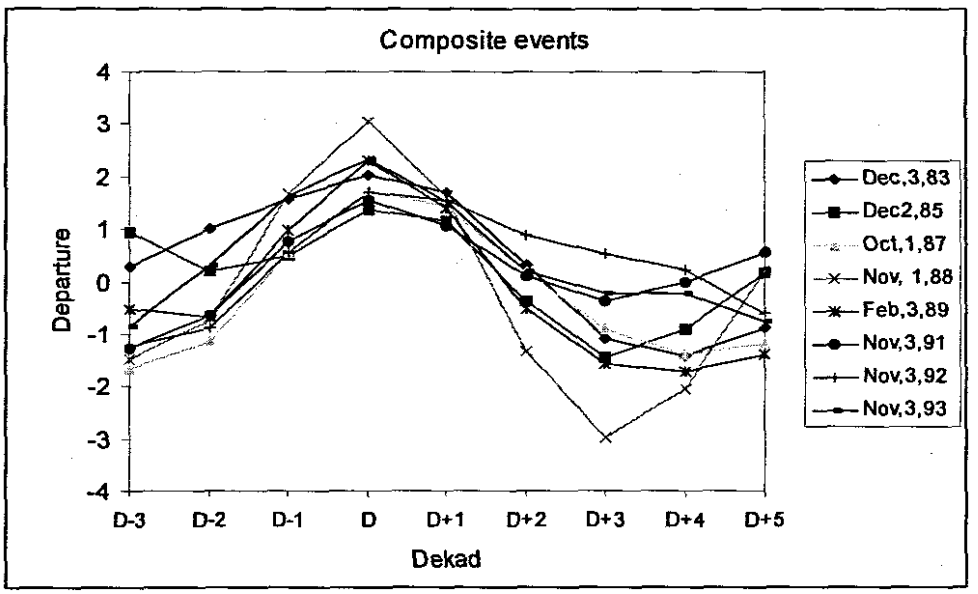

Fig. 2.2 Individual events with large amplitude change in NDVI carefully selected for the composite analysis in Chapter 6.

The events exhibit high coherence in their variability as shown in the Fig. 2.2. and they are based on dekad D and therefore the coherence is strongest then, diminishing with time away from this dekad.

2.3.5 Correlation analysis

NDVI data is analysed for seasonal means, standard deviations, and dekadal anomalies with a focus on the summer rainfall season. Cross-correlation is performed for relationships between NDVI and rainfall at seasonal and intraseasonal time scales using different leads and lags. A hindrance to this exercise is that rainfall data are at pentad resolution and vegetation NDVI data are at dekadal scales. There are 73 pentads and 36 dekads in the year and there is no direct method to reduce rainfall to the same time resolution as vegetation. A weighting average method is applied to bring rainfall to a dekadal (10-day) time step.

Evapotranspiration-related moisture fluxes are also correlated with NDVI and rainfall.

2.3.6 West-East transects

West-east gradients of NDVI and boundary layer parameters such as specific humidity, soil moisture and latent heat flux are shown using spatial sections. Mean and variance maps are presented along selected transects. Two transects between the dry-west and the moist-east are considered at 18°S and 27°S latitudes.

2.3.7 Moist boundary layer determination and budget analysis

As discussed in Chapter 1, many methods are available for determining boundary layer height. This study prefers the NCEP model specific humidity as a proxy for the moist boundary layer height. An increase in moisture fluxes from a moisture convergence and local evapotranspiration results in a deepening of the boundary layer. It is argued that fluctuations of specific humidity in the boundary layer correspond with fluctuations in boundary layer height.

A budget analysis is undertaken to establish the contribution of local and remote (external) forcings to the climate of southern Africa. This follows from the composite analysis for events with large amplitude changes of NDVI, to determine the relative contribution of positive vegetation feedback on the regional boundary layer.

2.4 Theoretical framework of the study

Based on the hypotheses stated in Chapter 1 and the methodology described here, a theoretical framework is offered (Fig. 2.2). Spatial and temporal patterns of variability at seasonal and intraseasonal timescales for NDVI and CMAP rainfall are determined using PCA. Co-located standing modes are of particular

interest to this study because they can be best related to interactions with the land surface. The standing modes are analysed and related to boundary layer response mainly through intraseasonal composite analysis.

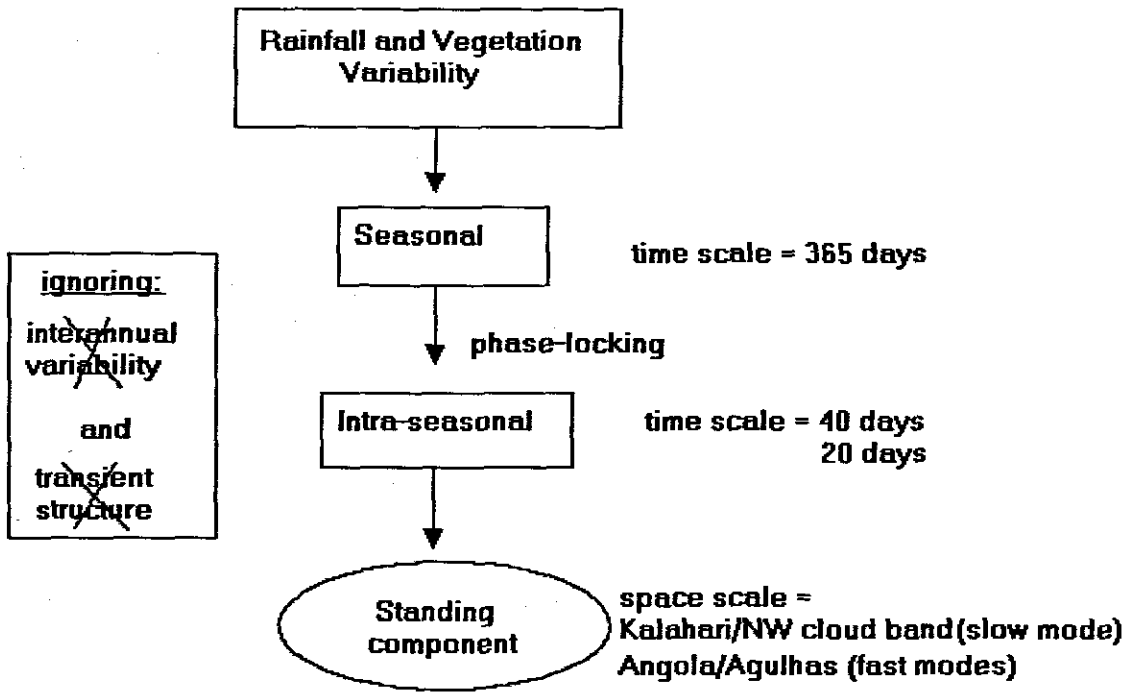

Fig. 2.3. Schematic illustrating the analysis for spatial and temporal modes of vegetation and rainfall variability used in this study.

While it has been noted in Chapter 1 that the vegetation-climate feedback is a mechanism involving such variables as soil moisture, albedo, and roughness, it is not the intention of this study to analyse all specific aspects of this mechanism. Instead, the correspondence between vegetation as a biospheric/land-surface variable and rainfall as a climate variable is tested at intraseasonal (event) time scales. This follows on the method of Wang (2004). Evapotranspiration-related moisture fluxes and 700 hPa wind and velocity potential are used to demonstrate this correspondence.

The vertical moisture flux into the boundary layer may be given by $w'q'$ which is related to a form of the latent heat flux equation: -

$$Q_e = \rho L w' q' \qquad (2.10; \text{Oke, 1987})$$

where Q_e is the latent heat flux, ρ is air density, L is the latent heat of vaporisation, w' and q' are the perturbations of vertical velocity and specific humidity. It is argued in this study that latent heat flux is a proxy for vertical moisture flux since it contains the flux term $w'q'$ multiplied by constants. It is useful to investigate the vertical flux of moisture which can result from moisture convergence, surface evapotranspiration, or convection (Kanamitsu and Mo, 2003). Several studies have established that moisture convergence is the dominant process (e.g. Robertson, 1999) and is assumed in this study to be related to the horizontal flow set up by tropical-temperate troughs.

This study focuses on surface evapotranspiration as it relates directly to the impact of the land surface. In order to separate the surface influence from the dominant moisture convergence; moisture flux, 700 hPa wind and velocity potential are analysed. The wind structure and moisture flux are analysed for events with large magnitude changes in NDVI so as to demonstrate that an earlier rainfall event and subsequent 'greening' result in an evapotranspiration flux that affects the next rainfall event. Here $w'q'$ values are taken from the NCEP model as latent heat flux at the intraseasonal (not turbulent) time scale.

2.5 Summary

The data used in this study, and the sources and methods of analysis have been presented in this chapter. Satellite NDVI, CMAP rainfall and NCEP latent heat flux constitute the major datasets analysed and discussed. Evapotranspiration-related moisture fluxes and circulation are also analysed. Major sources of data include the NCEP websites, ADDS websites and the South African Weather Service.

A theoretical framework has been offered. The analysis proceeds with a PCA on vegetation NDVI and CMAP rainfall for dominant spatial and temporal modes of

variability. The analysis focuses on co-located loading regions for insights. The climatology of evapotranspiration-related moisture fluxes is presented. An intraseasonal (event scale) composite analysis is done for events with large amplitude changes in NDVI to evaluate relationships and boundary layer responses. Finally, an analysis of the sensitivity of the atmospheric boundary layer over southern Africa to regional vegetation forcing is offered.

Chapter 3

SATELLITE-DERIVED INTRASEASONAL RAINFALL VARIABILITY OVER SOUTHERN AFRICA

3.0 Introduction

Rainfall is the most important meteorological parameter over southern Africa with profound impacts on human activities (Vogel, 2000). Its variability has far reaching impacts on society and livelihoods through agriculture and food security, water supply and human health, industry and national economies. Natural vegetation over the subregion is also impacted by temporal and spatial variability of rainfall especially in the deciduous savannas.

Many studies have detailed inter-annual rainfall variability over the subcontinent using station data and related it to remote forcing mechanisms but intra-seasonal variability has received little attention. The objective of this chapter is to establish the intraseasonal rainfall characteristics over southern Africa using CMAP pentad gridded rainfall data described in Chapter 2. Seasonal and interannual characteristics are described in less detail.

3.1 Annual march of rainfall

Rainfall over the summer rainfall region of southern Africa follows a distinct unimodal seasonal cycle. Most rains fall between October and April, peaking from December-February and reaching a minimum in June-July (Fig. 3.1a). Potential evaporation also follows a similar cycle but peaks earlier than rainfall (September-October) with lowest values in the middle of the austral summer (January-February). The absolute dryness in the winter and high evaporative losses in spring make the subregion highly vulnerable to climatic fluctuations.

The temporal pattern of annual rainfall over southern Africa shows well-defined wet and dry cycles of approximately four years in the 1980-2004 period (Fig. 3.1b). Wet years are observed for the seasons of 1984/85, 1988/89, 1996/97 and 1999/2000 whilst 1982/83, 1986/87, 1991/92 and 1997/98 are dry years. The 1992 drought is the most pronounced in the record whilst a distinct peak corresponds to the floods of 2000. Since the floods of 2000, southern Africa has experienced generally poor rains and a downward trend is evident (Fig. 3.1b). If the cyclical pattern were to persist, the years 2004-2005 would be on the trend for wet conditions.

3.2 Seasonal rainfall cycles

A PCA is carried out on pentad CMAP Xie-Arkin precipitation data for the twenty-year period 1981-2000 at 2.5° spatial resolution. The domain used for this PCA is from 10°E-50°E and from 10°S-40°S. Standardized unfiltered data are used to show the seasonal cycles. The first unrotated principal component (PC1) is the only mode retained for discussion according to scree test criteria. The succeeding modes reflect climate noise and do not provide useful insights. PC1 accounts for 34.2% of the total variance of rainfall across the domain of study.

Maximum spatial loadings are observed in the region of the Zambezi River valley (~15°S) extending from Angola through Zambia and Mozambique into the Channel (Fig. 3.2a). The loadings indicate wet conditions that prevail associated with the surface trough linking the Angola Low and a Low in the Mozambique Channel. It is also the zonal axis of the rain bearing ITCZ (Mulenga, 1998), a major determinant of seasonal rainfall over southern Africa. It is impinged on by easterly and westerly waves in summer (Mulenga, 1998).

Another localized region of spatial loading is KwaZulu-Natal on the east coast of South Africa (Fig. 3.2a).

Time scores show the seasonal oscillation peaking typically during the austral summer DJF becoming a minimum from June to August (JJA; Fig. 3.2b). The ITCZ is also at its southern-most position during DJF. Time scores show high amplitudes reflecting wet conditions corresponding to the 1984/85, 1988/89, 1996/97 and 1999/2000 rainfall seasons. Incoming Indian Ocean tropical cyclone induced rains are some causes of the wet anomalies. Low amplitudes associated with strong El Nino induced droughts are evident for the 1982/83 and 1991/92 rainfall seasons.

To determine the dominant frequency in the rainfall pattern, a wavelet modulus spectrum for seasonal CMAP rainfall shows dominant cycles at 73 pentads corresponding with the annual cycle (Fig. 3.2c). There is some leakage of the annual cycle energy into higher frequency harmonics with a '2-years at a time' characteristic (e.g. 81-82, 88-89, 93-94 and 96-97).

3.3 Intra-seasonal rainfall characteristics

Whereas, the seasonal cycles of rainfall over southern Africa have been identified, they form only a part of rainfall characteristics. The summer rainfall season is not entirely unimodal but it is characterized typically by alternating sequences of wet and dry weather (Makarau, 1995). The length of wet spells and dry spells has little correlation with seasonal rainfall totals. Tropical cyclones often result in above average rainfall totals for seasons which may be characterised by abnormally long dry spells. It is thus essential to study the intraseasonal activity, especially the timing and duration of dry spells. It would help a great deal if seasonal forecasts contained information about the midseason dry spell which often determines crop success or failure especially for shallow rooted crops.

Intraseasonal oscillations are cycles of variability whose frequencies are shorter than the seasonal cycle. Spectral analysis shows major cycles of intraseasonal

rainfall over southern Africa operating at approximately 40 days and 20 days. Wavelet filtering is applied to the data to retain cycles between 4-14 pentads (20-70 days) and also between 2-7 pentads (10-35 days). Filtering in the frequency space allows us to view dominant cycles in the specified bands.

Earlier studies by Levey (1993) and Makarau (1995) also found two major cycles for intraseasonal rainfall over southern Africa. The earlier studies however used station data and were limited to small domains. This study seeks to improve the earlier findings using more recent satellite CMAP rainfall data obtained for a larger domain.

3.3.1 40-day oscillations

From the results of the PCA for data filtered to retain cycles between 20-70 days, only the first PC is retained for discussion according to scree test criteria. PC1 accounts for about 12% of variance across the domain of study. The spatial loadings for PC1 maximize in an elongated region with a NW-SE orientation along the eastern edge of the Kalahari, extending from the western Zambezi toward central South Africa (Fig. 3.3a). The loading zone spans about 20° of latitude. Mulenga (1998) determined a similar loading pattern for mid-summer rainfall (December-February).

The loading region receives rainfall due to interactions between tropical easterly waves or heat lows and mid-latitude westerly troughs through tropical-temperate troughs. Tropical-temperate troughs and the attendant NW cloud bands are a major source of summer rainfall south of the Zambezi river (Levey and Jury, 1996) and good rains are often determined by the establishment of the NW-SE trough over periods of a few days (D'Abreton and Lindesay, 1993).

The time score amplitude peaks during December-January which is the peak of the annual cycle. Time scores reflect strong pulsing during the late 1980s (Fig.

3.3b) whilst a weak signal is observed for the dry summers of 1982/83 and 1991/92.

The modulus spectrum shows maximum energy varying between 30-50 days and may be attributed to the influence of the MJO.

3.3.2 20-day ISO

High frequency PCA modes are obtained from filtered data retaining cycles between 10-35 days. The modulus spectrum shows high frequency oscillations with maximum energy about 20 days. This high frequency oscillation shall be referred as the 20-day ISO.

Spatial loadings for rotated and unrotated components show similarity so rotated components are interpreted because they better represent the seasonality together with the ISO. The percentage of variance explained by each ISO mode is lower than that explained by the seasonal mode (34.2%) thus establishing the annual cycle and the associated ITCZ as the dominant factor in rainfall variability over southern Africa.

The first four 20-day modes of variability are significant according to scree test criteria but only PC1 and PC2 are discussed in this study. The loading 'centers of action' and variances are shown in the following table: -

Table 3.1 CMAP rainfall PCA modes and their locations

PC	Centers of action	Variance explained
1	Agulhas Current region (33°S, 33°E)	10.6%
2	Bie Plateau region, Angola (15°S, 17°E)	9.2%
3	Lower Zambezi (15°S, 30°E)	8.0%

4	SW Cape (35°S, 17°E)	4.9%

PC1 has strong positive spatial loadings over the Agulhas Current region and the adjacent southeast coastal margins (KwaZulu-Natal) of the subcontinent (Fig. 3.4a). This mode of variability may be linked to atmospheric planetary Rossby waves and the associated mid-latitude frontal bands. Ridging anticyclones behind cold fronts advect moisture producing extensive cloud along the KwaZulu-Natal coast and the adjacent interior. Comparisons with PC1 of the 40-day oscillation suggest that the dominant 20-day ISO over southern Africa is largely forced from the subtropical ocean (marine) whilst the lower frequency 40-day oscillation has terrestrial influence from the Kalahari transition zone. Although some seasonality is observed in the Agulhas time scores (Fig. 3.4b), significant oscillations are evident in winter suggesting that the oscillations continue throughout the year.

The loading pattern for PC2 of the 20-day ISO is focused on the Bie Plateau region of Angola (Fig. 3.5a) reflecting easterly waves particularly the Angola Low which is a significant feature of the summer climate over southern Africa. The Angola Low is generated by thermal heating of the surface and its depth is determined by the surface temperature. Time scores show that the Angola Low is almost exclusively a summer phenomenon with distinct seasonality peaking during DJF and becoming quiet in winter (Fig. 3.5b). The Angola ISO exhibits strong oscillations in the late 1980s and the late 1990s but is rather quiet during the early 1990s (Fig. 3.5b). Mulenga (1998) studied the Angola Low and determined that it is a quasi-stationary thermal heat low that drives moisture convergence over southern Africa.

The two rainfall modes for the 20-day ISO are loaded over tropical and subtropical regions. The tropical mode (PC2) is terrestrial whilst the subtropical mode (PC1) is marine and the terrestrial mode is of direct relevance to this study.

However, a fundamental observation is that the first mode of the 40-day oscillation connects PC1 and PC2 of the 20-day ISO, suggesting they elongate and join during the NW cloud band (Fig. 3.6). Hence, NW cloud bands are a slower harmonic of the faster modes at either end. This is a significant finding which supports the idea that tropical-temperate troughs form when a tropical low (Angola low) is coupled to a temperate westerly wave (Crimp *et al.*, 1998; Vogel, 2000).

3.4 Phases of seasonal and intraseasonal rainfall

It is important to establish whether the 20-day ISO is a harmonic of the 40-day oscillation. The spectral character of the rainfall oscillations is analyzed without band filtering in the two areas of maximum loading. The 40-day oscillation is the major spectral peak in the absence of the seasonal cycle for the terrestrial region while the 20-day ISO dominates the marine region (Fig. 3.7).

In the Agulhas current region (20-day PC1), intra-seasonal oscillations of rainfall continue through the year (Fig. 3.7b), whilst over the continent (40-day oscillation), they are quiet during the winter when rainfall is nearly absent (Fig. 3.8a). The regularity of oscillations over the oceans suggests that the Rossby waves are not random, but progress eastward to the south of Africa at certain times of the year. This is a remarkable finding, as it was previously considered that the waves are chaotic.

The 40-day oscillation and the 20-day ISO are phase locked to the seasonal cycle, especially at the onset of the summer rains (Fig. 3.8c). Tazalika (2003) observed a similar result for rainfall ISO over tropical Africa whilst Levey (1993) found seasonal dependence of intraseasonal oscillations even with a seasonal signal removed and suggested that the 20-day cycle may be embedded in the 40-day oscillation. Jury and Nkosi (2000) determined using Hovmoller analysis that westward propagating transient waves over the south Indian Ocean are

seasonally phase-locked. Intraseasonal oscillations for the Angola mode also show similar phase relationships with the seasonal cycles.

The mean 20-day Agulhas PC1 and 40-day Kalahari PC1 are in phase during the onset (October) and the cessation (March) wet spell but out-of-phase during summer (Fig. 3.9). However, when the 40-day oscillation is compared against the 20-day PC2 (Angola mode), the two coincide during the major wet spells of summer except in January. When the two intraseasonal oscillations are in phase, they produce copious rainfall or prolonged dry spells. It is concluded that 20-day marine systems are harmonics of the 40-day oscillation at the beginning and end of the rainy season, whilst the Angola low is a harmonic of the 40-day oscillation during December, February, and April wet spells.

The climatological mean 40-day rainfall oscillation exhibits three to six wet spells during summer rainfall period for the Zambezi/ITCZ region from October to April (Fig. 3.9a). The first major wet spell peaks during the middle of December lasting approximately 3 dekads, with the second peaking early February and the last in early March. This result agrees with Makarau (1995) who found wet spells to occur over southern Africa at nearly one monthly intervals from November to March. The time score exhibits an upward trend for the mean annual pattern, with stronger events in the late summer suggesting that the dominant ITCZ is more active over the Zambezi region in during this time. It is not entirely clear whether the 40-day oscillation is related to the global MJO.

The composite dry seasons of 1982/83, 1986/87, 1991/92, and 1997/1998 tend to have longer cycles, whilst wet years (1984/85, 1988/89, 1996/97 and 1999/2000) exhibit longer wet spells and shorter dry spells. This observation is consistent with that of Tennant and Hewitson (2002) in a study of intraseasonal rainfall over southern Africa. They also suggest that heavier rainfall events rather than several light rain events characterize wet seasons.

3.5 Summary

The seasonal and intraseasonal characteristics of rainfall over southern Africa have been determined. The major findings of this analysis are given below: -

(i) It is observed that the annual cycle is the most dominant mode (34%) of rainfall variability over southern Africa. The Zambezi ITCZ is the main synoptic feature associated with it.

(ii) ISOs over southern Africa exhibit spectral peaks about 20 days and 40 days. The 40-day mode is loaded in a NW-SE axis along the eastern edge of the Kalahari, spanning 20° of latitude whilst the 20-day ISO is focused on subtropical Agulhas current/Kwa-Zulu Natal, tropical Bie Plateau (Angola), lower Zambezi and SW Cape.

(iii) The first mode of the 40-day ISO connects PC1 and PC2 of the 20-day ISO, suggesting they elongate and join during the NW cloud band. Tropical-temperate troughs link the Angola low to westerly waves in the Agulhas region. This is a remarkable finding.

(iv) The 20-day and 40-day oscillations are phase locked to the seasonal cycle, especially at the onset of the summer rains. The two are in phase during major wet spells.

(v) The regularity of oscillations over the oceans suggests that the Rossby waves to the south of Africa progress eastward at certain times of the year. It was previously considered that the waves are chaotic.

(vi) The 20-day marine systems are harmonics of the 40-day oscillation at the start and end of the rainy season, whilst the Angola low is a harmonic of the 40-day oscillation during December and February wet spells.

Of particular relevance to this study are the terrestrial modes of variability and how they relate with the land surface and overlying vegetation.

(a)

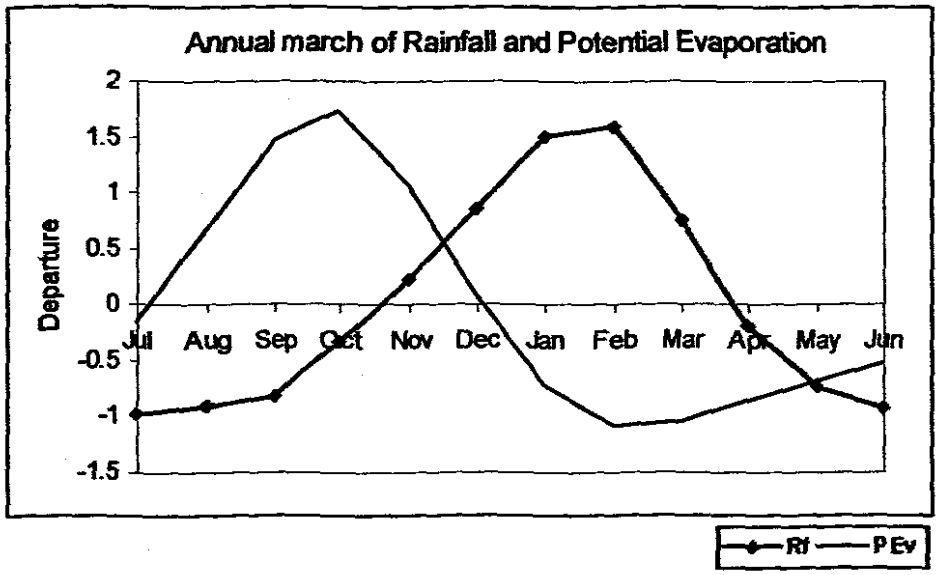

(b)

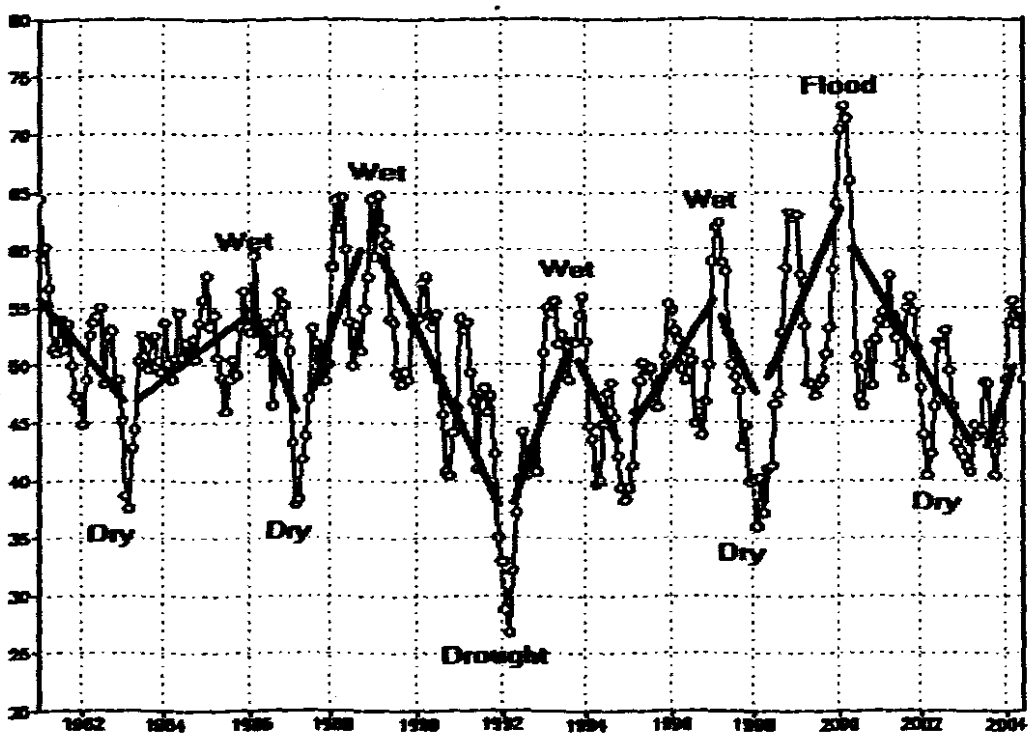

Fig. 3.1. (a) Annual march of rainfall and NCEP model potential evaporation over the summer rainfall region of southern Africa averaged for 1981-2000 (b) Percentiles of mean monthly rainfall over southern Africa. The 25 year mean is on the 50% mark.

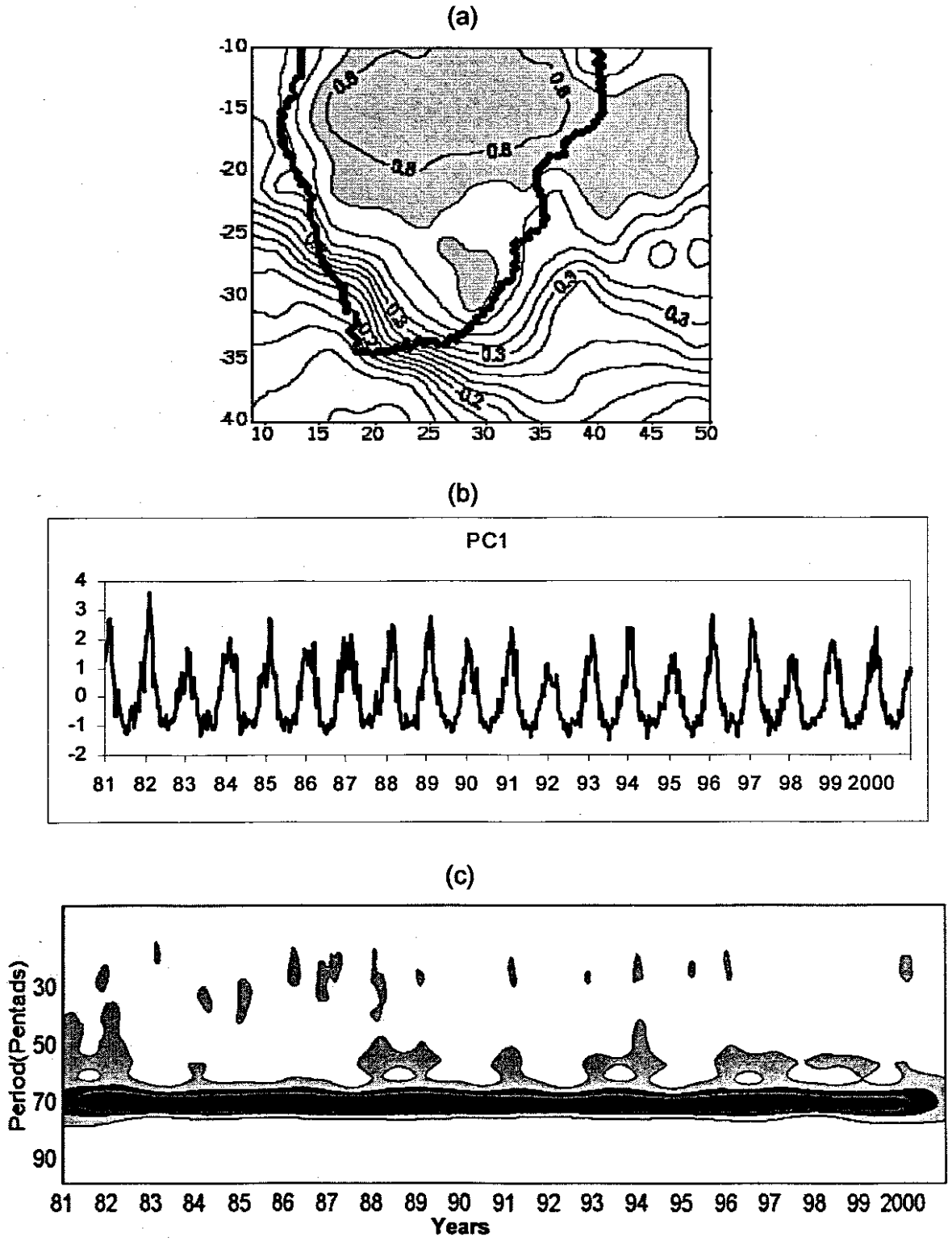

Fig. 3.2. (a) Spatial loading and (b) the associated time scores and (c) the modulus spectrum for seasonal rainfall (unfiltered and unrotated) for PC1 explaining 34% of total variance.

(a)

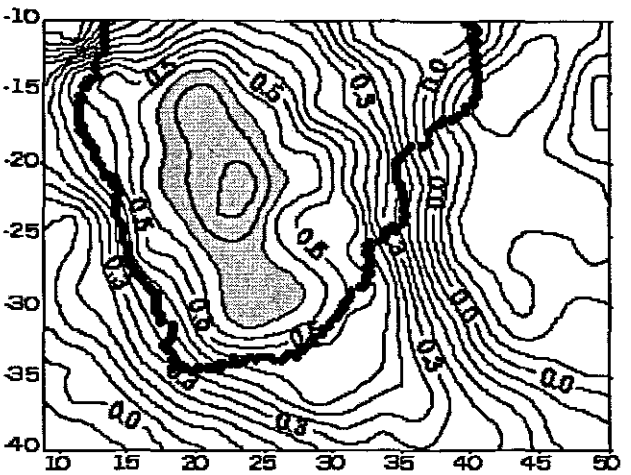

(b)

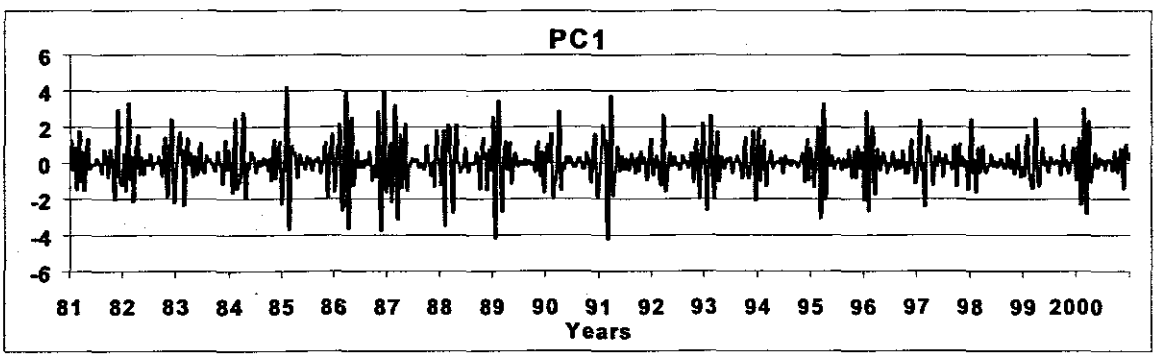

(c)

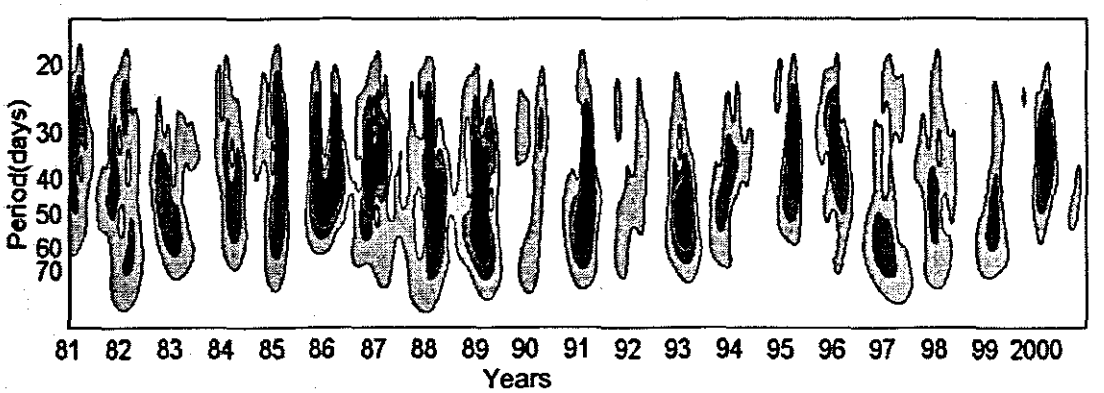

Fig. 3.3. (a) Spatial loading (b) the associated time scores and (c) the modulus spectrum for Intra-seasonal rainfall (filtered to retain cycles between 20-70days and unrotated) for PC1.

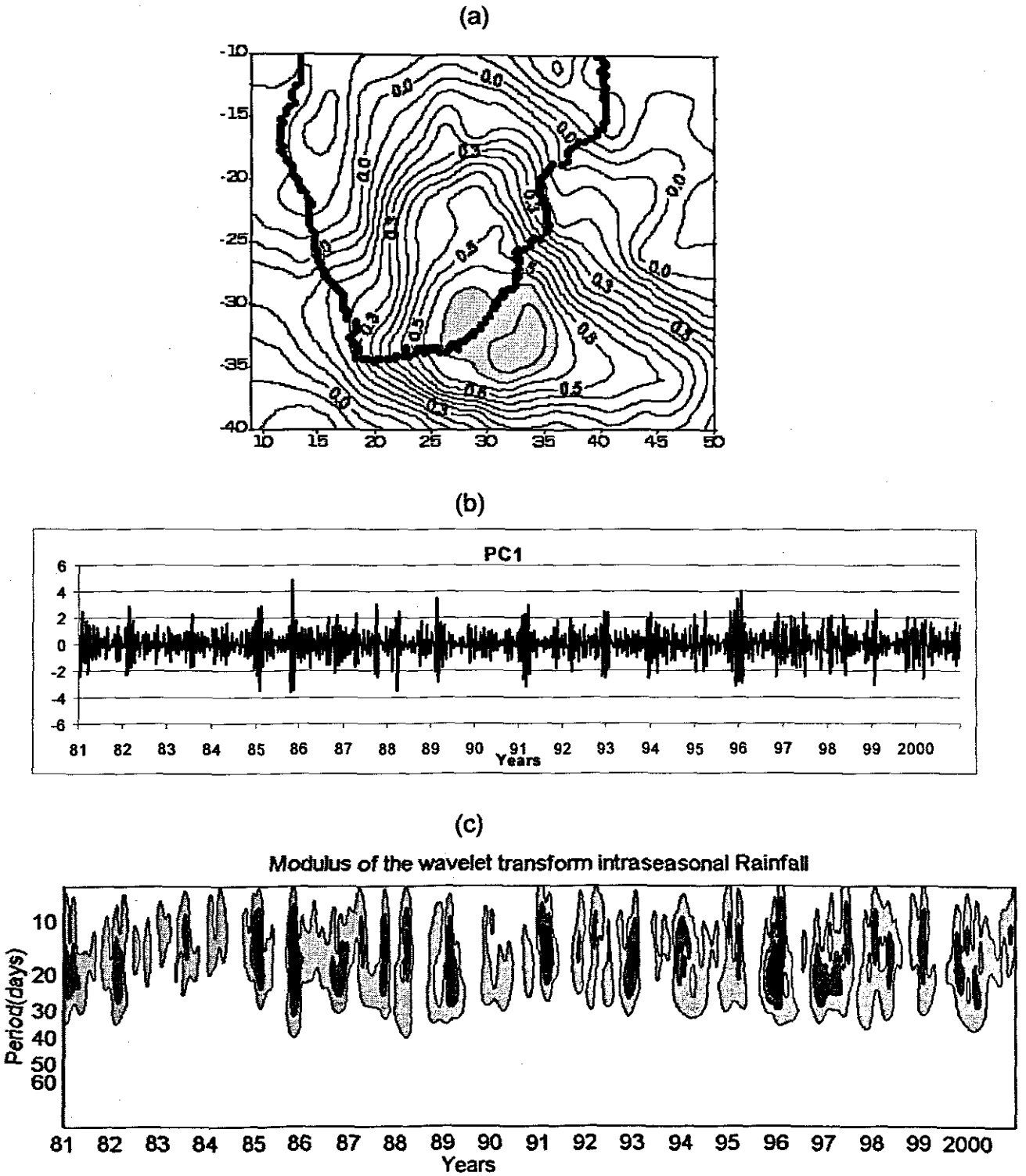

Fig. 3.4. (a) Spatial loading (b) the associated time scores and (c) the modulus spectrum for Intra-seasonal rainfall (filtered to retain cycles between 10-35 days and rotated) for PC1.

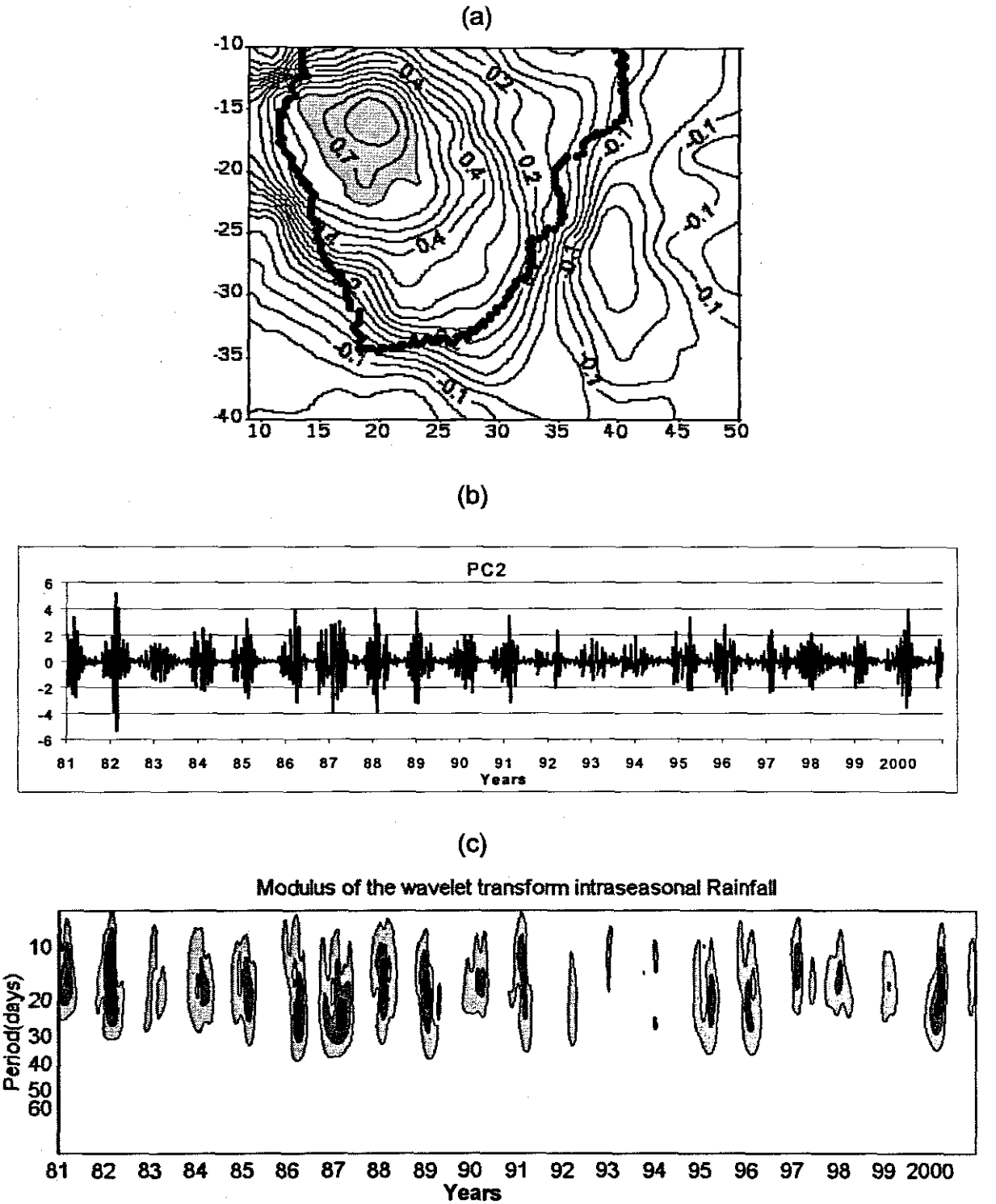

Fig. 3.5. (a) Spatial loading (b) the associated time scores and (c) the modulus spectrum for Intra-seasonal rainfall (filtered to retain cycles between 10-35 days and rotated) for PC2.

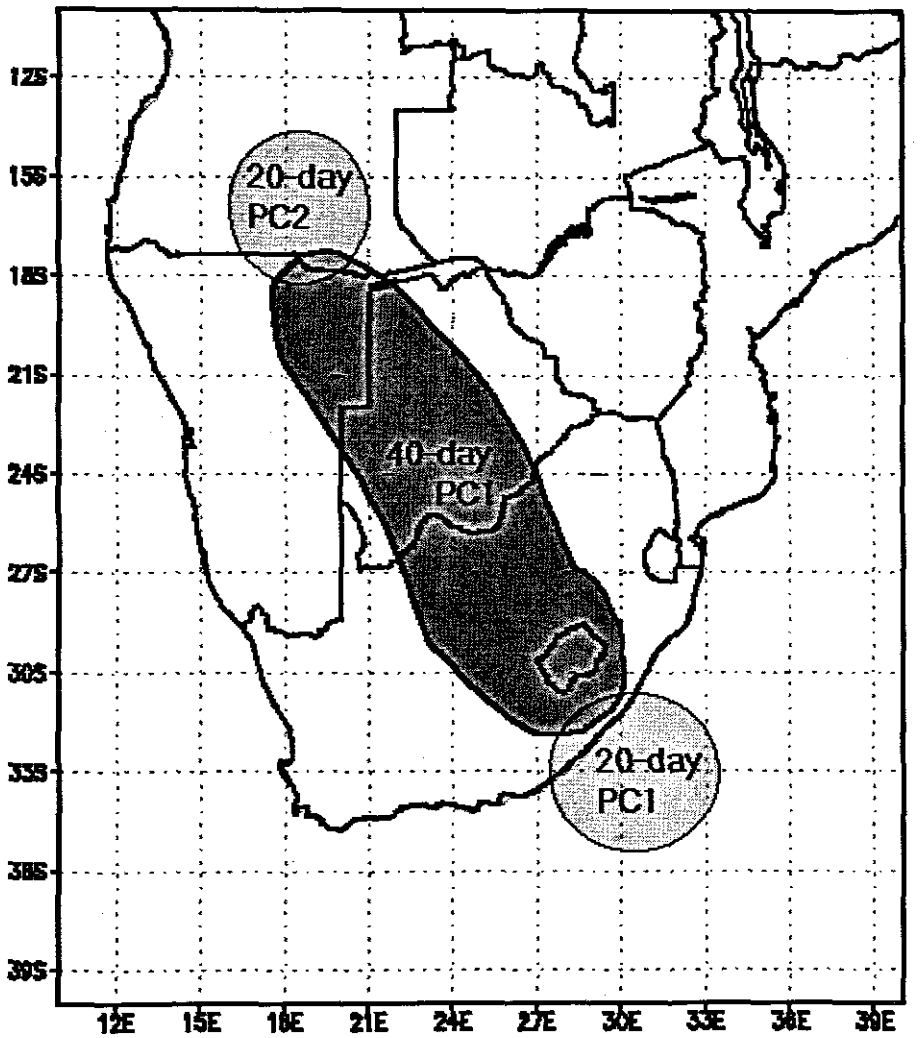

Fig. 3.6. The first mode of the 40-day ISO connects the two 20-day regions, suggesting they elongate and join during the NW cloud band

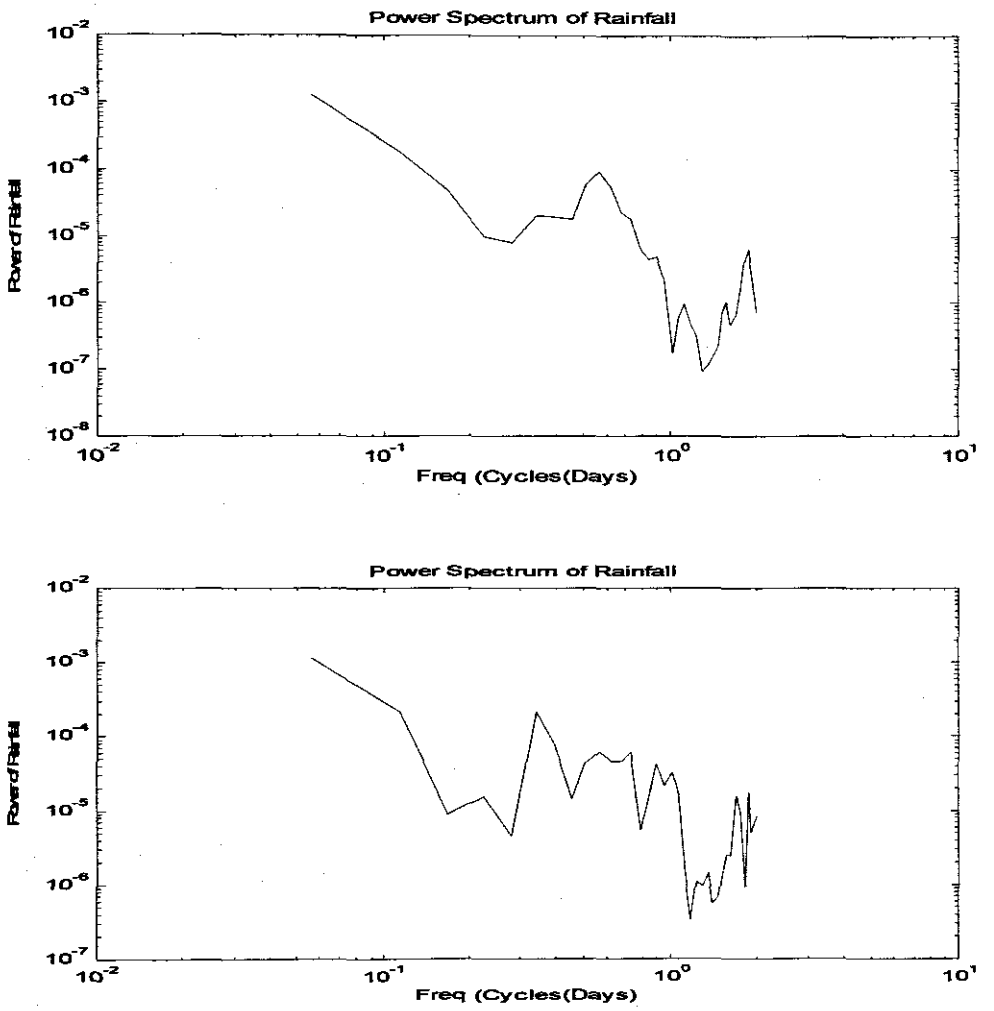

Fig. 3.7 Spectrum over the (a) Kalahari and (b) Agulhas regions

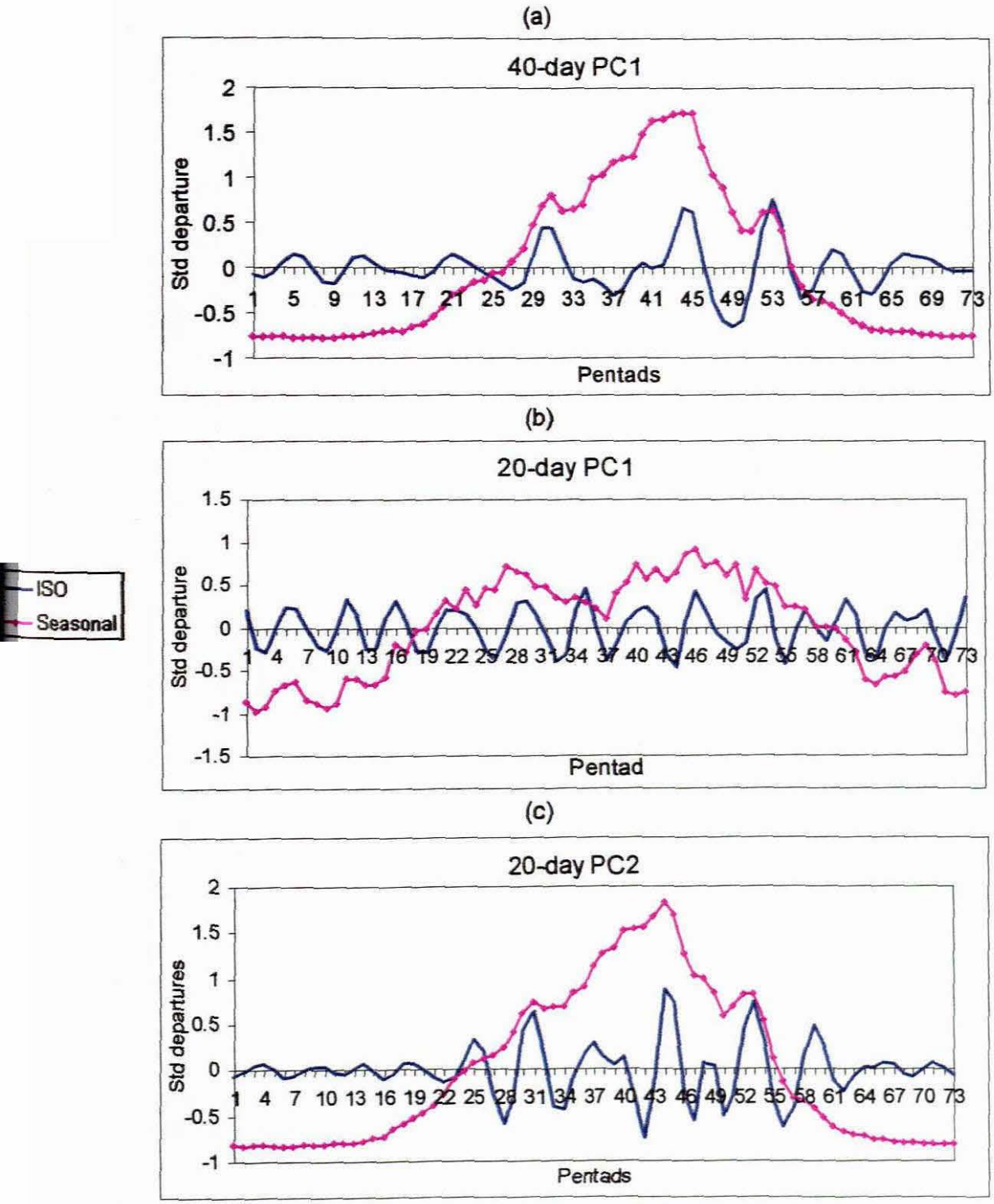

Fig. 3.8 Intraseasonal cycles of rainfall for (a) 40-day Kalahari PC1 (b) 20-day Agulhas PC1 and (c) 20-day Angola PC2 compared against climatology averaged over 20 years (1981-2000). Pentad 1 refers to 30 June to 4 July and pentad 73 refers to 25-29 June.

(a)

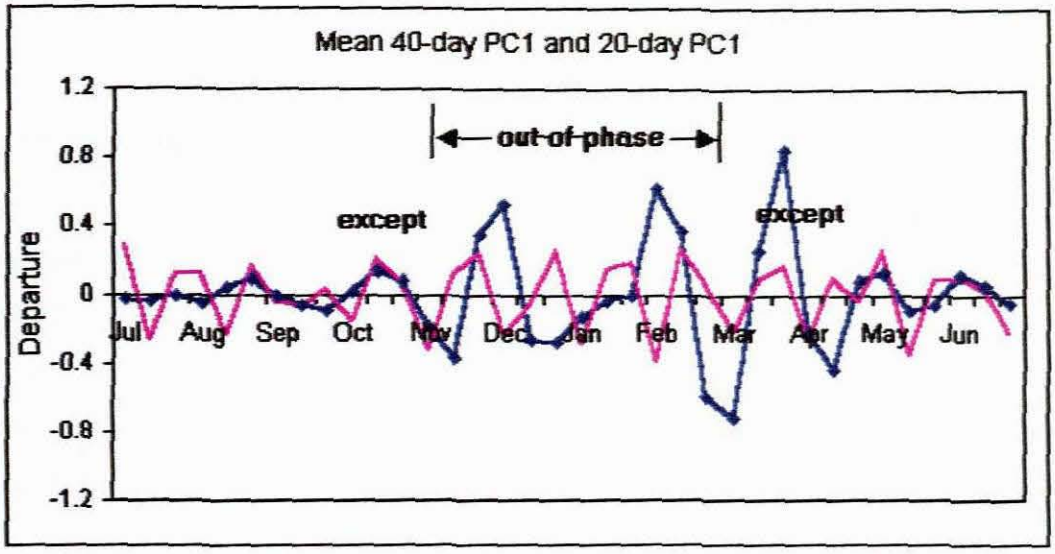

(b)

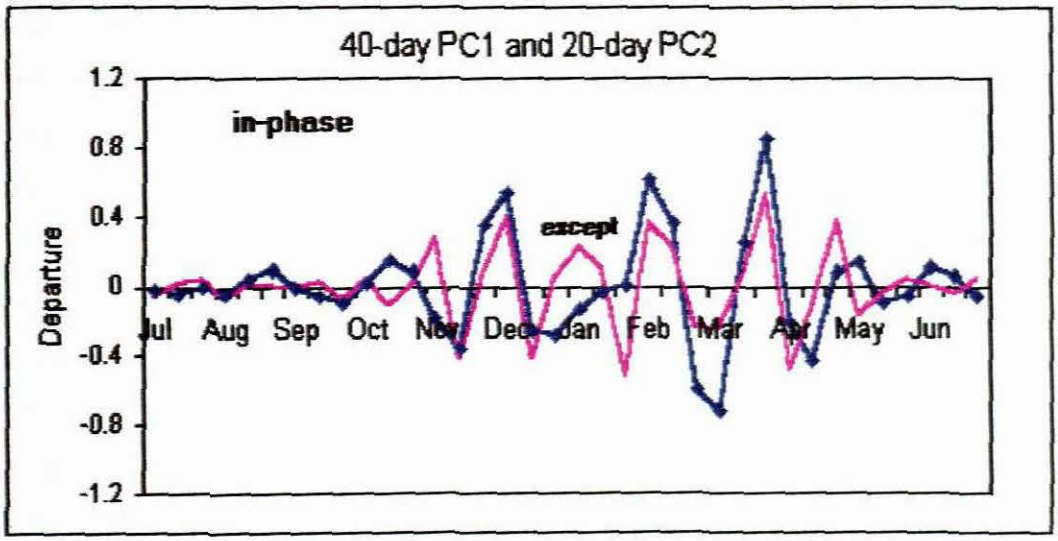

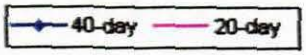

Fig. 3.9 (a) Climatological mean 40-day Kalahari PC1 compared against 20-day Agulhas PC1 and (b) 20-day Angola PC2.

Chapter 4

CHARACTERIZATION OF VEGETATION OVER SOUTHERN AFRICA

4.0 Introduction

Whereas, many studies have sought to characterize rainfall variability over southern Africa, little research has been done on the spatio-temporal variability of vegetation. Detailed spatial coverage of the presence and condition of vegetation has been provided by satellite indicators such as NDVI, leaf area index (LAI), fraction of vegetation cover (FVC), fraction of absorbed photosynthetically active radiation (FAPAR) and directional albedos. NDVI is commonly preferred because it provides a comprehensive dataset to represent vegetation responses to climatic effects. It is also an effective indicator of climate variability particularly in the semi arid regions (Davenport and Nicholson, 1993). The NDVI has also been related to net primary production as it exhibits a strong correlation (r=0.82) with annual maize yield over southern Africa (Jury *et al.*, 1997a) and is useful for crop and drought monitoring.

Whilst NDVI fluctuations have been related to vegetation density, photosynthetic activity and agricultural activity (e.g. Tucker and Sellers, 1986; Gutmann, 1990), intraseasonal oscillations of vegetation are not well understood. Previous studies in many regions have used NDVI data at monthly resolution which is too coarse for intraseasonal analysis. This study pioneers research on intraseasonal variability of vegetation over southern Africa using dekadal NDVI and advances the understanding of associated processes.

The objective of this chapter is to establish the spatial and temporal dynamics of vegetation over southern Africa at seasonal, intraseasonal and interannual time scales. The progression of analysis and interpretation follows that of CMAP rainfall in the previous chapter.

4.1 Annual march of NDVI

The phenological evolution of vegetation over southern Africa is analysed in terms of dormancy, growth and senescence. An important use of NDVI images is for comparisons between vegetation condition at different times. The seasonal variation of greenness is shown in Fig. 4.1 from the dry season to the 'green' summer. Evidence of 'greening' in winter is shown for the coastal areas of the Western Cape and the east coast of southern Africa, opposing a drying trend elsewhere. 'Greening' starts to occur along the eastern edge of the Kalahari in October reflecting early summer rainfall systems including the NW cloud bands consistent with Gondwe and Jury (1997) whilst the influence of the zonal ITCZ manifests itself during January and February (Fig. 4.1).

Most natural vegetation over southern Africa exhibits a profound unimodal seasonal cycle shedding off leaves and withering in the long and dry winter/spring and reaching a minimum in late September just prior to the onset of summer rains (Fig. 4.1). The vegetation NDVI rises steadily through the season until it reaches a plateau between February-March. A gradual decline in NDVI occurs due to senescence of vegetation during the dry season whilst rainfall events in the late summer serve to slow the seasonal decline of NDVI.

A comparison between NDVI and potential evaporation shows a strong inverse relationship ($r=-0.92$) such that when NDVI peaks, potential evaporation is at a minimum (Fig. 4.1). Since potential evaporation refers to atmospheric demand for water vapour (Roderick and Farquhar, 2004), it suggests that when vegetation is at its 'brownest' the demand for water vapour is greatest. Rainfall (water supply) is also absent during the spring when vegetation is depleted and desiccating winds are greatest.

An analysis of the annual march of NDVI during 'green' years (1984/85, 1988/89, 1996/97 and 1999/2000) and during 'brown' years (1982/83, 1986/87, 1991/92

and 1997/98) is made and compared against the 20-year mean. The analysis shows that the march for 'brown' years is such that the greening is earlier than the mean by at least two dekads and the seasonal decline is early (Fig. 4.2a). This suggests that the rainfall patterns for 'dry' years favour an early onset and a poor late summer. For the composite of wet years the NDVI is significantly higher than the long term mean especially during December-February (Fig 4.2b). This indicates that good rainfall occurs during DJF and strengthens the view that the NDVI is a good indicator of climate variability. Similarly, Anyamba *et al.* (2002) also demonstrated that during the warm ENSO event of 1997/98, the NDVI was above normal for the early part of the growing season.

4.2 West-east transects

January mean NDVI values are extracted along two transects at 18°S and 27°S. West-east plots show distinct gradients of NDVI with high values in the east (Fig. 4.3). This agrees with observed satellite imagery shown in the figure. Persistently low values (~ 0.1) are observed over the western desert despite variations in rainfall. Hence there is little response to climate west of ??°E.

Along the 27°S transect (Fig. 4.3b), NDVI increases markedly from the central desert to the moist east. A vegetation transition zone along the edge of the Kalahari (Kalahari transition zone) is dynamic; shifting westwards from 26°E to about 23°E during wet years. This suggests that this zone of high year-year variability is very sensitive to rainfall variability and may be linked to seasonal variation of the NW cloud band. In a related study, Tucker *et al.* (1991) demonstrated using NDVI the equatorward retreat of the southern edge of the Sahara during dry years. Several modelling studies have also demonstrated the sensitivity of vegetation transition zones to climate variability (e.g. Charney, 1975; Zeng *et al.*, 1999).

By contrast, NDVI along the 18°S transect remain mostly above 0.3 even in dry years (Fig. 4.3a). NDVI values of up to 0.45 are evident over the northeast of the subcontinent largely due to the proximity of the transect to the deep tropics and the associated ITCZ. Gondwe and Jury (1997) determined that vegetation of the Zambezi Valley region is less sensitive to climate fluctuations than the southern plateau. Davenport and Nicholson (1993) also noted the small year-year variation of NDVI in the more humid forests even when rainfall changes significantly. This strengthens the view that the NDVI-rainfall relationship is more pronounced in the semi-arid regions (where mean annual precipitation is in the range 600-800 mm) than the wetter forests. Of note is that west-east gradients over southern Africa are generally preserved in both wet and dry years because they are controlled by long term mean climate conditions rather than short term fluctuations (Wang *et al,* 2001).

A distinct contrast between the semi-arid southwest and the forests in the northeast is evident. Annually integrated NDVI values are often used in vegetation studies (e.g. Davenport and Nicholson, 1993) and to determine interannual variability (Fig 4.4a,b). The mean annual values range from 2.3 in the southwest to 4.9 for the Zambezi forests for monthly NDVI whilst the annual march shows little variability for the southwest but distinct seasonality over the Zambezi (Fig. 4.4c).

4.3 Seasonal cycles of NDVI

A PCA is carried out on vegetation NDVI at 2.5° spatial resolution for the period 1982-2000 to determine the dominant modes of variability at seasonal time scales. The NDVI are useful for studying vegetation cycles because they provide spatially continuous long-term information whilst PCA is particularly relevant in identifying seasonal patterns of vegetation greening related to seasonal rainfall patterns. Several studies have used this method to analyse NDVI time series (e.g. Anyamba and Eastman, 1996; Young and Anyamba, 1999).

Results for the unrotated component of PCA for standardized unfiltered NDVI are presented. As with the rainfall analysis, only PC1 for vegetation is retained for analysis and discussion. The analysis is done for continental Africa, south of 10°S.

PC1 explains 34% of variance, maximizes in a broad zonal region around 17°S (Fig. 4.5a), and co-locates with the area of maximum loading for CMAP rainfall which also explains 34% of variance (Fig. 3.2a). This finding agrees with a hypothesis of the study (Chapter 1) and suggests strong coupling between seasonal rainfall and vegetation greenness especially in the Zambezi/ITCZ. As with rainfall, a local maximum is also loaded in the direction of KwaZulu-Natal. The apparent strong gradients observed near the coasts are an artifact of the contour analysis.

Time scores for NDVI show distinct cycles which peak in the late summer (Fig 4.5b) whilst the wavelet transform of vegetation NDVI shows the major period of oscillation over the respective loading areas as the annual cycle at 36 dekads (Fig. 4.5c).

4.4 Intraseasonal oscillations of NDVI

Satellite vegetation NDVI is filtered using wavelet analysis to retain cycles between 20-70 days. Since the data are at dekadal resolution, cycles shorter than twenty days cannot be determined. A PCA is also performed on filtered data to obtain intraseasonal characteristics. The first unrotated mode is retained for discussion.

PC1 is positively loaded in a NW-SE band in the central interior extending through the western Zambezi toward central South Africa on the eastern edge of the Kalahari (Fig. 4.6a). Gondwe and Jury (1997) determined a similar loading

pattern and high standard deviations over the central plateau (Botswana). The loading pattern is co-located with the region of maximum loading for the 40-day rainfall oscillation except for a slight truncation on the southern flank (Fig. 3.3a) which may be due to the contour analysis. This is an important result and most of the subsequent analysis hinges on this co-location.

Intraseasonal PC1 accounts for 12% of variance across the domain and reflects the fundamental role of the NW cloud band in this region in regulating variability of vegetation greening. NW cloud bands are a major source of rainfall for this region (Harrison, 1984).

Time scores for vegetation do not exhibit seasonally confined pulsing of intraseasonal oscillations unlike rainfall PC1. Significantly high amplitudes are evident for the wet summers of 1989, 1994 and 2000 (Fig. 4.6b). High NDVI PC1 amplitudes during the dry season may be an artifact of standardized data due to low values in winter and spring. Major oscillations are evident in the modulus spectrum with cycles between 25-50 days (Fig. 4.6c).

4.5 Seasonal mean ISO

Seasonally averaged intraseasonal oscillations for vegetation and rainfall are analyzed for climatological features over the twenty-year period. There are two major oscillations during the summer rainfall period, one peaking in December/January and the other in April (Fig. 4.7a). The mean ISO for 'green' years shows shorter cycles than for 'brown' years which become quiet in the mid-season (Fig. 4.7b).

The NDVI oscillations are not confined to summer but continue through the year, with a distinct dry season minimum in September-October before the onset of summer rains (Fig. 4.7a,b). This minimum is in phase with the seasonal minimum which also occurs at this time (Fig. 4.8). Superimposed oscillations

and seasonal mean plots of vegetation show that the ISO are phase lagged to the seasonal cycle, particularly at the onset of the rainfall season in October (Fig. 4.8).

It can be concluded from the results that the vegetation oscillations are less well defined than the rainfall oscillations particularly in February-March which is the peak rainfall period. This is because of 'biotic memory' and suggests that NDVI does not diminish rapidly in the absence of rainfall and therefore the oscillations are of lower magnitude. Wang *et al.* (2001) established that NDVI is better correlated with running mean averaged precipitation than short-term rainfall events. It is a critical finding of this analysis that intraseasonal oscillations of NDVI exist over southern Africa.

4.6 Summary

The spatial distribution and temporal variability of vegetation over southern Africa have been studied at seasonal, intraseasonal and interannual time scales. Important findings of this chapter are: -

(i) Strong west-east gradients of vegetation greenness are evident over the subcontinent and are consistent with mean rainfall.

(ii) The regional vegetation exhibits a unimodal cycle reaching a plateau between February-March and a minimum in September before the onset of the summer rains.

(iii) The relationship between potential evaporation and NDVI is analyzed with respect to the average cycle, for "green" and "brown" years. This empirical analysis shows clearly that years of poor rainfall have an earlier start to the rainy season and deficient rainfall from December to January.

(iv) The Kalahari 'transition zone' is dynamic, locating farther west during wet summers but retreating eastwards in drier years. This zone reflects the dominant influence of NW cloud bands and rainfall introduces the most

variation in NDVI and hence primary production. There is little response to climate west of 20°E.

(v) The seasonal vegetation mode co-locates with the rainfall mode suggesting the dominance of the ITCZ at seasonal timescales.

(vi) Intraseasonal oscillations in vegetation exist. The ISO maximizes at about 40 days in a NW-SE band extending from western Zambezi through to central South Africa along the eastern edge of the Kalahari. The spatial loadings also co-locate with rainfall loadings despite the different data and independent analysis.

(vii) Intraseasonal oscillations of vegetation are not as seasonally distinct as their rainfall counterparts. This is partly because of responses during winter/spring and to the continuous nature of the data.

(viii) Climatologically, three to six 'green' spells alternate with 'brown' spells at nearly monthly intervals during summer over southern Africa. Dry summers tend to have longer ISOs than wet summers.

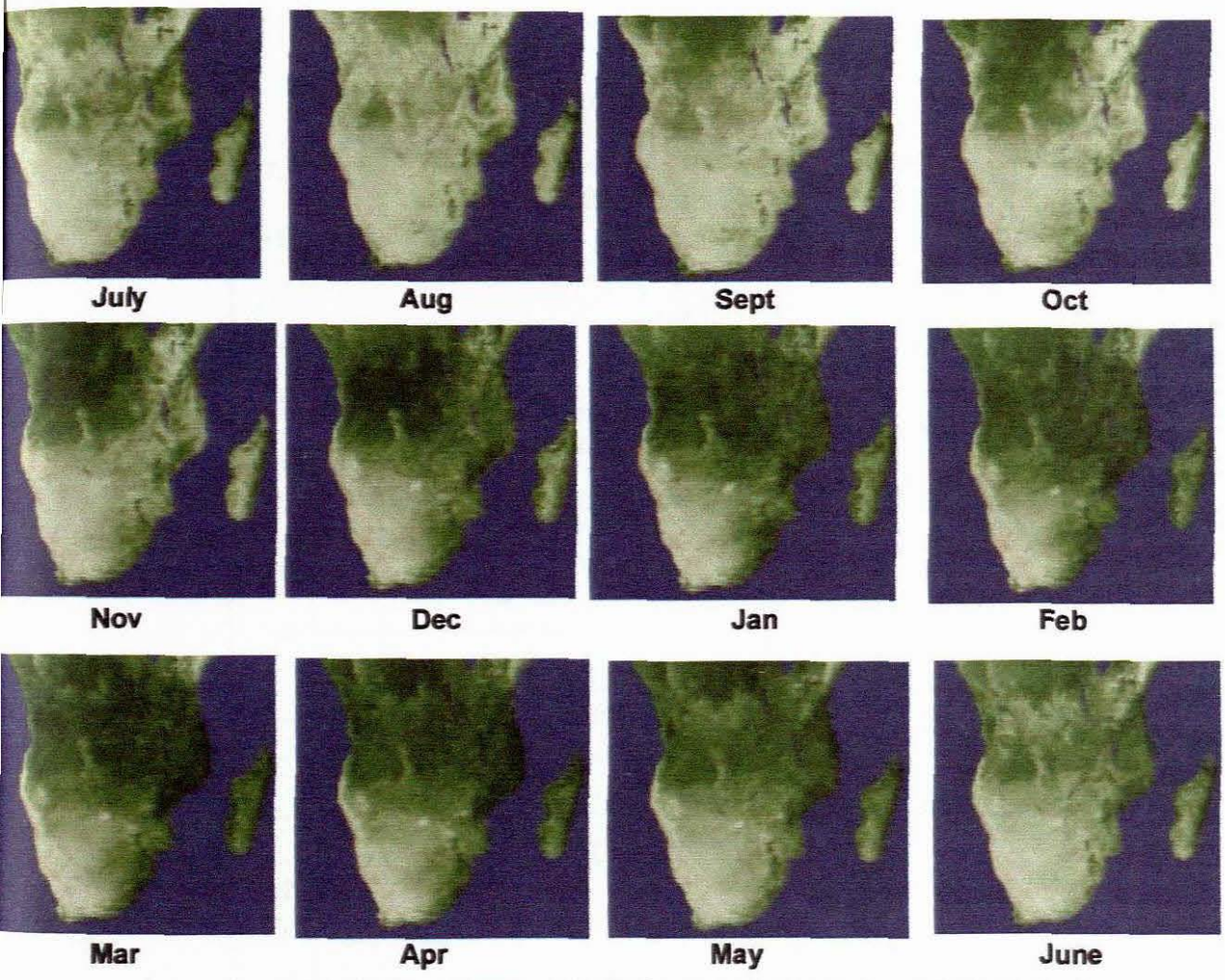

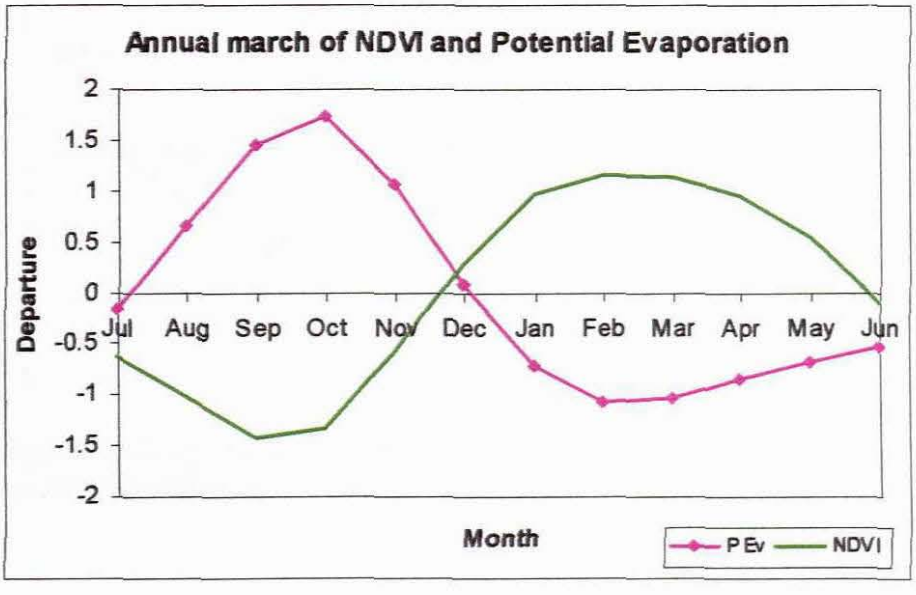

Fig. 4.1 Mean monthly NDVI images over southern Africa (1981-2000). (Source: NASA -Goddard Space Flight Center Scientific Visualisation Studio). The mean annual march of satellite NDVI and NCEP model potential evaporation are shown below.

(a)

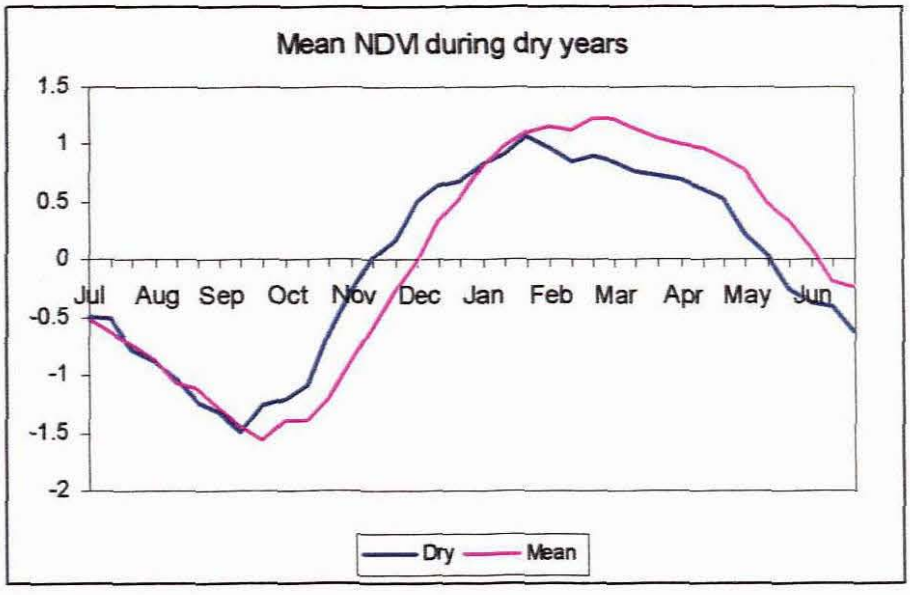

(b)

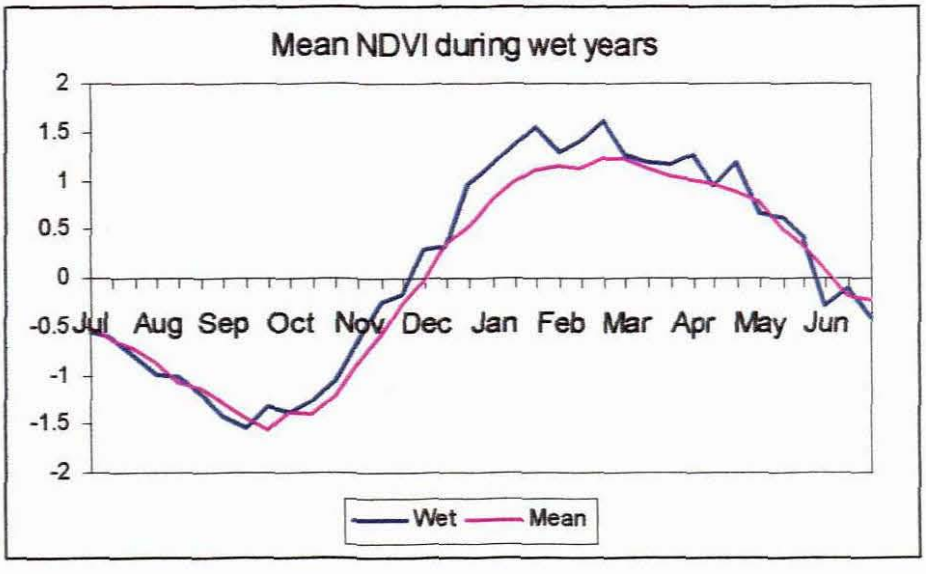

Fig. 4.2 Mean NDVI during (a) 'brown' years and (b) 'green' years compared against the 20-year mean.

(a)

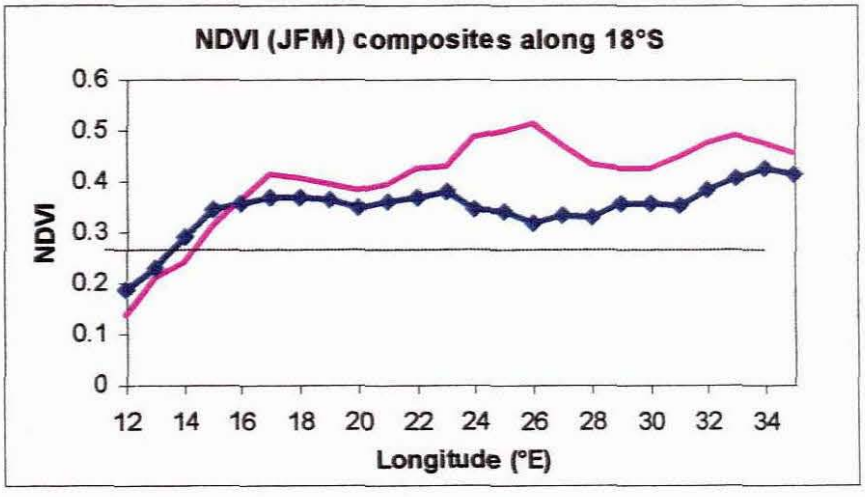

(b)

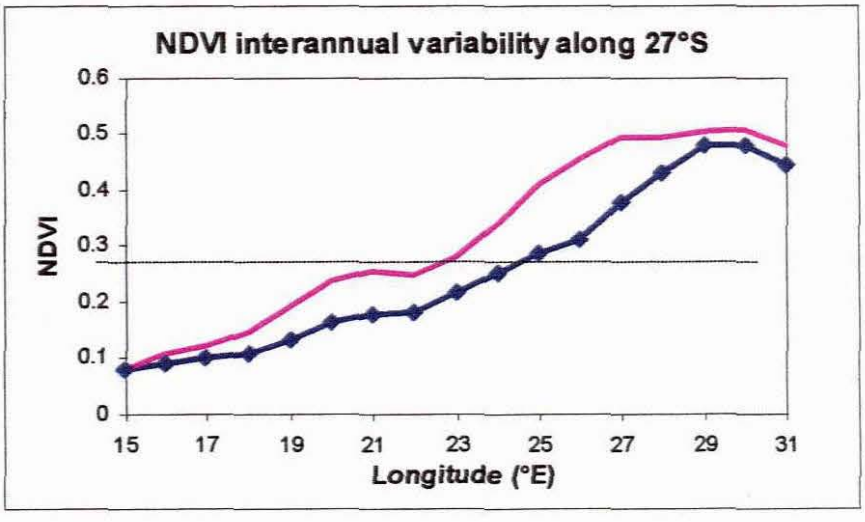

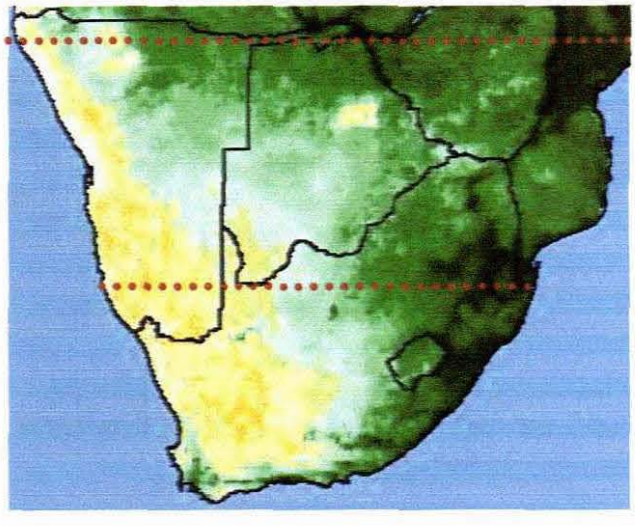

Fig. 4.3 January mean NDVI composite values for 'green' years (1986, 1989,1994, 1997 and 2000) and 'brown' years (1983, 1987, 1992 and 1998) along the18°S and 27°S west-east transects. The corresponding satellite image for 'green' years is shown in the lower panel.

(a)

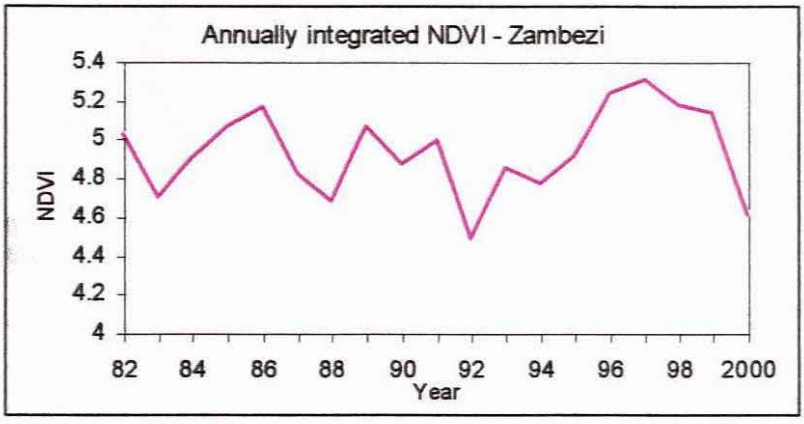

(b)

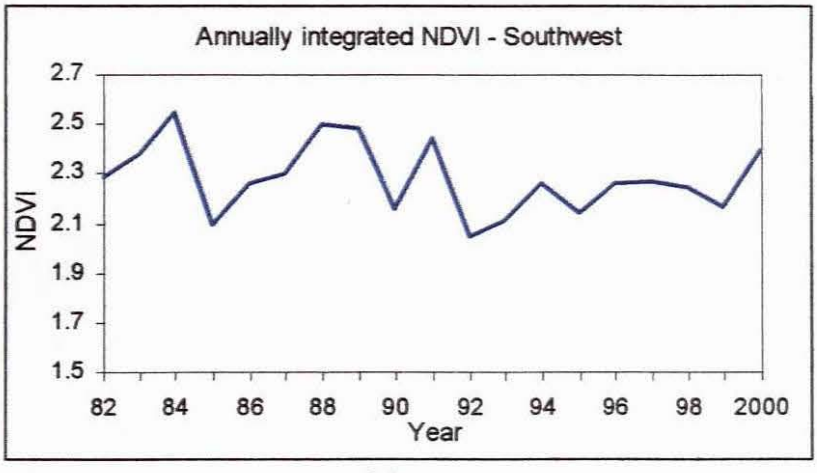

(c)

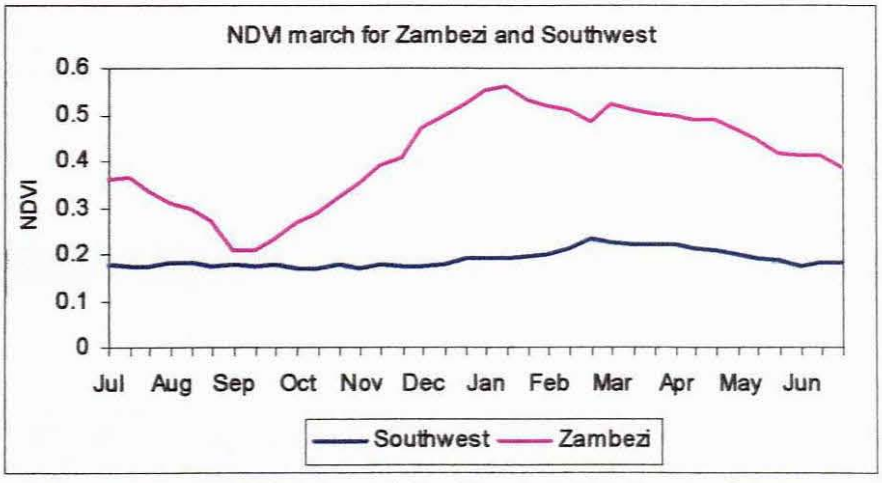

Fig. 4.4 Annually integrated NDVI for (a) the Zambezi Valley and (b) the Southwest. The mean march is shown in (c).

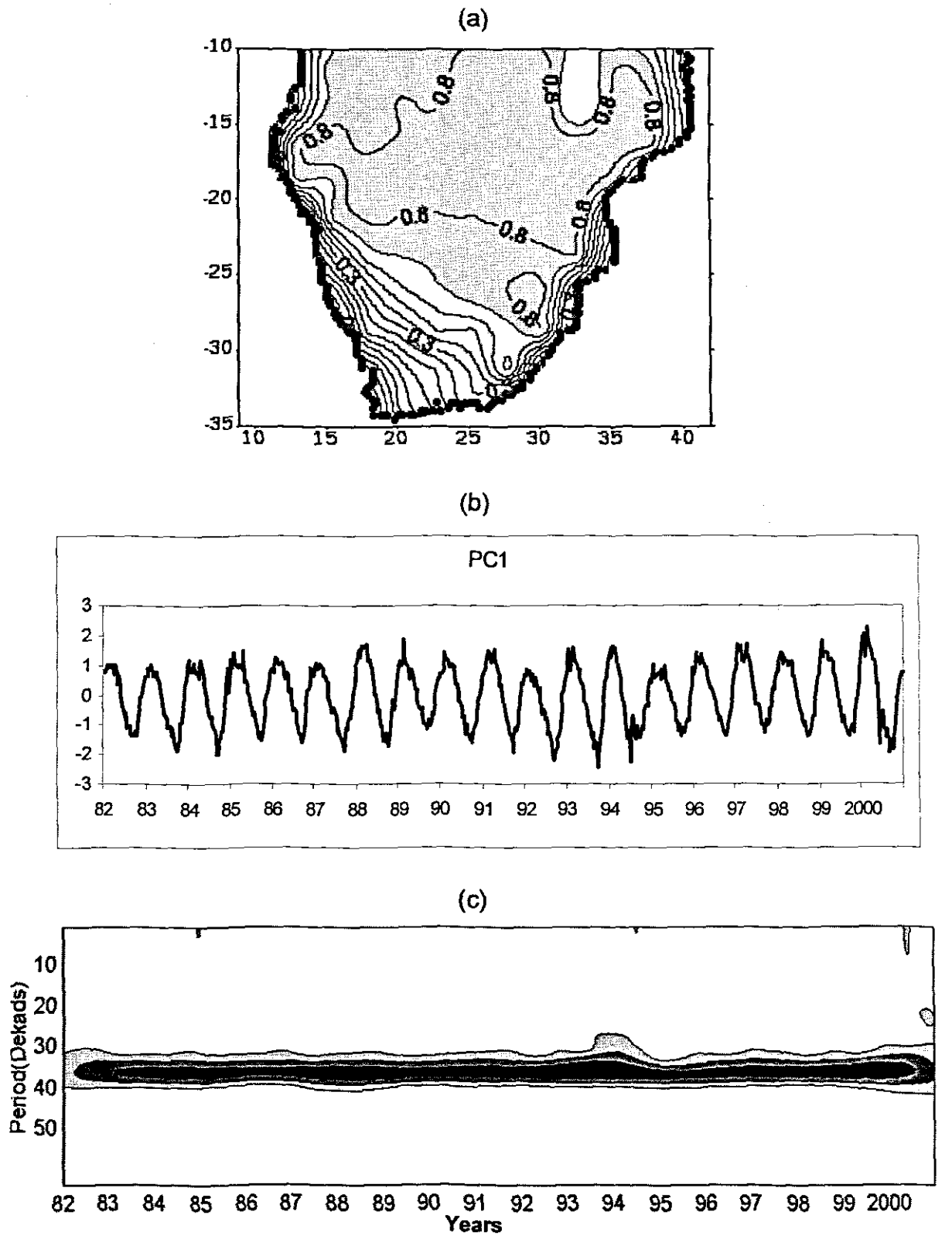

Fig. 4.5 (a) Spatial loading and (b) the associated time scores and (c) the modulus spectrum for seasonal vegetation NDVI (unfiltered and unrotated) for PC1 accounting for 34% of total variance.

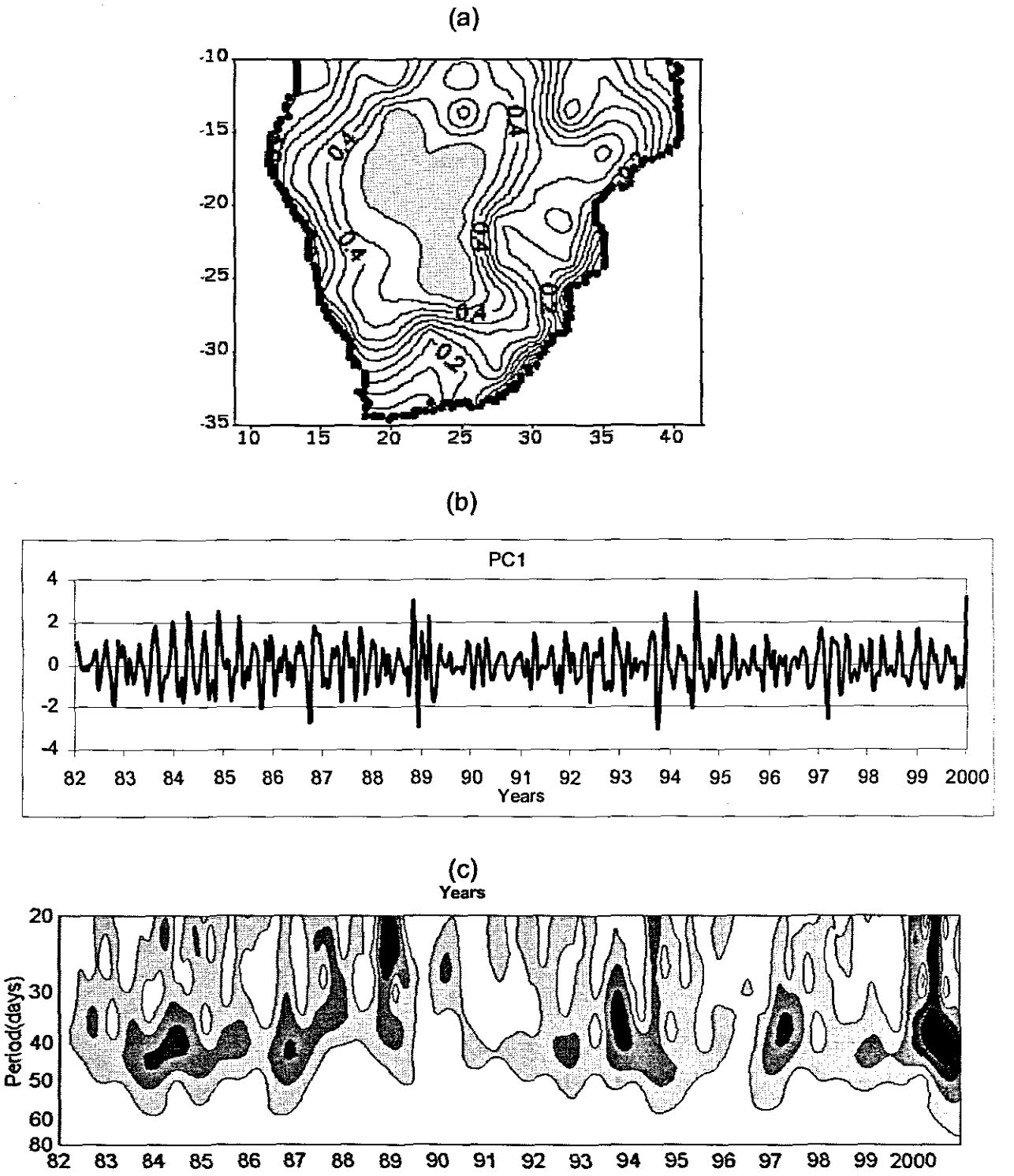

Fig. 4.6. (a) Spatial loading (b) the associated time scores and (c) the modulus spectrum for Intra-seasonal vegetation NDVI (filtered to retain cycles between 20-70 days and unrotated) for PC1.

(a)

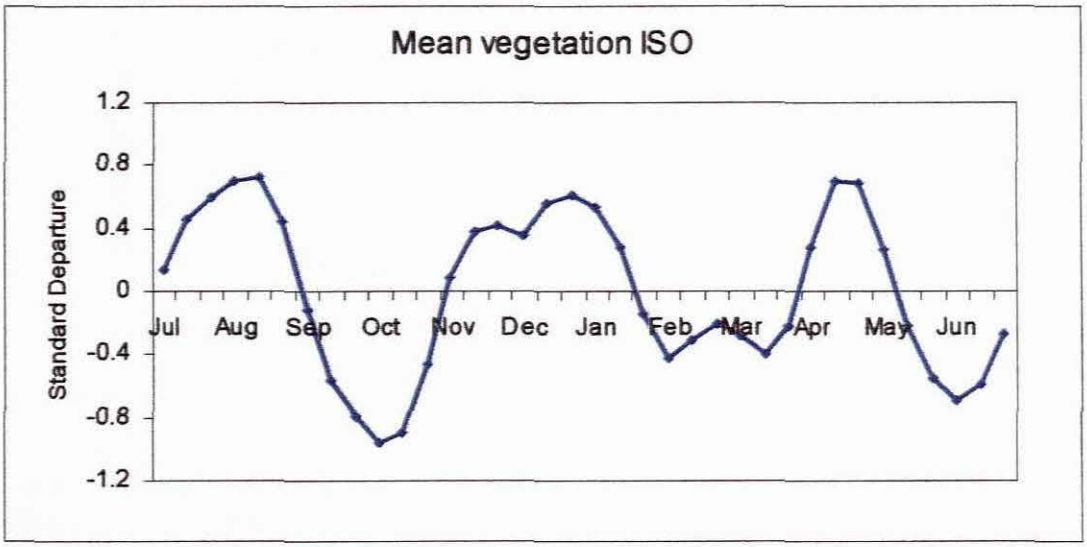

(b)

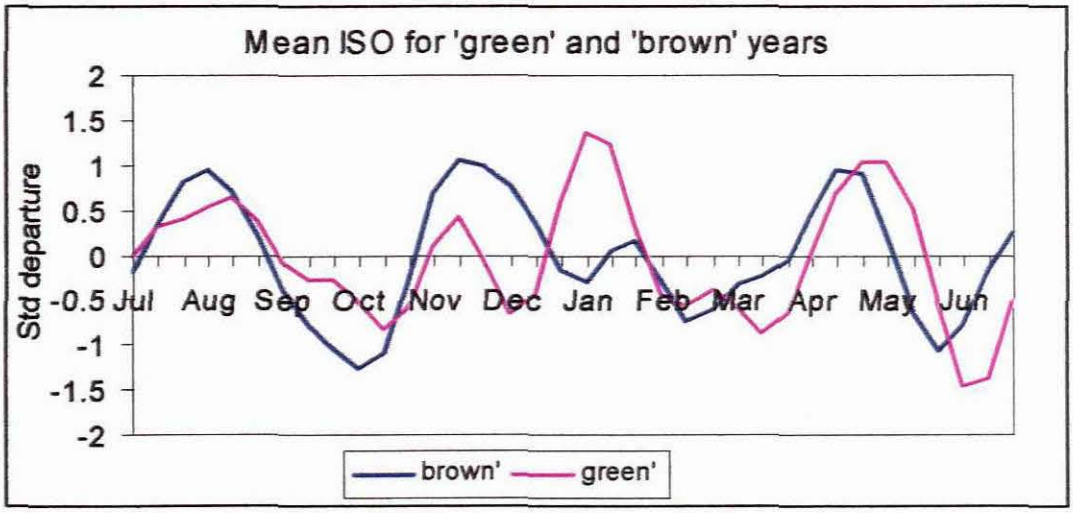

Fig. 4.7 (a) Seasonal mean ISO for NDVI over the Kalahari PC1 region and (b) mean ISO for 'green' and 'brown' years averaged over nineteen years (1982 - 2000).

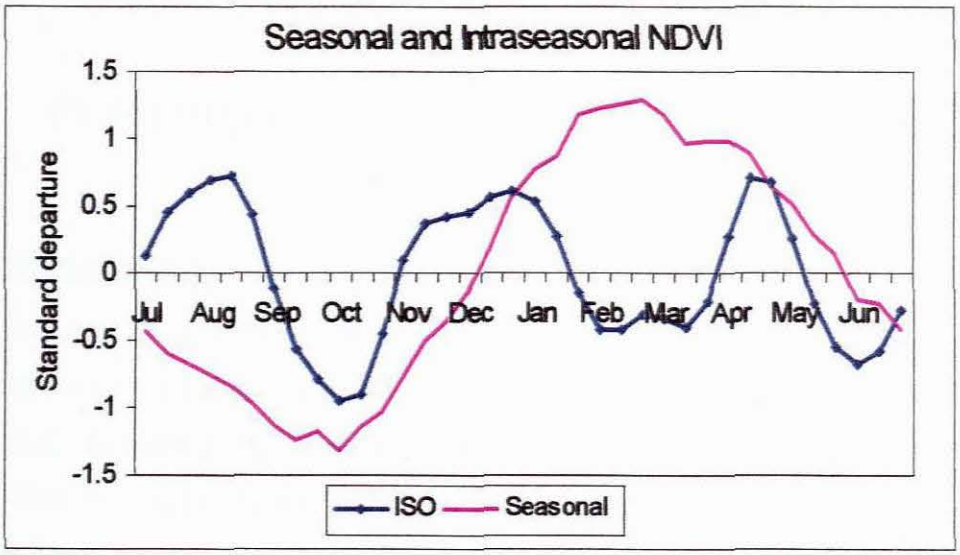

Fig. 4.8 Intraseasonal cycles of NDVI for PC1 compared against climatology averaged over 20 years (1982-2000)

Chapter 5

EVAPOTRANSPIRATION-RELATED FLUXES OVER SOUTHERN AFRICA

5.0 Introduction

The preceding chapters have characterized rainfall and vegetation variability over southern Africa. Before the correspondence between NDVI and rainfall is tested, this chapter presents the climatology and variability of evapotranspiration-related fluxes over the subcontinent. This is essential for understanding the linkages and feedback mechanisms between the land surface and rainfall events.

Boundary layer fluxes have not been studied extensively over southern Africa. However, considerable research effort has focused on latent and sensible heat fluxes and convection above the adjacent oceans and the Agulhas current system (e.g. Walker and Mey, 1988; Jury and Reason, 1989; Jury *et al.*, 1997b; Rouault *et al.*, 2003). It is thought that the fluxes above the Agulhas have significant effect on cloud formation and rainfall events particularly over the east-coast of South Africa (e.g. 20-day PC1).

Solar radiation is a major 'driver' of the climate system. A fraction of solar radiation incident on the earth's surface is reflected back to space whilst the remainder is either absorbed and partitioned into sensible heat and latent heat or emitted as outgoing longwave radiation. Partitioning of incident radiation depends largely on the surface albedo, aerodynamic roughness and soil moisture availability, which are influenced by vegetation cover (Bounoua *et al.*, 2000). This affects boundary layer height and the vertical transfer of heat and moisture in the lower atmosphere.

5.1 Evaporative losses

In general, there is a west-east variation of evapotranspiration over southern Africa (Fig. 1.2a). This pattern agrees with the spatial variation of rainfall. Mean summer evaporation over southern Africa is high over the Congo rainforests and the southwest Indian Ocean (Fig. 5.1). The Congo forest basin is a major source of evaporation whilst the warm Agulhas current is dominant over the adjacent Indian Ocean. Topographic 'hot spots' are evident to the south and north of Madagascar. Very little evaporation occurs over the west coast because of the desiccating effects of the cold Benguela current and the south Atlantic anticyclone.

Potential evaporation is often used as a measure of the amount of water that could be evaporated were it available. Since it is a function of surface and air temperatures, insolation, and wind speed, potential evaporation is uniformly high over the Kalahari and Namib Deserts (Fig. 5.2a). The mean seasonal march of potential evaporation over southern Africa has been discussed and compared with rainfall and NDVI in the preceding chapters.

A composite of wet years minus dry years for potential evaporation shows high variability in the Kalahari 'transition zone' reflecting lower potential evaporation (lower demand) during wet years in this region (Fig. 5.2b). It is remarkable that the eastern edge of the Kalahari is also the loading region for intraseasonal oscillations of rainfall and vegetation and is thus a 'center of action' for variability on several time scales.

5.2 Latent heat flux

Latent heat is the heat absorbed for change of state during the processes of evaporation and melting, but released as sensible heat during condensation and freezing. Since latent heat flux is associated with phase changes of moisture, it can be used as a good estimate of available moisture or vertical moisture flux.

NCEP reanalysis latent heat climatology shows low values over the southwestern desert region of the subcontinent (Fig. 5.3a) whilst high values over the Zambezi region co-locate with mean rainfall patterns. In general, the mean pattern agrees with that for evaporation (Fig. 5.1).

The influence of the Agulhas Current on latent heat fluxes is evident over the adjacent Indian Ocean and the retroflection region of the southern Ocean (Fig. 5.3a). Previous studies have determined that heat fluxes into the atmosphere above the warm Agulhas current have significant influence on the regional climate (e.g. Jury *et al.,* 1993; Crimp *et al.,*1998; Rouault *et al.*, 2003).

The standard deviation of interannual variability of latent heat flux shows significantly high values (> 15 W m^{-2}) along the eastern edge of the Kalahari (Fig. 5.3b), and may be related to year-year variability of tropical-temperate troughs and the attendant NW cloud bands. Regions of high variability are also evident over the ocean adjacent to the east and south coasts. The strong signal from the ocean reflects the influence of the Agulhas current on heat and moisture fluxes into the overlying atmosphere.

5.2.1 Seasonal cycles

A PCA is done on standardised and unfiltered NCEP model-estimated latent heat flux data at 2.5° resolution. The spatial loadings for seasonal cycles of latent heat flux show similar patterns as for rainfall and vegetation NDVI reflecting the dominance of the ITCZ as a climate factor over southern Africa (Fig. 5.4a). Terrestrial signcal dominates the annual cycle. Strong gradients near the coasts are artifacts of the contour analysis. The seasonal mode accounts for 38% of variance across the domain of study.

The time scores show seasonal cycles of NCEP latent heat flux similar to satellite NDVI and CMAP rainfall peaking in the austral summer and reaching a minimum

in winter (Fig. 5.4b). An increasing trend of latent heat flux from the early 1980s to the turn of the century is evident and could point to global warming.

The modulus spectrum shows maximum energy at 36 dekads corresponding with the annual cycle (Fig. 5.4c).

5.2.2 Intraseasonal oscillations

A PCA of intraseasonal latent heat flux shows three significant modes according to scree test criteria loaded over marine and terrestrial regions.

Table 5.1 NCEP model latent heat flux PCA modes and their location

PC	Centers of action	Variance explained
1	Western Agulhas	16%
2	Kalahari	13%
3	Eastern Agulhas	12%

PC1 is loaded over the western Agulhas south of Cape Town (Fig. 5.5a) whilst PC3 maximizes over the eastern Agulhas of Durban (Fig. 5.7a). These modes further demonstrate the influence of the Agulhas current system on evaporation and latent heat fluxes. The Agulhas current turns to become the Agulhas return current in the PC1 region and has significant influence on passing cyclones (Majodina and Jury, 1996). Apart from the contouring package, the steep gradients along the east coast may be a result of topographical factors. Cold and unsaturated westerly winds persistently induce heat losses from the ocean surface into the overlying atmosphere (Walker and Mey, 1988). This mode is also related to easterly winds associated with the south Atlantic anticyclone in summer. The mean wind is much higher in the marine environment due to lower friction, so the variability is greater too. Consequently, time scores for Agulhas modes show high frequency oscillations occurring throughout the year (Figs. 5.5b and 5.7b).

Rainfall variability over eastern South Africa has been linked to variability of the Agulhas current system in a number of studies (e.g. Jury *et al.*, 1993; Mason, 1995). The large heat fluxes from the Agulhas current may have significant influence on atmospheric circulation and weather over southern Africa (Reason, 2001) when onshore (southerly) winds occur.

Spatial loadings for PC2 maximize in a zone with a NW-SE orientation, extending from the Kalahari to the Karoo of South Africa (Fig. 5.6a). This mode coincides with the sensible heat flux maximum but is displaced westwards of the rainfall and NDVI modes of the 40-day oscillation. Time scores of latent heat flux for the terrestrial mode (PC2) exhibit some seasonality with regular pulsing during the austral summer, which become quiet in winter (Figs. 5.6b). The mode reflects the influence of the land surface and the overlying vegetation on evapotranspiration and latent heat flux.

The modulus spectra for PC1, PC2 and PC3 show that the intraseasonal oscillations are of high frequency with maximum energy between 20-30 days. Results from this analysis and from the rainfall analysis in Chapter 3 agree that the terrestrial mode is more seasonal than the marine modes which exhibit randomness and continue throughout the year.

5.3 Surface soil moisture

As expected, surface soil moisture fraction climatology from NCEP reanalysis shows high values of soil moisture in the northeast (Zambezi) and very dry soils in the southwest desert region (Fig. 5.8). A composite of 'green' years minus 'brown' years shows high variability of surface soil moisture in a NW-SE axis consistent with the PC2 of latent heat flux (Fig. 5.6a). Since vegetation growth and senescence are largely a function of soil moisture, it suggests that vegetation is highly variable in this region in concert with soil moisture. This agrees with the results of the vegetation analysis in Chapter 4. In a related

study over semi-arid Botswana, Farrar *et al.* (1994) suggested that vegetation growth is enhanced by exogenous soil water originating from the surrounding ground as runoff.

5.4 Specific Humidity

Boundary layer (850 hPa) specific humidity over southern Africa follows similar patterns as rainfall and other meteorological variables discussed in this study. The mean summer monthly specific humidity over southern Africa is characterised by high values over the deep tropics (Fig. 5.9). Spatial gradients of specific humidity from west to east are evident over the southern regions. This agrees with a W-E vertical cross section of mean specific humidity shown earlier (Fig. 1.4b). A sharp gradient and slope at the edge of the Kalahari is evident.

A composite of 'green' years minus 'brown' years shows significant difference over the eastern edge of the Kalahari extending from eastern Namibia through to central South Africa (Fig. 5.10a). The vertical section reflects a shift of boundary layer moisture westwards during wet years (Fig. 5.10b) suggesting that tropical-temperate troughs and the attendant NW cloud bands locate farther west during wet years. Most importantly, the signal is strongest at the surface and decreases rapidly with height.

5.5 Summary

An analysis of evapotranspiration related surface and boundary layer fluxes has been presented in this chapter. The agreement between different NCEP model-estimated flux patterns and satellite-derived rainfall and vegetation is striking. Fundamental results of this chapter are: -

(i) The mean distribution of moisture and heat fluxes is strongly related to the observed patterns of vegetation and rainfall across southern Africa suggesting strong local coupling.

(ii) Despite a focus on the land surface, the dominance of the Agulhas current system in modulating variability of evaporation-related fluxes has been demonstrated.

(iii) The seasonal mode of variability for latent heat flux is loaded over the Zambezi valley with an annual cycle similar to those for rainfall and NDVI.

(iv) Intraseasonal modes of variability for latent heat flux include two marine and one terrestrial mode. As with rainfall, the marine oscillations continue throughout the year whilst the terrestrial mode becomes 'quiet' in the intervening dry season.

(v) The 'center of action' for vegetation and rainfall along the eastern edge of the Kalahari shifts westwards during wet years suggesting a corresponding shift of the NW cloud band.

The correspondence between rainfall and vegetation at intraseasonal/event timescales is tested in the next chapter.

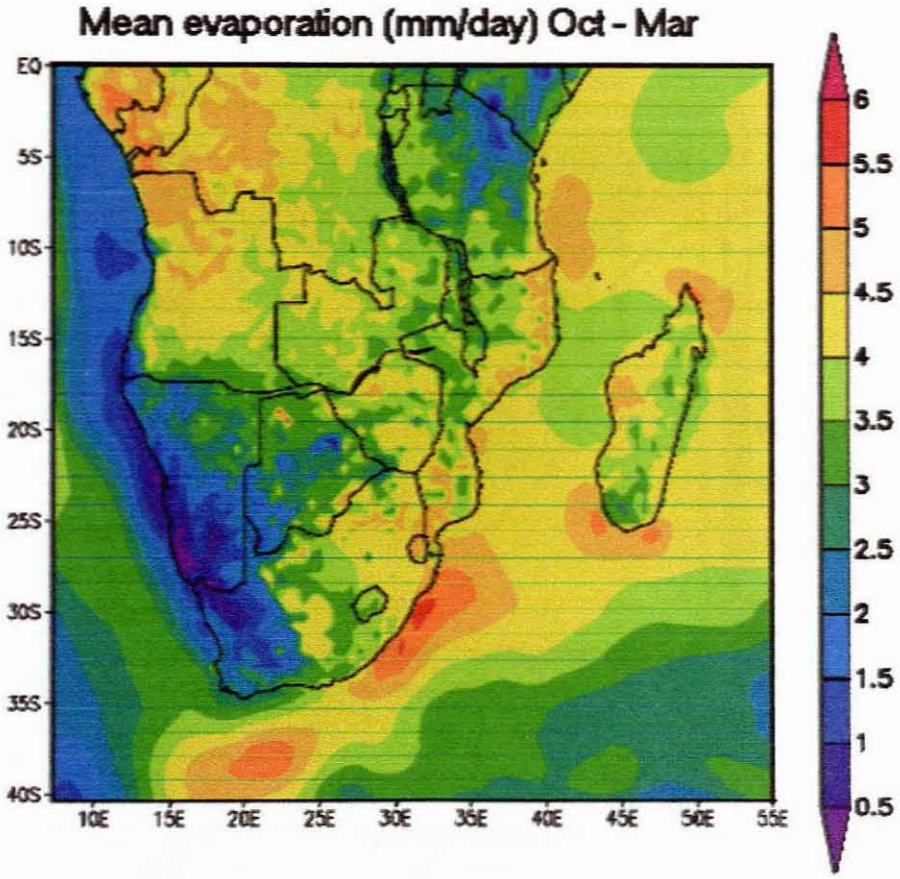

Fig. 5.1 RegCM3 model mean summer evaporation over Africa south of 10°S.

(a)

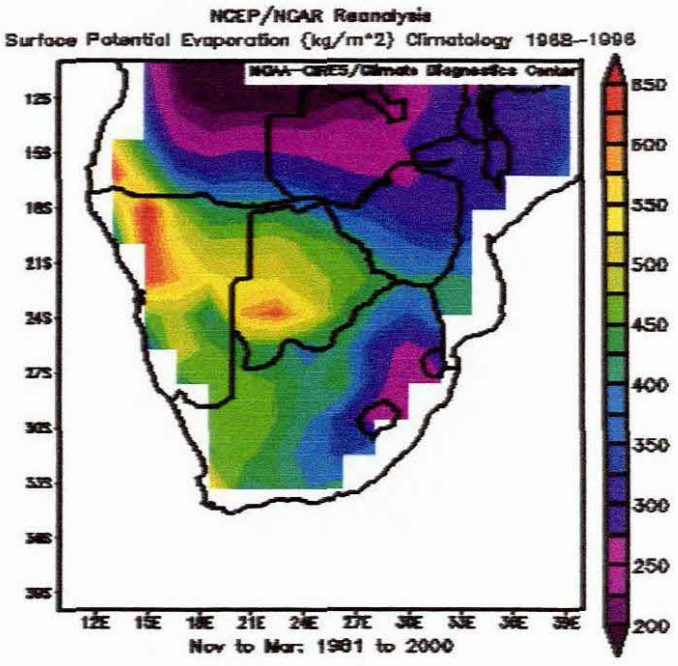

(b)

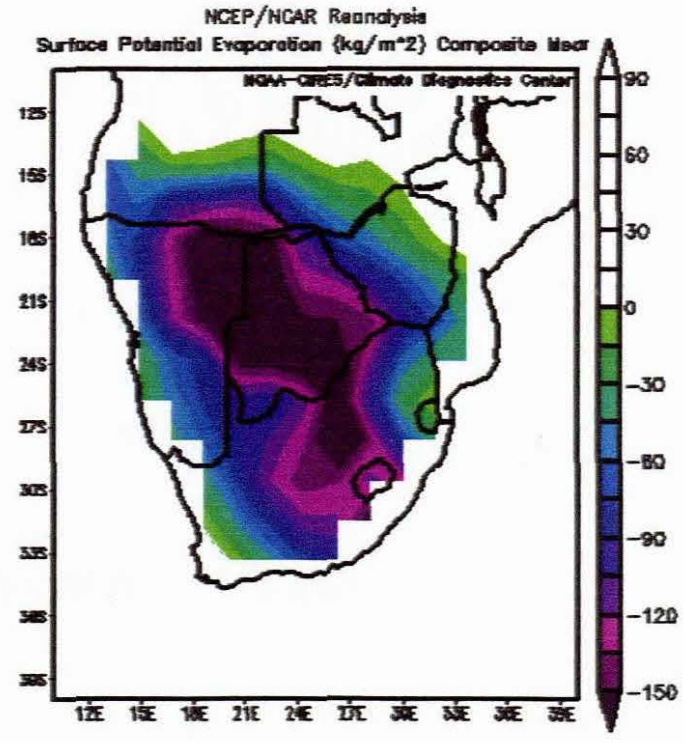

Fig. 5.2 (a) Surface NCEP model potential evaporation climatology over southern Africa and (b) a composite for 'green' minus 'brown' years.

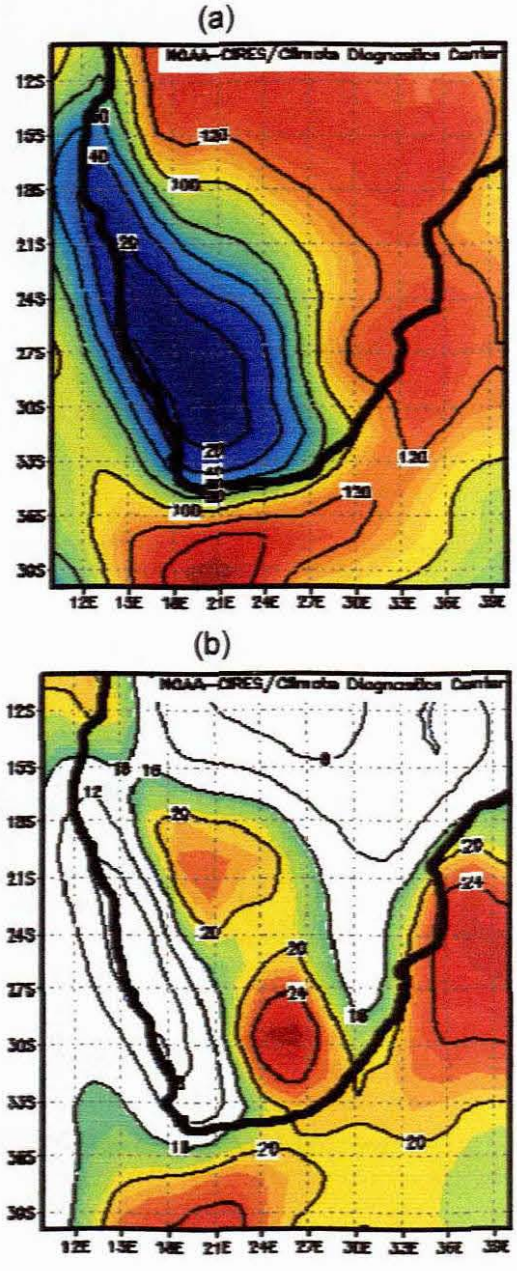

Fig. 5.3 (a) DJF NCEP model latent heat flux climatology (1968-1996) and (b) the interannual standard deviation (1982-2000)

(a)

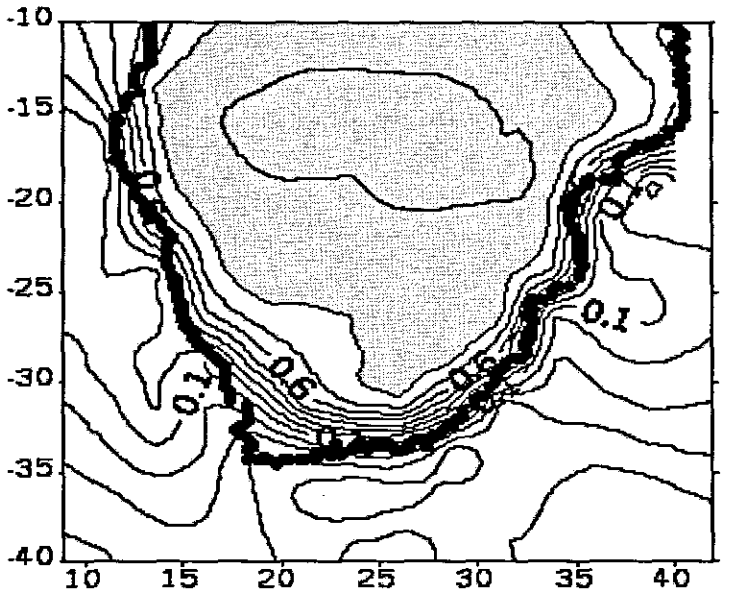

(b)

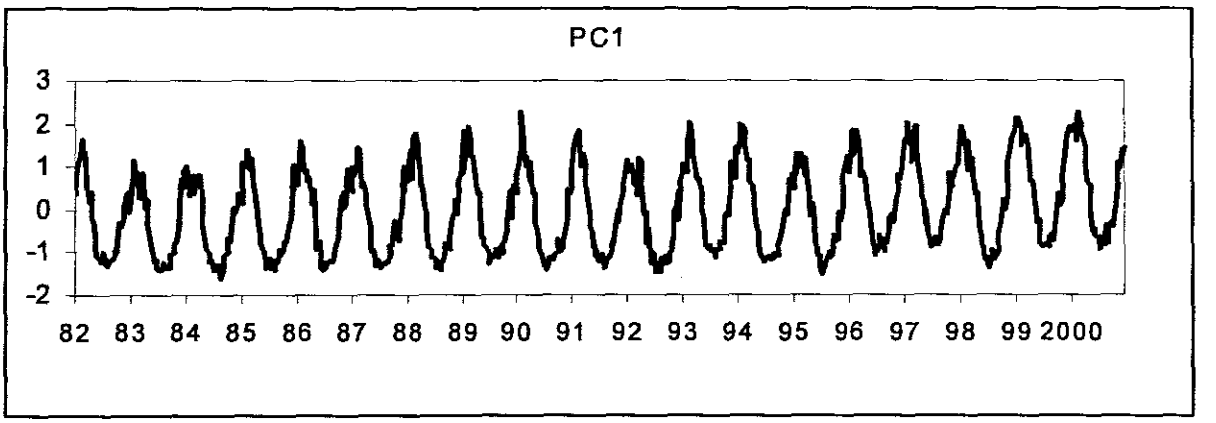

(c)

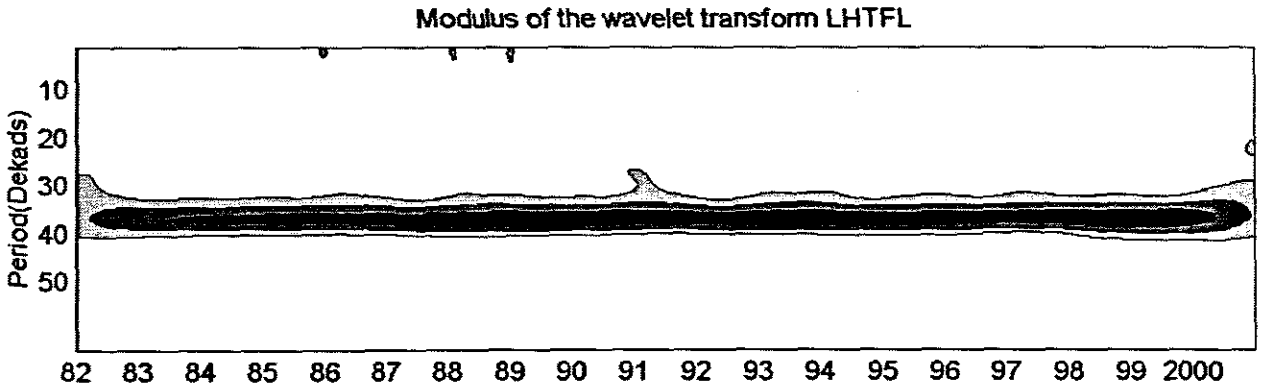

Fig. 5.4 (a) Spatial loadings (b) time scores and (c) modulus spectrum for NCEP model latent heat flux (unfiltered and unrotated) seasonal cycles (PC1) over southern Africa.

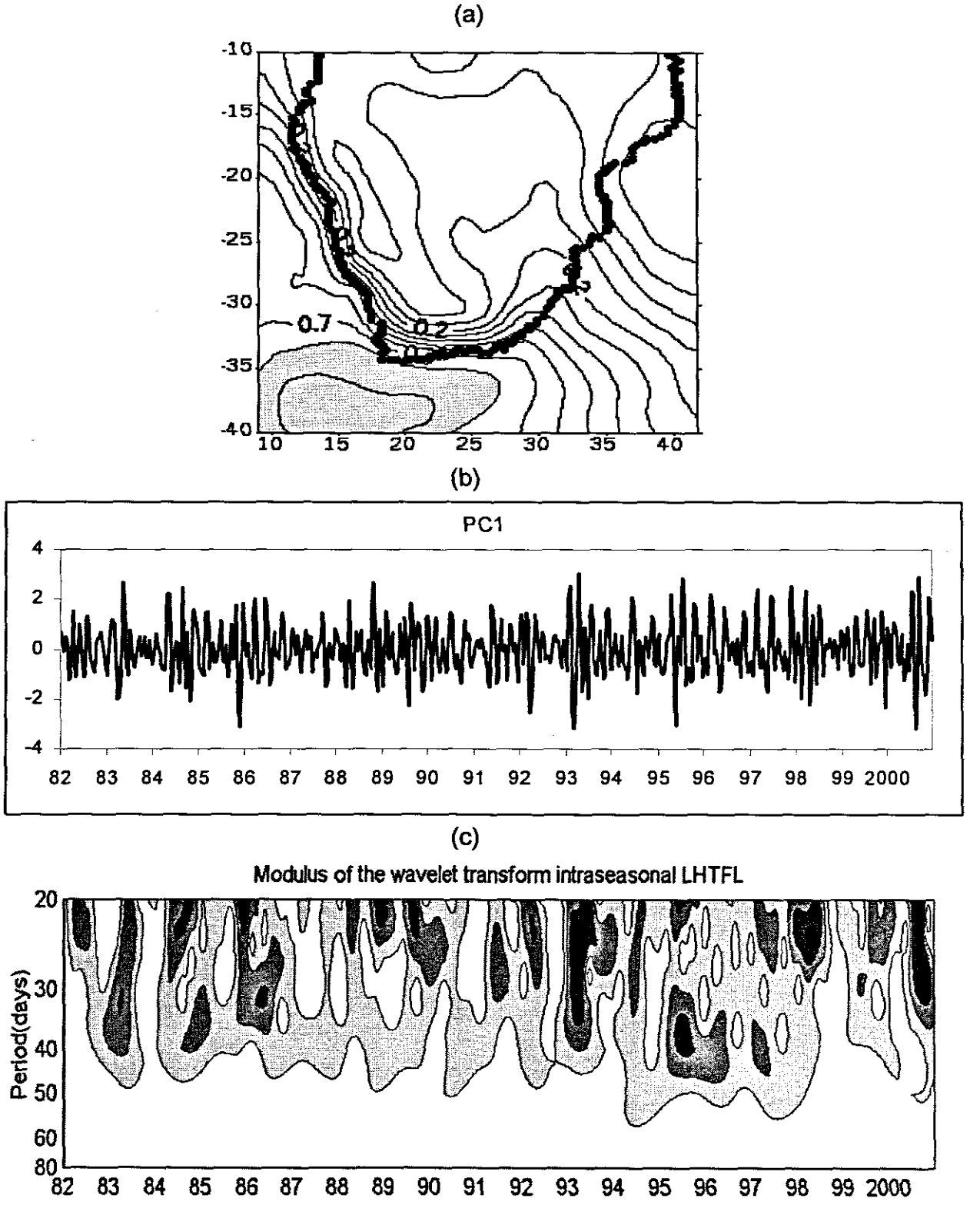

Fig. 5.5 (a) Spatial loadings (b) time scores and (c) modulus spectrum for intraseasonal NCEP model latent heat flux (filtered and rotated) PC1 over southern Africa.

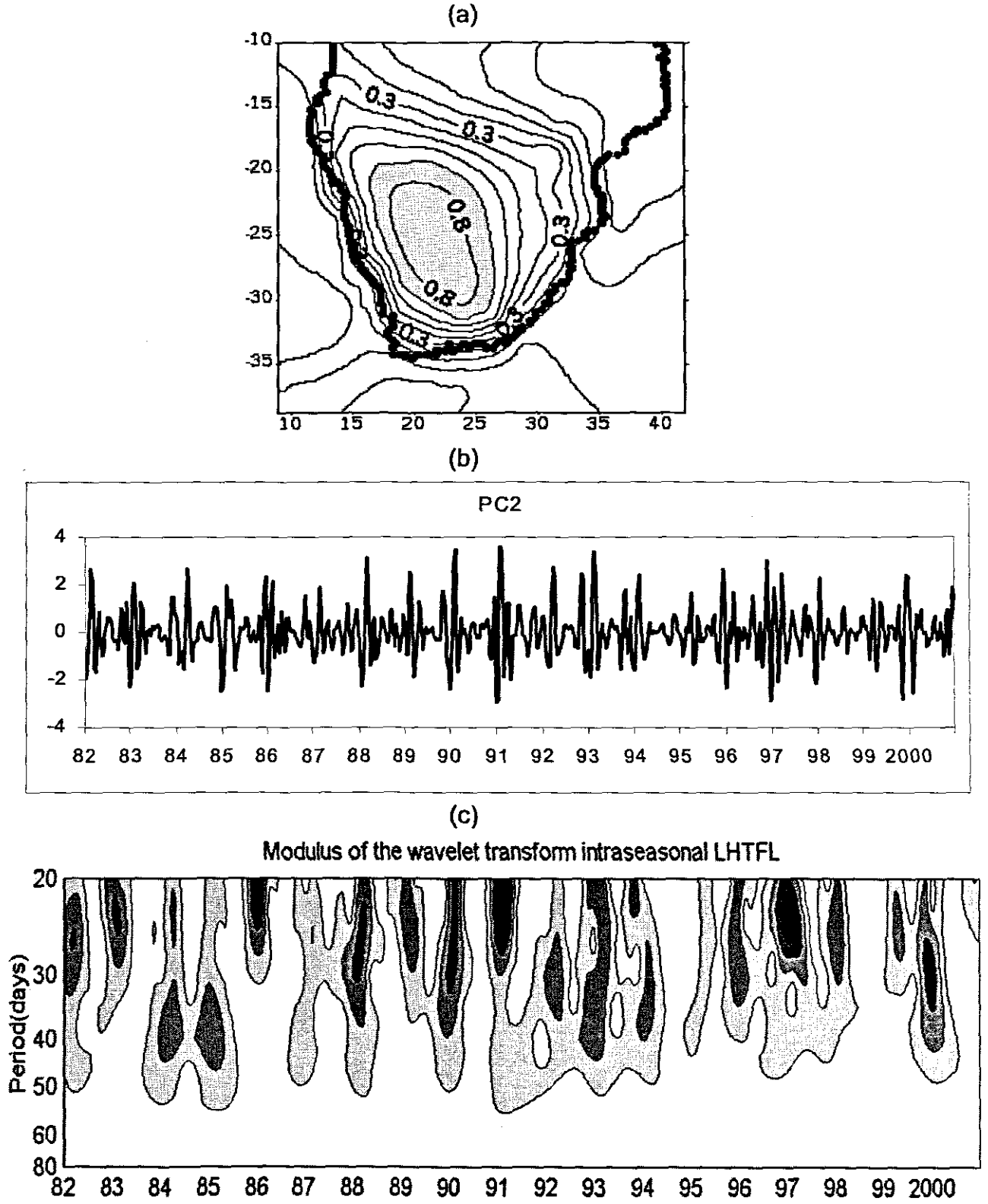

Fig. 5.6 (a) Spatial loadings (b) time scores and (c) modulus spectrum for intraseasonal NCEP model latent heat flux (filtered and rotated) PC2 over southern Africa.

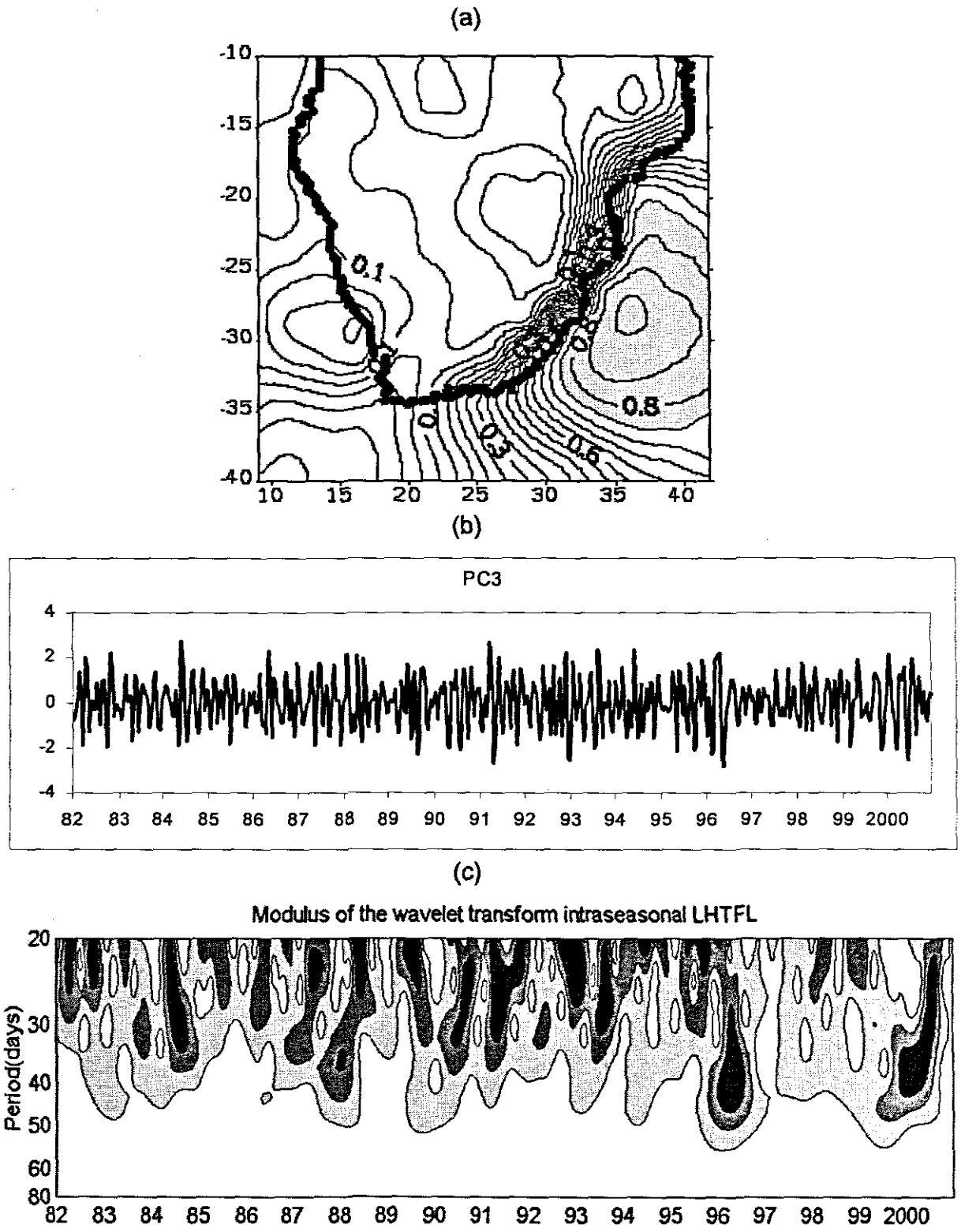

Fig. 5.7 (a) Spatial loadings (b) time scores and (c) modulus spectrum for intraseasonal NCEP model latent heat flux (filtered and rotated) PC3 over southern Africa.

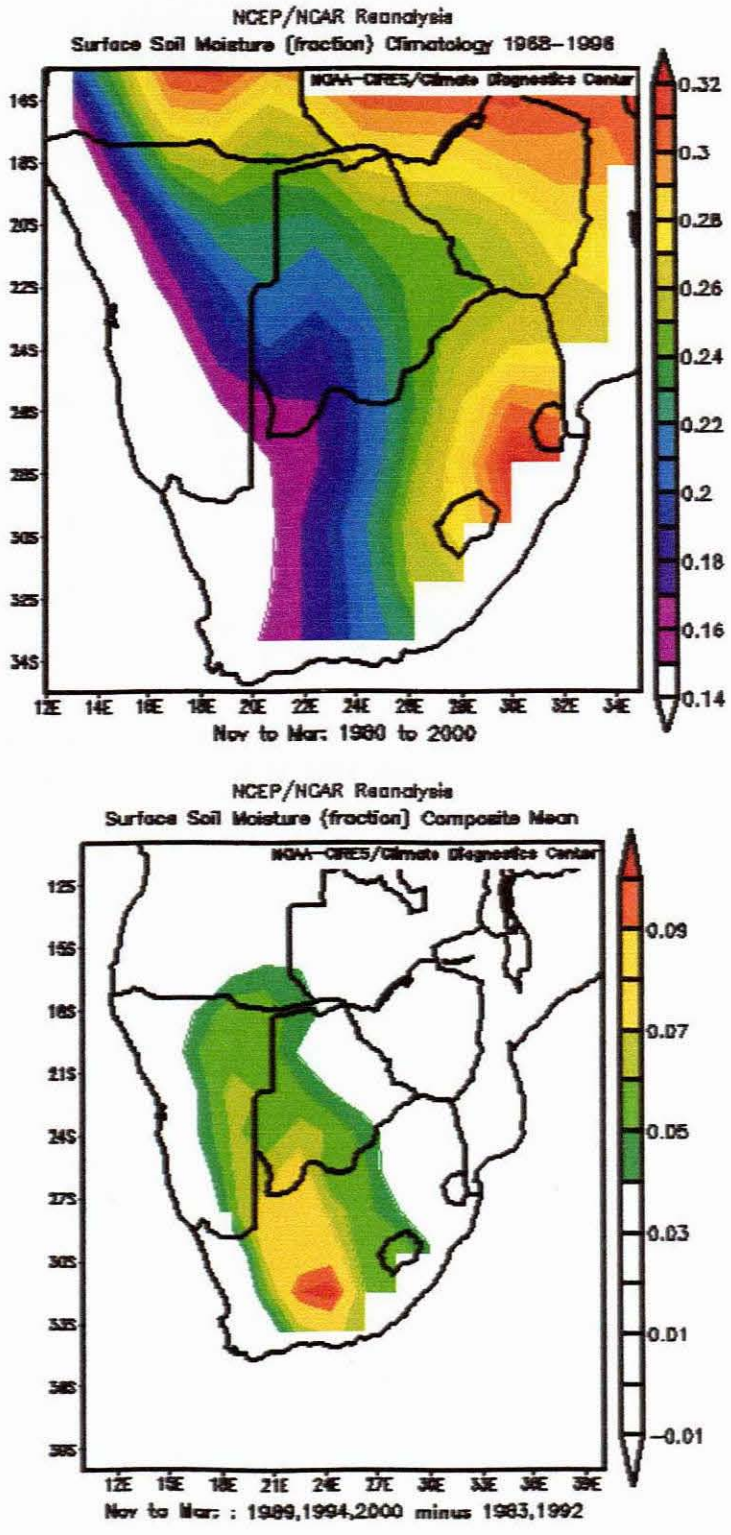

Fig. 5.8 NCEP model surface soil moisture climatology (upper panel) for summer season and the composite difference of 'green' minus 'brown' years.

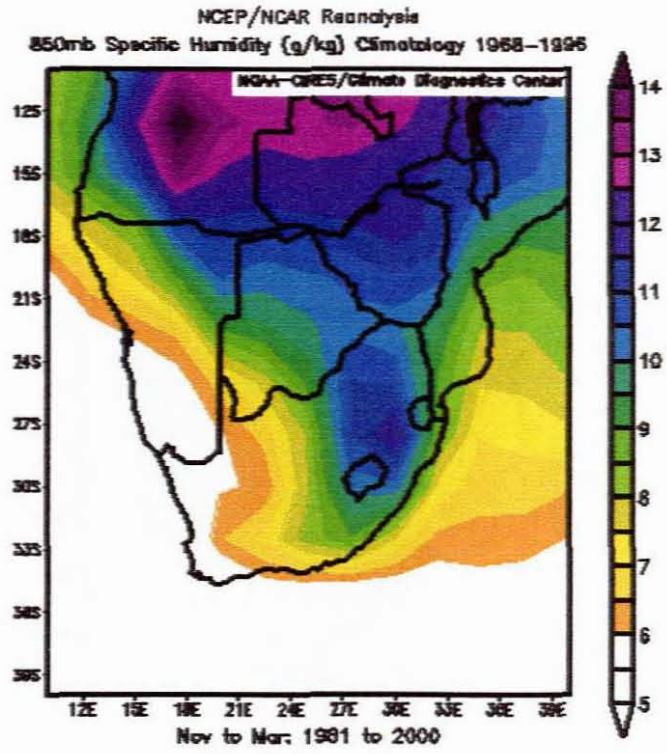

Fig. 5.9 Summer mean monthly 850 hPa NCEP model specific humidity over southern Africa. A sharp gradient and slope at the edge of the Kalahari is evident.

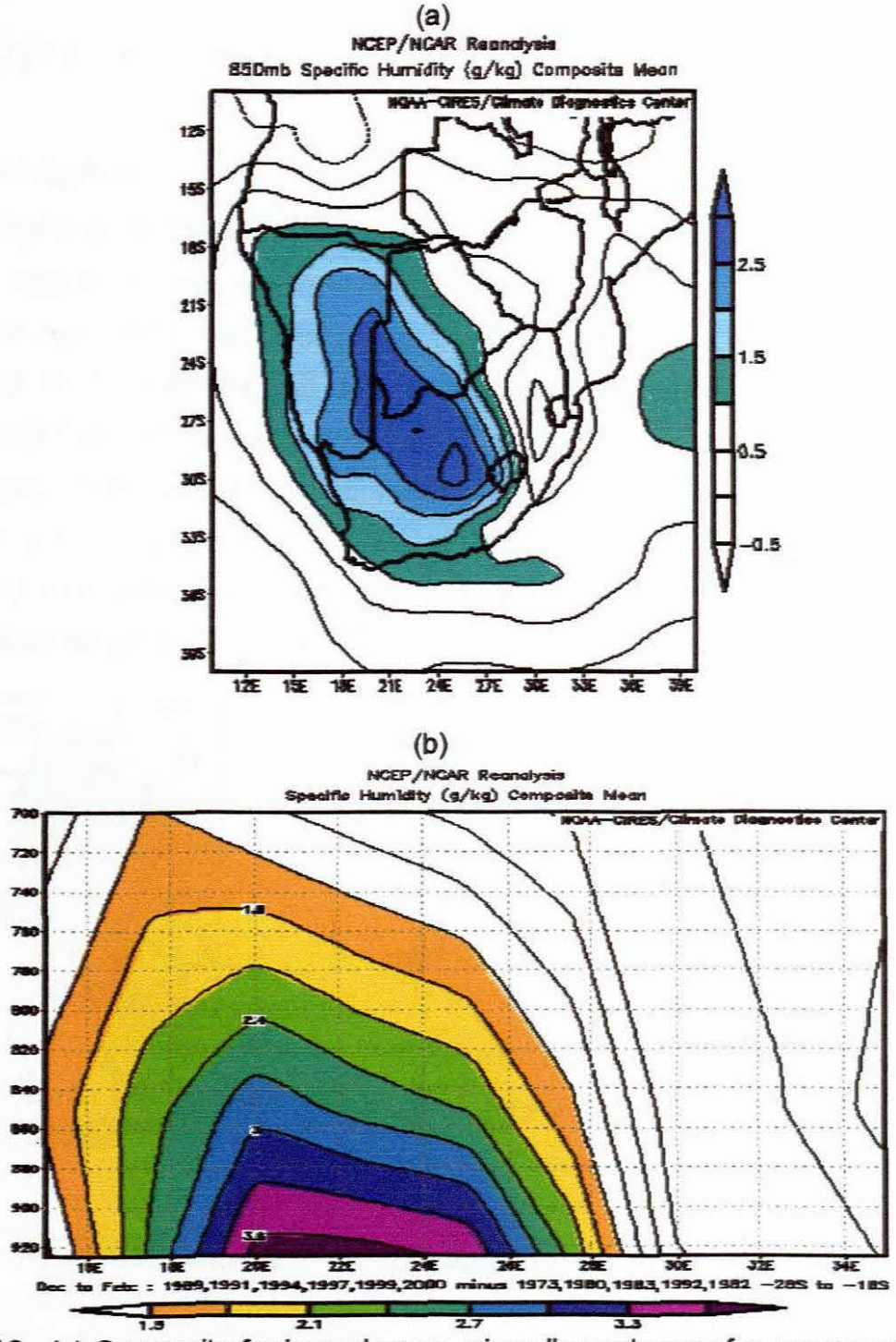

Fig. 5.10. (a) Composite for 'green' years minus 'brown' years for summer mean monthly 700 hPa specific humidity over southern Africa and (b) averaged from 17.5°S to 27.5°S. The moist boundary layer shifts westwards during wet years.

Chapter 6

VEGETATION-RAINFALL DYNAMICS OVER SOUTHERN AFRICA

6.0 Introduction

The preceding chapters have determined the space and time variability of rainfall, vegetation, and evapotranspiration-related moisture fluxes at seasonal, intraseasonal, and to less extent interannual time scales. The co-location of dominant PCA modes for seasonal and intraseasonal rainfall, vegetation and latent heat flux and the high correlation of slightly lagged time scores suggest that strong coupling exists. A 'center of action' along the eastern edge of the Kalahari extending from the western Zambezi through to central South Africa (Fig. 6.1) has been determined and the analysis now focuses on that axis to obtain more insights.

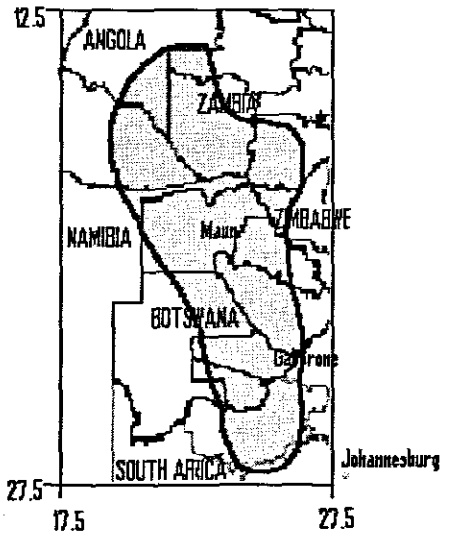

Fig. 6.1 'Center of action' for vegetation-rainfall feedbacks over southern Africa

The 'center of action' is a semi-arid region where vegetation-rainfall feedbacks are thought to be strongest (Davenport and Nicholson, 1993; Zeng *et al.*, 2002) due to high evaporative losses.

The main objective of this chapter is to investigate the correspondence between temporal patterns of vegetation and rainfall in the 'center of action' at the intraseasonal (or event) timescales.

It is also intended to establish the processes responsible for observed patterns using related moisture fluxes and circulation. The sensitivity of the regional boundary layer atmosphere to local vegetation forcing is also tested.

Relationships between rainfall events and vegetation response are investigated using case studies for events with large amplitude changes of NDVI. Composite analysis and cross-correlation analysis are used at different leads and lags. The timing of NDVI response to rainfall events is not well understood (Davenport and Nicholson, 1993) but it is assumed that vegetation lags rainfall at intra-seasonal time scales. It is also recognised that rainfall is not the only determinant of vegetation growth but other factors such as soil moisture, nutrient availability, soil fertility, soil type, and land use are also important (Farrar *et al*, 1994).

6.1 Spatio-temporal patterns of rainfall and NDVI

The analysis in this section follows that of Wang *et al.* (2001) in a study of spatial patterns of NDVI in the central Great Plains of the United States.

Principal component analysis has identified co-located spatial loadings for rainfall and vegetation over the Zambezi region at seasonal time scales (Fig. 6.2a,b). Rainfall and NDVI exhibit pronounced unimodal seasonal cycles over the summer rainfall region of southern Africa. Vegetation clearly lags the rainfall in its annual march by up to 3 dekads reaching a plateau during February-March (Fig. 6.1c,d). The phase lag maximizes after consecutive droughts such as after the droughts of 1982/83 and 1991/92 with up to 4 dekads lag. Vegetation memory of the previous droughts is suggested to delay the greening response to wet spells in the following year (Zeng *et al.*, 1999). This process may be assisted by weather conditions in the intervening winter.

At seasonal time scales, rainfall and vegetation are highly correlated (r=0.67), as expected due to autocorrelation. A near-linear relationship between growing season NDVI and rainfall has been determined by previous studies (e.g. Nicholson *et al.*,1990; Tucker and Nicholson, 1999).

Dominant modes of variability for intraseasonal rainfall and vegetation over southern Africa also co-locate in a region along the eastern edge of the Kalahari spanning about 20° of latitude except in the south (Fig. 6.3a,b). Tropical-temperate troughs and the attendant NW cloud bands are the main synoptic features associated with the loading pattern. The surface variability strengthens and 'anchors' the cloud band to determine rainfall over the eastern Kalahari.

Time scores show 'pulsing' of intraseasonal oscillations but the mean patterns for two ISOs do not show significant relationship (Fig. 6.3d). This strengthens an earlier supposition that the variability of in-season NDVI is less well developed than that of rainfall largely due to 'biotic memory'. This may also be due to high year-to-year in-season variability of vegetation such that the reference mean is unstable.

However, stronger relationships are evident at the 40-day event scale. A composite analysis of events with large amplitude changes of NDVI is made for events with change exceeding 2 standard departures occurring between October and April. Eighteen events are selected according to these criteria. Satellite CMAP rainfall, NCEP model latent heat flux, boundary layer height and circulation composites for the same periods are also made to enable comparisons and cross-correlation.

6.2 Event response analysis

Correlation analysis is performed for rainfall against NDVI for each of the 'big' events to reveal the strength of relationships. The results are shown in the following table: -

Table 6.1 Correlation coefficients (r-values) for dekadal NDVI and rainfall at different lags based on events with large amplitude changes in NDVI ('big' events). Dates are given in dekads and significant coefficients are highlighted.

Event with large amplitude changes in NDVI	Lags			
	0	1	2	3
December, 3, 1983	0.25	**0.42**	-0.08	0.19
November, 3, 1984	0.13	0.02	-0.14	-0.34
December, 2, 1985	0.23	**0.69**	-0.05	-0.87
November, 1, 1986	0.07	0.18	0.18	-0.61
December, 1, 1986	0.18	0.12	-0.50	-0.75
October, 1, 1987	0.15	**0.70**	**0.49**	-0.35
November, 1, 1988	-0.17	**0.76**	**0.79**	-0.01
February, 3, 1989	-0.24	**0.68**	**0.85**	-0.10
November, 3, 1991	-0.68	-0.75	**0.41**	**0.95**
November, 3, 1992	-0.38	-0.39	**0.44**	**0.83**
November, 3, 1993	**0.76**	**0.63**	-0.60	-0.95
December, 2, 1995	0.01	**0.39**	0.09	-0.37
January, 3, 1997	**0.84**	**0.91**	0.44	-0.61
January, 1, 1999	-0.88	-0.82	-0.21	**0.93**
January, 1, 2000	**0.65**	**0.73**	-0.59	-0.72
November, 2, 2000	0.16	**0.60**	0.01	-0.88
December, 2, 2000	-0.72	0.04	-0.68	-0.45

10 out of 17 events show a response, either simultaneous (zero lag) or delayed by 1 or 2 dekads. The remaining events show either delayed response or no response at all suggesting that the external forcing is too strong. These events are excluded from further composite analysis.

Significant NDVI-rainfall correlations occur at either 1 or 2 dekads (10-20 days) lag. It is remarkable that events with large amplitude changes in NDVI occur mostly during the early summer, suggesting that the vegetation-rainfall relationship may be strongest then - prior to NDVI reaching a 'plateau'. This is possibly due to the co-linear effect of higher temperatures then. During the late summer (Feb-Apr), the diurnal temperature cycle is weak with lighter winds.

A correlation analysis is also made for composites of the 'big' events described above and another for 'discrete' rainfall events for comparison. 'Discrete' rainfall events are defined in this study as events that occur after extended dry periods (dry period > 3 dekads). The results for the composites are shown below: -

Table 6.2. Correlation coefficients of events with large amplitude changes of NDVI and discrete rainfall events against the corresponding rainfall at different lags and leads.

Correlation coefficients		
Lags(-)/Leads(+) (dekads)	NDVI 'big' events	'Discrete' rainfall events
- 3	**0.32**	
- 2	**0.92**	
- 1	**0.80**	
0	**0.15**	**0.14**
+ 1		**0.77**
+ 2		**0.60**
+ 3		**0.26**

Lag intervals of up to 3 dekads are examined. As expected, events with large amplitude changes of NDVI lag rainfall and discrete rainfall events lead NDVI. The weakest correlations between rainfall and vegetation in either case occur at zero lag. High correlations occur at lag 1 and lag 2, for both NDVI 'big' events and 'discrete' rainfall events. This result confirms a hypothesis of this study that rainfall leads vegetation by 10-20 days. Similar results were obtained by Justice *et al.* (1991) who determined a lag of 10-20 days between rainfall and vegetation in semi-arid Niger and Mali. In a similar study, Wang *et al.* (2001) found that NDVI is better correlated with running mean averaged precipitation than short-term rainfall events in the central Great Plains of the United States.

The composite of selected events shows vegetation to lag rainfall by 2 dekads at intraseasonal time scales (Fig. 6.4). This agrees with the correlation analysis. Whilst it is expected that NDVI 'big events' occur after a significant rainfall event, some critical research questions arise: -

1. To what extent does the evapotranspiration flux from vegetation greening after a rainfall event affect the next wet spell?
2. Does the vegetation help to 'anchor' cloud bands regardless of external forcing?

As offered in Chapter 2, NCEP model latent heat flux, boundary layer height, 700 hPa wind and velocity potential and 700hPa Bloemfontein dew-point depression are analysed for composite events with large magnitude changes in NDVI. This is done to determine whether an earlier rainfall event and subsequent 'greening' result in an evapotranspiration flux that affects the next rainfall event.

6.2.1 Latent heat flux

A composite of NCEP model latent heat flux for events with large amplitude change in NDVI is made (Fig. 6.5). The comparison shows that rainfall leads latent heat flux by 1 dekad which in turn leads NDVI by a dekad. It suggests the latent heat flux, which represents vertical moisture flux, is the 'middle man' between rainfall events and vegetation. It 'carries the message' through soil moisture to the moist boundary layer. Surface evaporation after a rainfall event results in an increased latent heat flux into the boundary layer. It suggests that the vapour flux is dominated by direct evaporation from the surface soil moisture. The sequence of events before and after the NDVI 'big event' is shown in Table 6.3.

Table 6.3 The sequence of events before and after the NDVI 'big event'.

Time lag/lead	Situation
D-3	Dry
D-2	Rainfall maximum
D-1	Latent heat flux maximum
D	NDVI maximum
D+1	Boundary layer responses?
D+2	
D+3	

The response of the boundary layer is observed in the dekads D+1, D+2, up to D+5. However, it is recognised that composites may become unreliable with increasing time away from D.

6.2.2 Dew-point depression and boundary layer height

Radiosonde profiles for Bloemfontein are analysed for 700 hPa dew-point depression. It is recognized that a single level may not indicate convective potential and also that Bloemfontein is at the southern edge of the 'center of action'. However, when compared against NCEP model area-averaged boundary layer height, agreement is found (Fig. 6.6). As the dew-point depression decreases (reflecting moist conditions), the moist boundary layer height deepens (Fig. 6.6). A turning point occurs at D-1, coinciding with the latent heat flux maximum. A general upward trend in moist boundary layer height after a NDVI 'big' event is also noted.

The peaking of latent heat flux one dekad after the rainfall event agrees with fluctuations of boundary layer height and dew-point depression. The composite moist boundary layer deepens markedly after a rainfall event at D-1 but does not diminish as much after the event (Fig. 6.7). The increase of boundary layer height is distinct over the western semi-arid regions. Changes over the more humid east and northeast are not as marked. The mean composite boundary layer height increases after the rainfall event, and deepens further after the vegetation maximum. This supports the supposition that additional moisture flux into the boundary layer from the land surface and transpiring vegetation helps sustain the moisture in the absence of external forcing. However, the boundary layer height (hence moisture) seems to reinforce the external forcing, which is remarkable.

6.2.3 700 hPa wind and velocity potential

The composite of winds for certain phases of NDVI 'big' events is shown in Fig. 6.8. The vector winds at D-3 and D+1 show anticyclonic circulation over the subcontinent whilst D-1 shows a trough west of the plateau. Thus, the circulation seems to inhibit cloud development before and after the rainfall event. Velocity potential for the compositing period is also analysed for divergence. The variation of NCEP model velocity potential is in phase with the variation of satellite vegetation NDVI (Fig 6.9). Whilst it was thought the low-level velocity potential would reflect external forcing and relate to rainfall, it seems to be related to vegetation better. It peaks at D coinciding with the NDVI maximum suggesting that a sharp increase in vegetation 'draws' airflow towards itself, in a self sustaining way. Perhaps the evapotranspiration adds to the low-level buoyancy that causes uplift and convergence. In addition, the higher canopy height would increase friction, slowing the winds and causing convergence.

6.3 Sensitivity of the regional atmosphere to local vegetation forcing

Positive upward feedbacks of vegetation on rainfall are more distinct in intermediate precipitation regions (Zeng *et al.*, 2002). While it has been demonstrated that the external forcing is the dominant forcing mechanism as regards the 'center of action' through tropical-temperate troughs and the attendant NW cloud bands, results of this analysis suggest strong coupling between the land surface and the boundary layer over southern Africa.

This chapter sought to establish vegetation-rainfall dynamics over southern Africa including processes of vegetation feedback in land-atmosphere interactions. The major findings are summarized.

(i) Strong spatial and temporal relationships exist between rainfall and NDVI over southern Africa particularly in the semi-arid regions of the subcontinent.

(ii) The evapotranspiration flux from the land surface into the boundary layer after a rainfall event deepens the boundary layer, even after the convergence has declined.

(iii) The latent heat flux seems to be dominated by direct evaporation from the surface soil moisture. The boundary layer height peaks coinciding with the latent heat flux and it seems to reinforce the external forcing.

(iv) A most significant finding is the agreement between vegetation and low-level velocity potential. A sharp increase in vegetation appears to draw airflow towards itself, in a self-sustaining way.

(v) The vegetation seems to have more influence on the horizontal convergence than the vertical moisture flux.

A synthesis of the major findings and conclusions of this study is given in the next chapter.

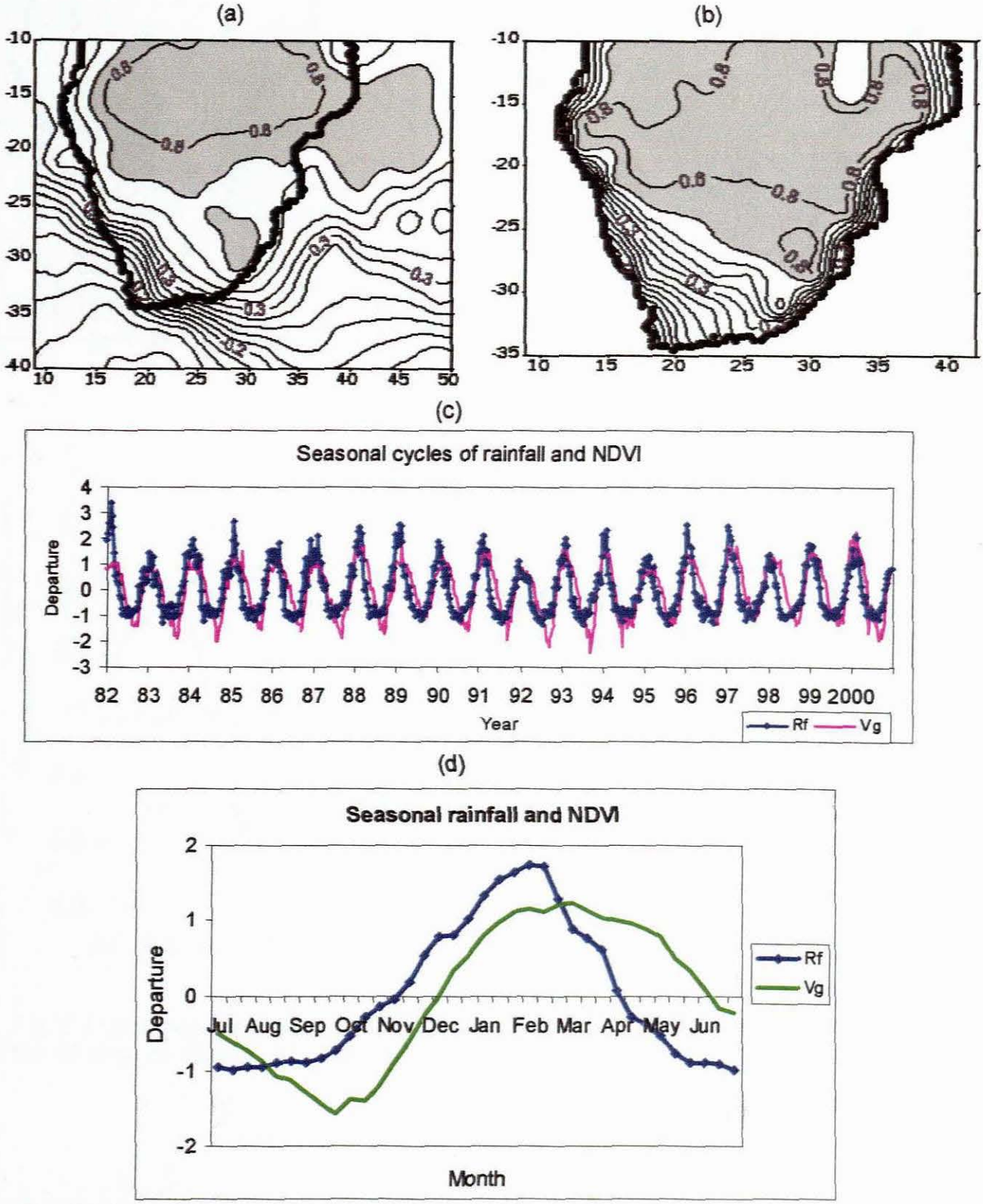

Fig. 6.2 Seasonal spatial loadings for (a) rainfall and (b) NDVI (c) the associated time scores showing pronounced cycles and (d) the seasonal mean.

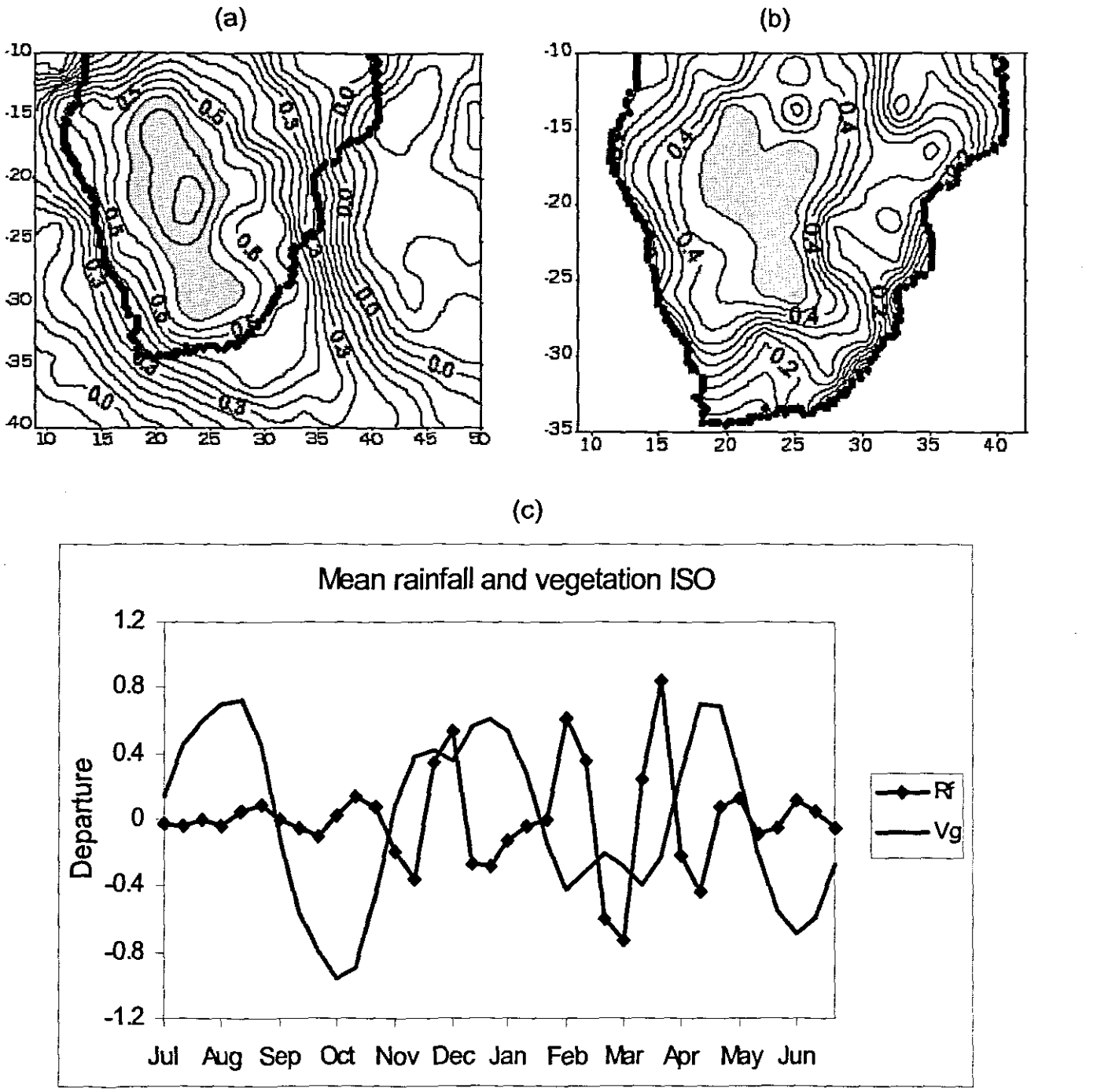

Fig. 6.3 Intraseasonal spatial loadings for (a) rainfall PC1 and (b) NDVI PC1 for the 40-days oscillation and (c) the seasonal mean ISOs.

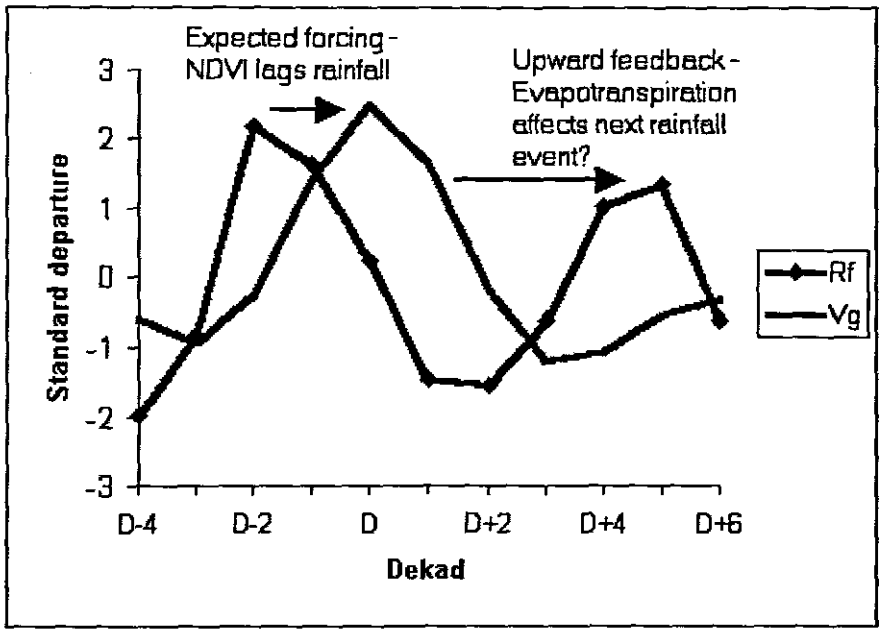

Fig. 6.4 Composite 'big' event ISO for rainfall and vegetation over the Kalahari transition zone. The key question is 'to what extent is the evapotranspiration flux from one rainfall event influencing the next event?

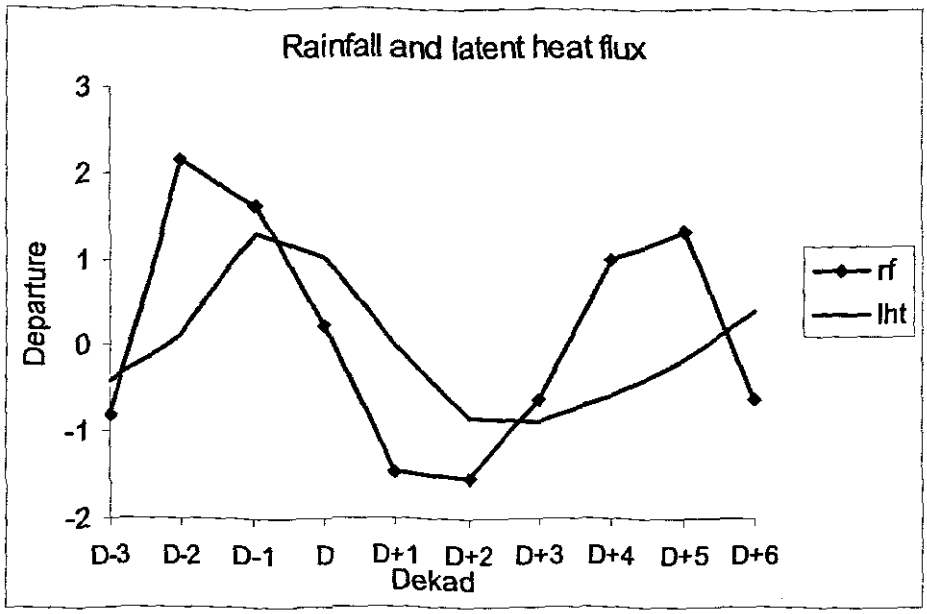

Fig. 6.5 Mean composites of rainfall and latent heat flux for NDVI 'big events'

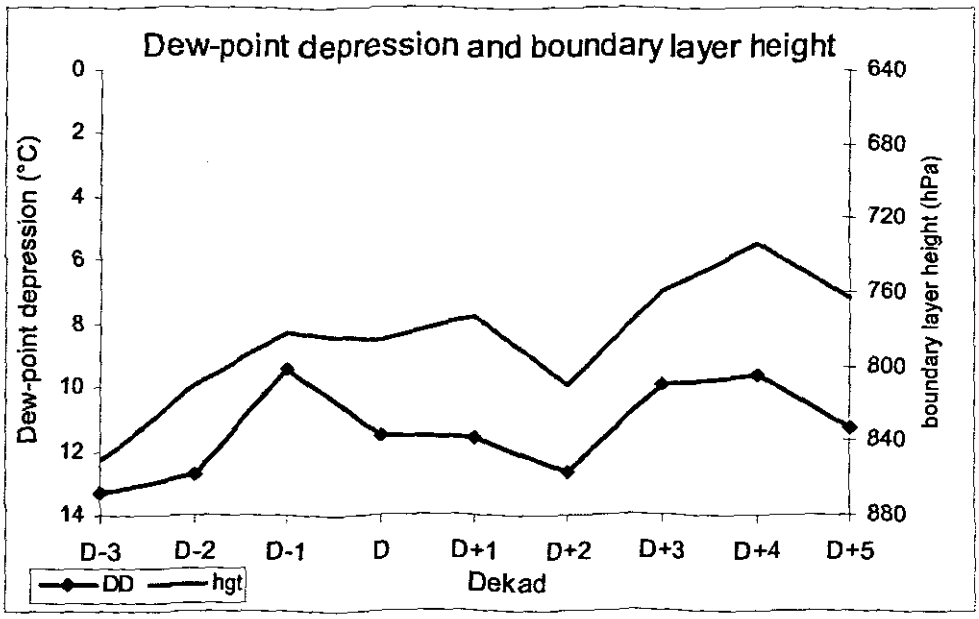

Fig. 6.6 Composite analysis of NCEP model boundary layer height and inverted Bloemfontein 700 hPa dew-point depression

(a) D-3

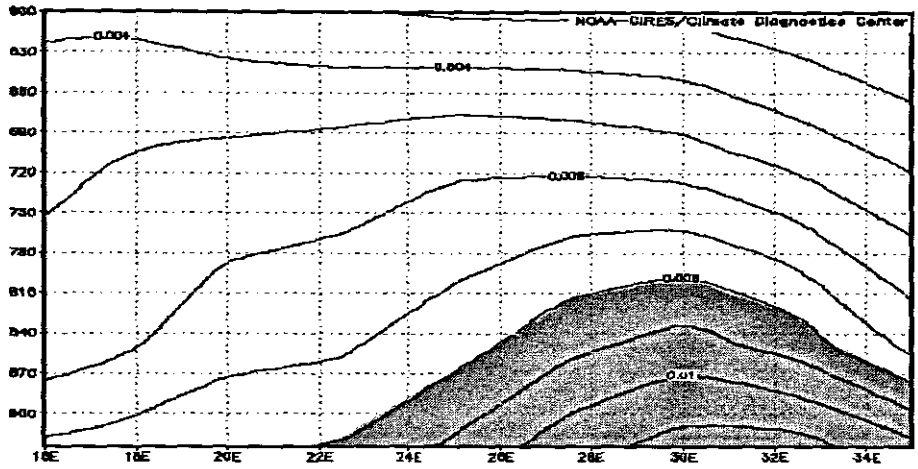

(b) D-1

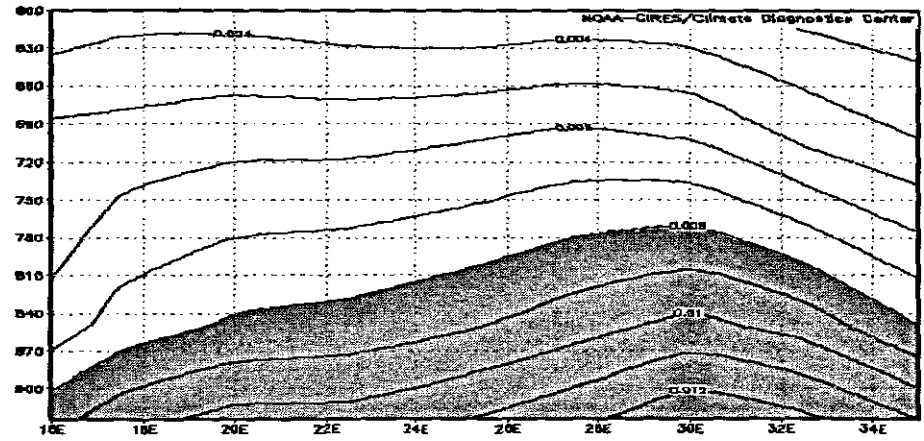

(c) D_0

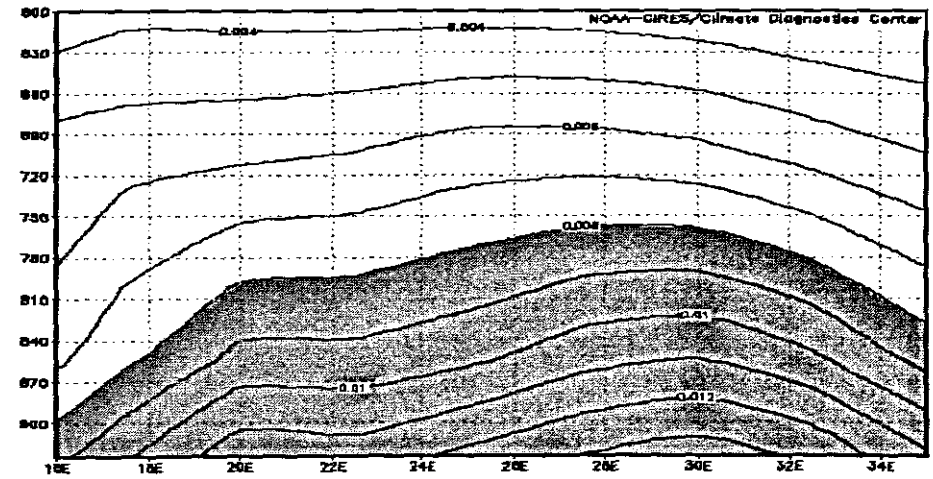

Fig. 6.7 Dekad mean composite NCEP specific humidity in the boundary layer from 925 hPa to 600 hPa averaged from 17°S to 27°S and from 16°E to 35°E, for NDVI 'big' event cases. The layer > 0.008 g/kg is shaded.

(c) D+1

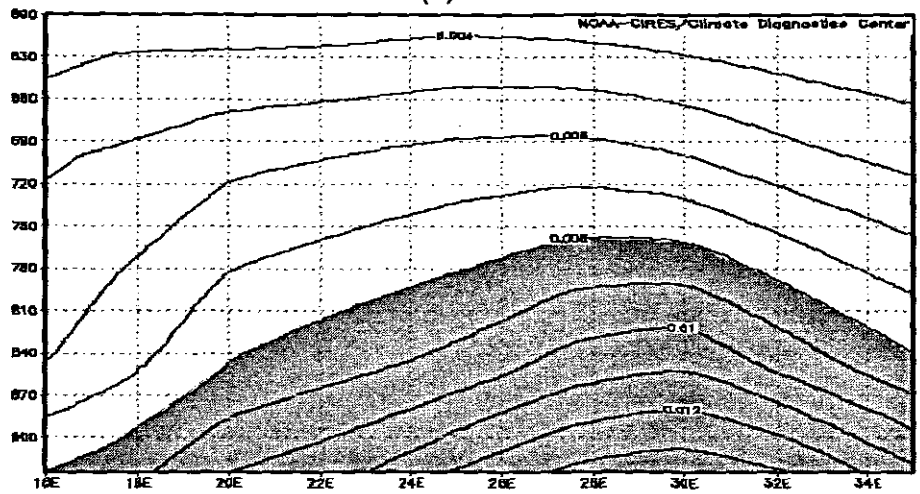

(d) D+3

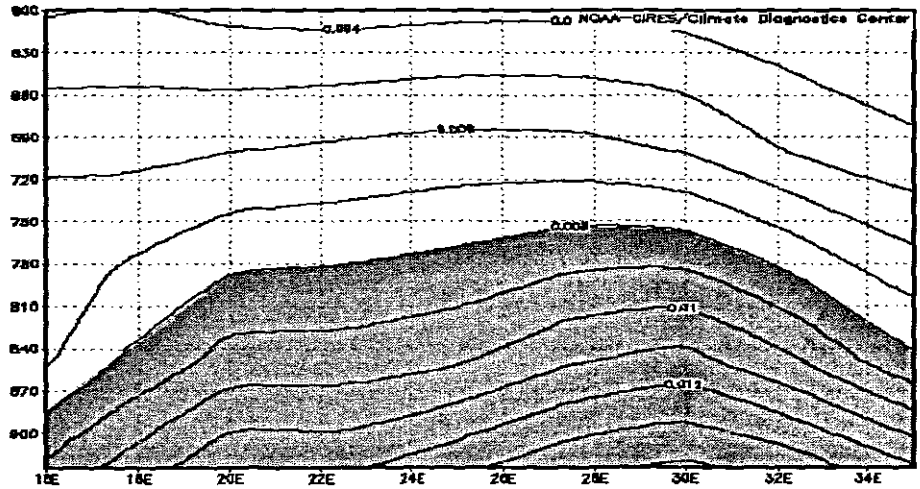

(e) D+5

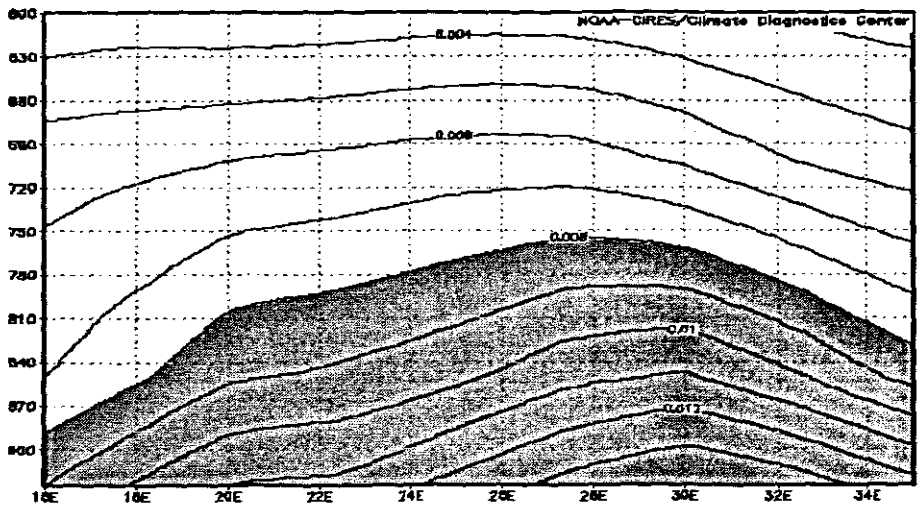

Fig. 6.7 cont.

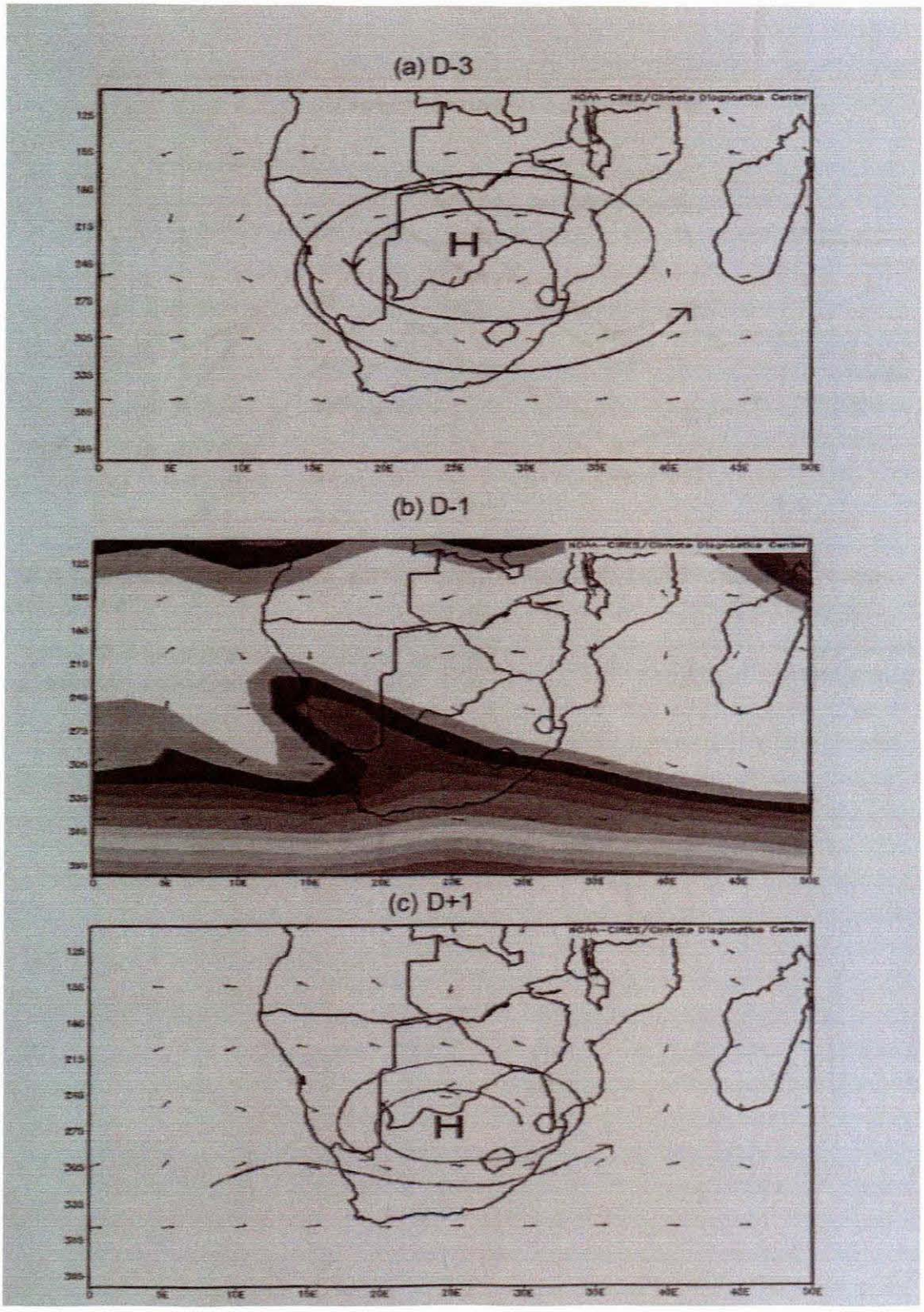

Fig. 6.8 NCEP model decadal mean composites of wind vectors for (a) D-3, (b) D-1 and (c) D+1 with streamlines imposed

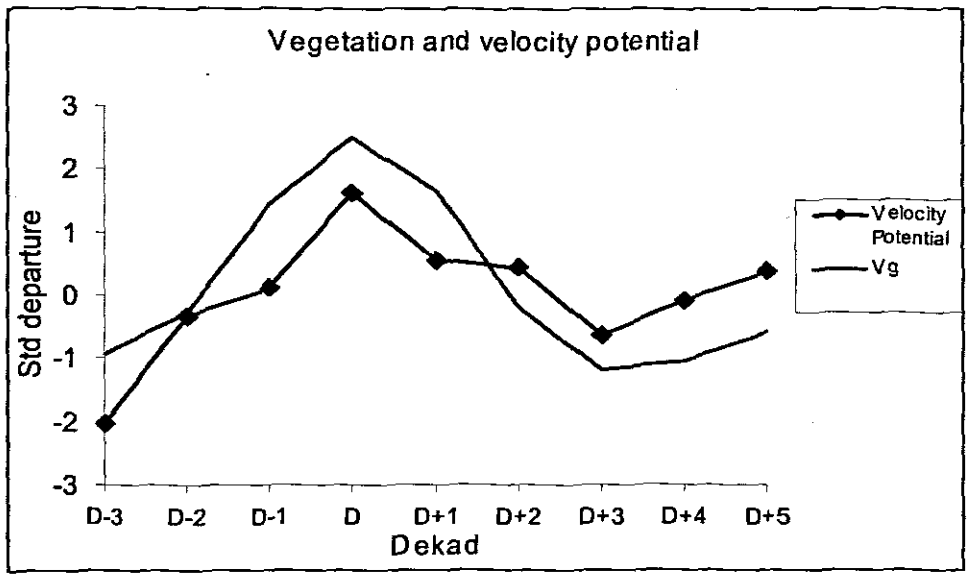

Fig. 6.9 Composite analysis of satellite vegetation and NCEP model low level velocity potential.

Chapter 7

DISCUSSION AND CONCLUSIONS

7.0 Introduction

This study has detailed the spatio-temporal variability of rainfall and vegetation over southern Africa at seasonal, intraseasonal and interannual timescales. The climatology and variability of evapotranspiration-related moisture fluxes over the subcontinent have been discussed. An attempt has been made to establish the influence of vegetation and related moisture fluxes on rainfall events over southern Africa. The sensitivity of the regional climate to land surface forcing has also been tested.

Whilst this study has characterised the vegetation of southern Africa using satellite based observations and climate factors, the human aspects of land cover and its variability are less well known. Thus, impacts of land use on climate are briefly discussed qualitatively in this chapter before a synthesis of the major findings and conclusions of this study is presented. The recommendations and implications for future research are offered at the end.

7.1 Land use influences on climate

Hoffman and Jackson (2000) have suggested that land use patterns may alter the climate of tropical savannas by reducing precipitation and increasing surface temperature. Land use refers to the exploitation of land in anthropogenic activities (e.g. agriculture, industry, residential etc) including the nature of vegetation. Southern Africa experiences land use and land cover change because of land clearing through slash and burn agriculture.

High quality land use and land cover maps are important for monitoring, research and policy making especially in terms of optimising land use. A land use and land cover map for southern Africa is shown in Fig. 7.1.

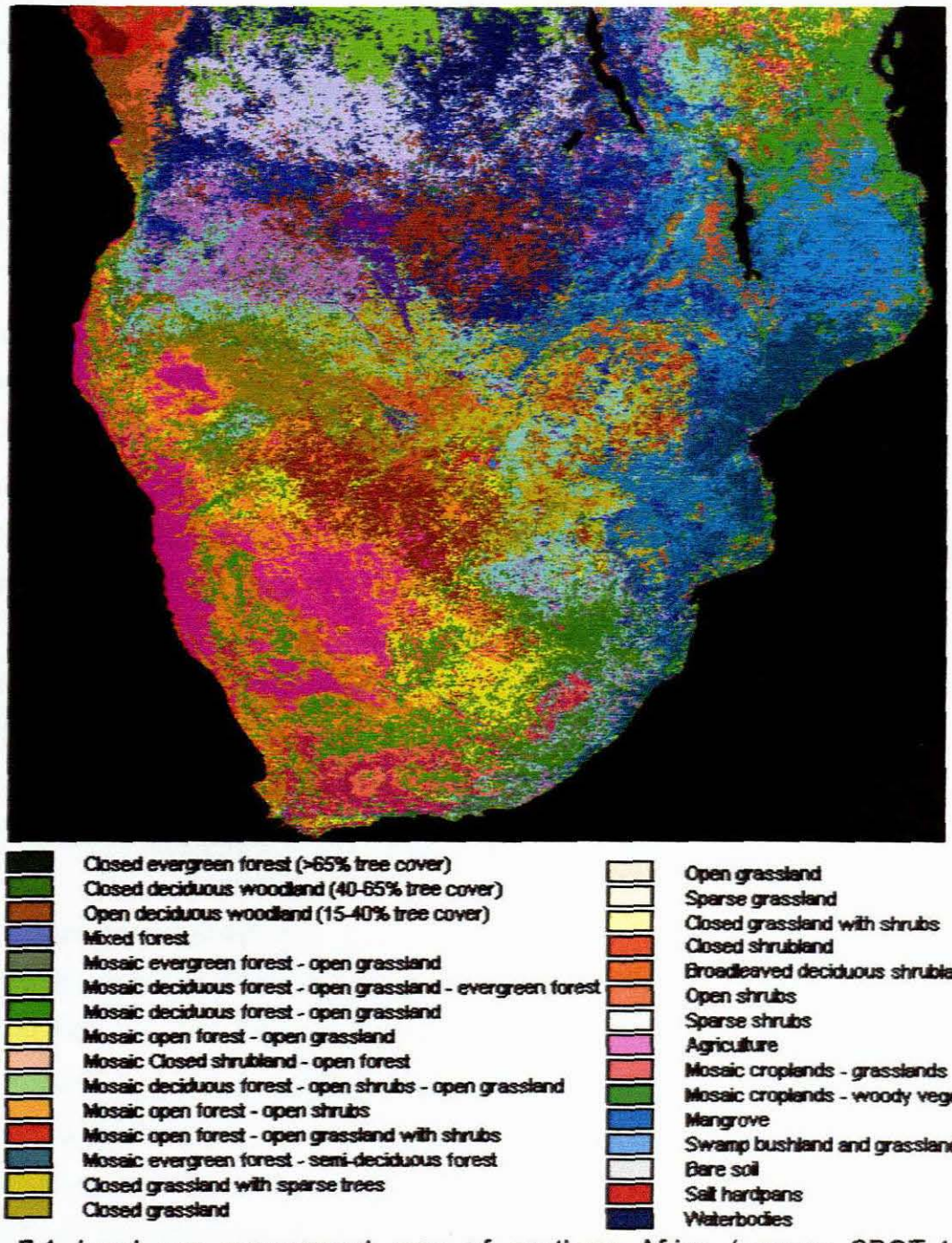

Fig. 7.1 Land use assessment map of southern Africa (source: SPOT-4 VEGETATION)

The natural land cover is dominated by grasslands and open forests over the southern plateau and mixed forests in the Zambezi. Commercial agriculture is also evident in the mean pattern with extensive livestock ranching in the Karoo of South Africa. Whilst the NDVI is a good indicator of vegetation greenness as viewed by satellite, it does not distinguish between sub-tropical forests and grasslands and cannot account for canopy characteristics such as canopy height and roughness length. Canopy height affects the frictional drag on the wind and mechanical turbulence. Human activities such as agriculture, deforestation, overgrazing, fire burning and urbanisation of the peripheral areas can significantly affect the climate through the roughness length.

The roughness length can significantly affect the boundary layer climate through human activities such as agriculture, deforestation, overgrazing, fire burning and urbanization of the peripheral areas. Surface roughness is a key land surface variable which can alter the fluxes of heat, moisture and large-scale circulation patterns. Many studies have shown that a reduction in roughness length results in reduced precipitation (e.g. Pitman *et al.,* 1993; Hahmann and Dickinson, 1997). The influence of surface roughness was not tested in this analysis because of the complex nature of land-atmosphere interactions. However, Drew (2004) modelled a 20% increase in roughness length over southern Africa but the results did not reveal a clear signal and suggested that the MM5 model was relatively insensitive to that change.

7.1.1 Commercial agriculture

Natural vegetation of many regions of the world has been replaced with crops. Large-scale commercial agriculture may have profound impacts on the boundary layer climate of southern Africa. Irrigating farmland means more seasonally-confined evapotranspiration into the atmosphere with potential influence on cloudiness and rainfall. Bare surfaces during the winter/spring have negative feedback on sensible heat resulting from reduced latent heat (Schlesinger *et al.*,

1987) and may be related to heat waves during the spring. Several large land areas are under irrigation

Hoffman and Jackson (2000) ran simulations using a National Center for Atmospheric Research (NCAR) Community Climate Model (CCM3) coupled with the NCAR Land Surface Model (LSM). They sought to simulate human impact on the climate by changing the savanna to open grassland and commercial agriculture over southern Africa. Results reflected a reduction of precipitation and an associated increase in summer dry spells. They attributed the reduction in precipitation to higher albedo and reduced roughness length.

7.1.2 Deforestation and biomass burning

Deforestation may result in decreased precipitation and higher surface temperature (Dickinson and Kennedy, 1992; Lean and Rowntree, 1997) and also increased carbon dioxide (CO_2) levels in the atmosphere. GCM projections of climate show increased temperatures of 1-2°C over southern Africa but not much in rainfall. Higher temperatures imply increased water stress and high evaporative losses.

Population growth in rural communal lands has increased pressure on pastures leading to overgrazing. Modelling studies have simulated overgrazing to cause reduced precipitation and higher surface temperature in semi-arid regions (e.g. Charney, 1975).

Tree harvesting and biomass burning have become more frequent especially in the tropical savannas affecting tree densities (Hoffman and Jackson, 2000) and altering the climate. A regional science initiative, the Southern African Fire-Atmosphere Research Initiative (SAFARI) was launched in 1992 focusing on understanding the basic principles of biomass burning in the subtropical savannas.

7.1.3 Urbanisation

Urban areas currently make up 6% of all land cover in southern Africa due to expansion of urban areas into the neighboring areas which are under agriculture or other land covers such as forests. Urban population growth (36% of the population of southern Africa lives in urban areas) and rural-urban migration in search of employment have caused a rapid expansion of the built up area over southern Africa resulting in significant land-use changes. Urbanisation alters the local wind patterns and heat and moisture regimes. Urban areas are warmer than the surrounding countryside associated with reduced nocturnal cooling (IPCC, 2001). This may be attributed to the nature of the urban land surface with tall buildings and industrial emissions which alter the composition of the atmosphere.

7.2 Summary of Important Results

7.2.1 Space-time variability of rainfall

The seasonal and intraseasonal characteristics of rainfall over southern Africa were determined in Chapter 3. The annual cycle is a dominant mode (34% of variance) of rainfall variability and the ITCZ is the main synoptic feature associated with it.

Intraseasonal oscillations over southern Africa exhibit spectral peaks at 40 days and 20 days. The 40-day oscillation is loaded in a NW-SE axis on the eastern edge of the Kalahari spanning 20° of latitude whilst the 20-day ISOs are focused on Agulhas current/KwaZulu-Natal, Bie Plateau (Angola), lower Zambezi and the SW Cape. A remarkable finding of this study is that the 40-day oscillation 'connects' the two 20-day ISOs during the cloud band (Fig. 7.2). NW cloud bands are a major source of rainfall over the interior plateau and are a slower harmonic of the faster modes at either end. Tropical-temperate troughs link the Angola low to a westerly wave in the Agulhas region. This pulsing is caused by the 'right hook' ridging that undercuts the poleward flowing tropical air.

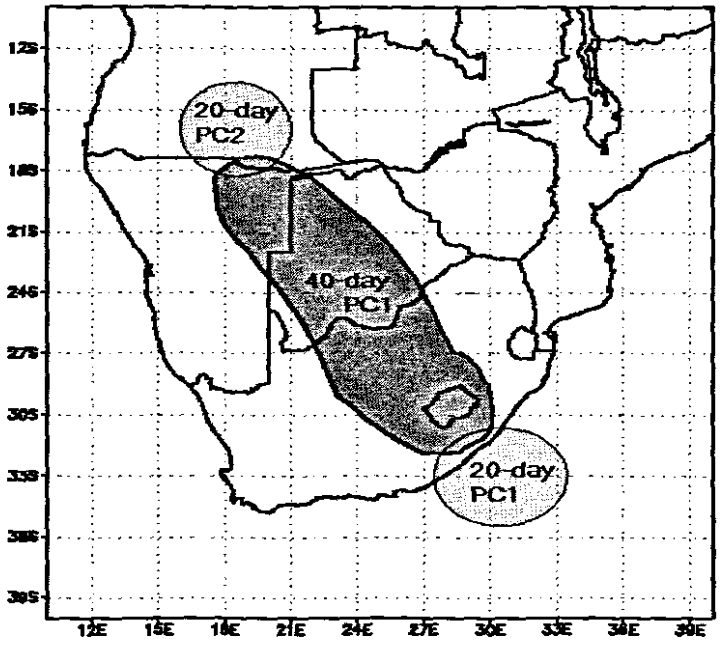

Fig. 7.2 Schematic shows that the 40-day oscillation 'connects' PC1 and PC2 of the 20-day ISO.

The intraseasonal oscillations are phase locked to the seasonal cycle, especially at the onset of the summer rains whilst the two ISOs are in phase during the major wet spells. The 20-day marine systems are harmonics of the 40-day oscillation at the start and end of the rainy season, whilst the Angola low is a harmonic of the 40-day oscillation during December and February wet spells. The regularity of oscillations over the oceans suggests that Rossby waves progress eastward to the south of Africa at certain times of the year. This is an important result as it was previously thought that the waves are chaotic.

Climatologically, there are three to six wet spells alternating with dry spells in the summer rainfall season over southern Africa. This agrees with a previous study by Makarau (1995) which found prominent wet spells to occur over southern Africa at nearly monthly intervals from November to March. It was also determined that dry summers tend to have longer intraseasonal oscillations than wet summers.

7.2.2 Vegetation variability

The distribution and time-space variability of vegetation at seasonal, intraseasonal and interannual time scales over southern Africa were analysed and discussed in Chapter 4. Strong west-east gradients of vegetation greenness were determined from the western desert to the forest over southern Africa. High variability and sensitivity to rainfall characterize the eastern edge of the desert - the Kalahari transition zone. This zone reflects the influence of boundary layer-vegetation coupling within the tropical-temperate troughs and associated NW cloud bands.

One of the major findings of this study is the determination of intraseasonal oscillations of vegetation over southern Africa. Especially with a long NDVI time series, this study pioneers this area of research. The ISO maximizes at about 40 days and spatial loadings are co-located with loadings for CMAP rainfall's 40-day oscillation along the eastern edge of the Kalahari. This is a unique and important contribution of the thesis to our understanding of vegetation dynamics and this has the potential to indicate areas where satellite data can be useful in early warning systems for assessing agricultural production and possible shortfalls due to drought.

The pulses of the vegetation ISO are weaker than CMAP rainfall's 40-day oscillation partly because of 'biotic memory' suggesting vegetation greenness (NDVI) does not diminish rapidly even in the absence of rainfall. It is recorgnised that despite its temporal resolution, vegetation may not exhibit a 20-day oscillation as with rainfall since NDVI does not fluctuate in concert with rainfall at the time scale of days.

7.2.3 Evapotranspiration-related fluxes over southern Africa

The climatology and variability of evapotranspiration-related moisture fluxes over southern Africa were analysed and discussed in Chapter 5. The mean distribution of moisture fluxes is significantly related to the observed patterns of

rainfall, vegetation and marine winds around southern Africa suggesting strong coupling. Seasonal cycles and spatial loadings for surface latent heat flux show similar features as CMAP rainfall and NDVI. The Zambezi region is an important source of atmospheric water vapour and latent heat flux at seasonal time scales. Another important source is the Indian Ocean Agulhas current 'warm pool' east and south of the subcontinent. Whilst the Agulhas current system is not of particular relevance to land-atmosphere interactions, its dominance in modulating variability of evaporation-related fluxes has been demonstrated.

The loading region for rainfall and NDVI 40-day oscillations along the eastern edge of the Kalahari is not only a region of strong gradients of heat and moisture fluxes, but also a region of high sensitivity to interannual variations. Analysis of boundary layer heat and surface moisture fluxes suggests that the tropical-temperate troughs and the attendant cloud bands locate farther west during the wetter years. Consequently, there is high standard deviation for meteorological parameters in this zone. In an earlier study, Gondwe and Jury (1997) determined that the Kalahari transition zone is a dynamic system.

7.2.4 Vegetation-climate dynamics

The vegetation feedbacks on the climate of southern Africa were investigated in Chapter 6. Results from this study demonstrate that NDVI spatial patterns are largely a function of rainfall distribution. The NW cloud band region extending from western Zambezi to central South Africa along the eastern edge of the Kalahari is a focus of analysis. Case studies of events with large amplitude change in NDVI were selected and compared against cases for satellite CMAP rainfall, NCEP model latent heat flux, boundary layer height, vector winds, velocity potential and Bloemfontein dew-point depression.

Boundary layer analysis has shown that the atmosphere over southern Africa is sensitive to the forcing from the land surface at the intraseasonal (event) time scales. The evapotranspiration flux from the land surface into the boundary layer

after a rainfall event deepens the boundary layer, even after the convergence has declined. The moist boundary layer height does not diminish as much after the rainfall event. The latent heat flux seems to be dominated by direct evaporation from the surface soil moisture after a rainfall event. The boundary layer height also peaks to coincide with the latent heat flux maximum suggesting that additional moisture flux into the boundary layer from the land surface and transpiring vegetation helps sustain the moisture in the absence of external forcing.

The results of this study are not conclusive that the additional vertical moisture flux from the vegetation affects the next rainfall event. Instead, the vegetation seems to reinforce the externally forced horizontal convergence. A most significant finding of this thesis is the agreement between vegetation and low-level velocity potential (divergence). A sharp increase in vegetation appears to draw the airflow towards itself, in a self-sustaining way. Perhaps the evapotranspiration adds to the low-level buoyancy that causes uplift and convergence. In addition, the higher canopy height would increase friction, slowing the winds and causing convergence.

Variability of the rainfall of southern Africa has also been strongly linked to SSTs in many regions of the oceans (e.g. Nicholson and Entekhabi, 1987; Walker, 1990; Jury and Pathack, 1991; Mason *et al.*, 1994; Makarau and Jury, 1997; Mason and Jury, 1997; Rocha and Simmonds, 1997; Reason and Lutjeharms, 1998). Pacific ENSO responses generate significant external influences on the rainfall. CMAP rainfall over eastern highlands of southern Africa is negatively correlated with Pacific Nino3 (NDVI > 0.4 there; Fig. 7.3). This may have implications for seasonal prediction of rainfall over Zambia, Zimbabwe, Mozambique and northeast South Africa in cases of strong ENSO signal. Botswana and the Kalahari transition zone are not as strongly correlated with ENSO (NDVI < than 0.3 there). It can be argued that vegetation (land surface) feedback acts to reduce the influence of remote forcings on the regional rainfall.

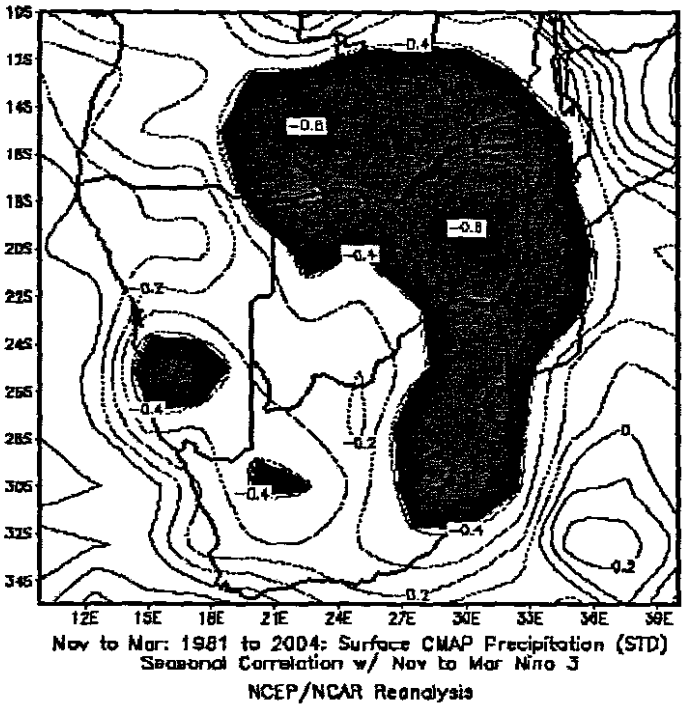

Fig. 7.3 Correlation of Nov.-Mar. CMAP rainfall anomalies with Pacific (Nino 3) SSTs.

Composite analysis for rainfall for 'green' minus 'brown' years shows a signal covering much of the interior plateau (Fig. 7.4). The western side fluctuates internally, the eastern flank is modulated externally, and in both cases NW cloud bands may be present.

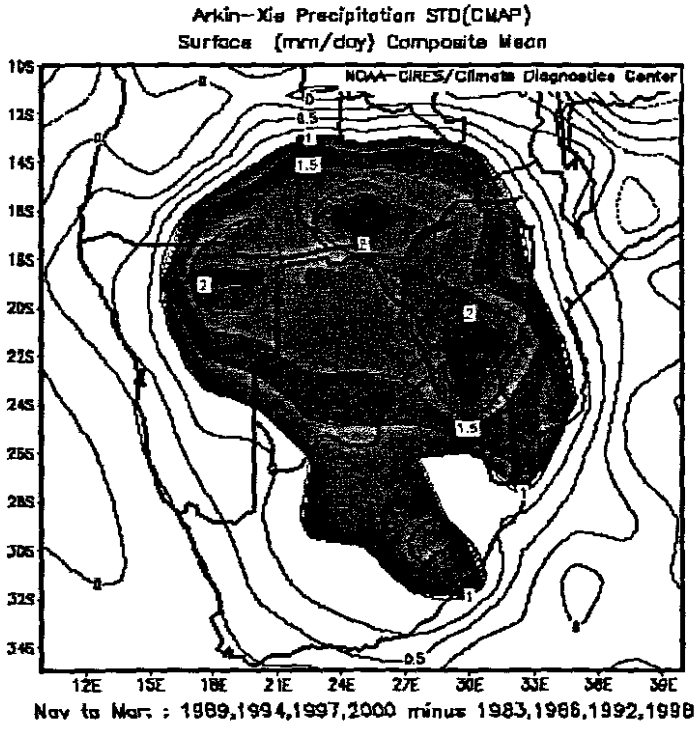

Fig. 7.4 Composite CMAP rainfall for 'green' minus 'brown' years

Boundary layer (700 hPa) winds for a composite of 'green' minus 'brown' years show a cyclonic low-pressure cell as the distinguishing feature over the central plateau (Fig. 7.5). The low also locates over the 'center of action' where a large scale Botswana upper high 'anchors' during drier years. Upper westerlies are reduced south of Africa, suggesting remote influences or a poleward shift of the jet stream due to moisture loaded to the north.

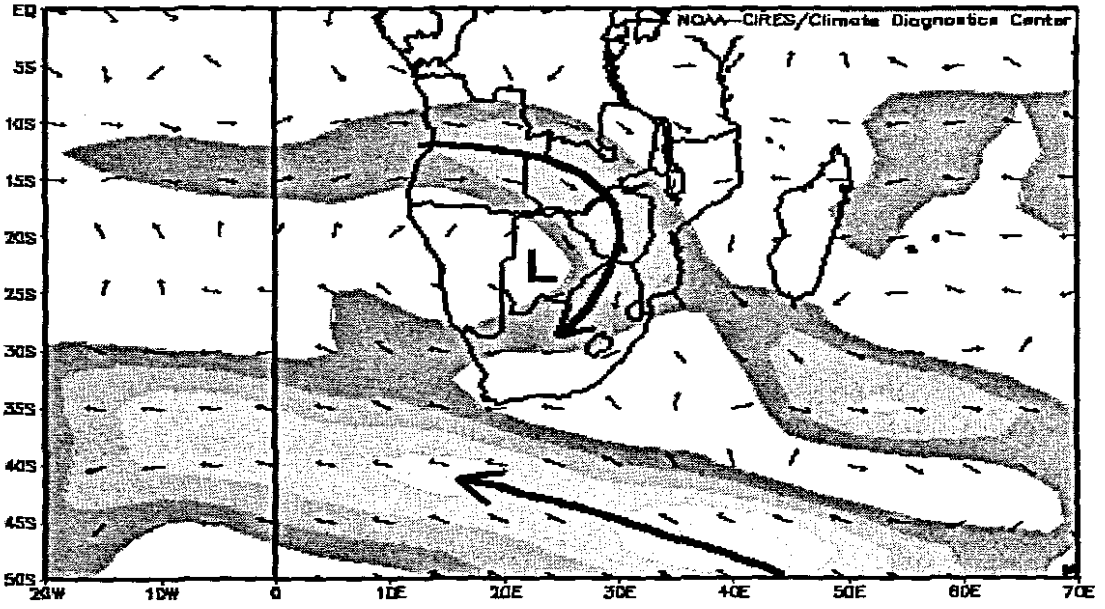

Fig. 7.5 Boundary layer (700 hPa) winds for a composite of high minus low NDVI years.

Overall, results of this study suggest a distinct role of the land surface and vegetation of southern Africa in determining climate variability apart from the dominant large scale systems.

7.3 Potential limitations and challenges

As discussed in Chapter 1, vegetation-climate interactions occur through various thermal, hydrological and biogeochemical processes (Wang, 2004) involving such variables as soil moisture, surface albedo, evapotranspiration (hence precipitation), surface roughness and atmospheric dynamics. It has also been recorgnised that rainfall is not the only determinant of vegetation growth but other

factors such as soil moisture, nutrients availability, soil fertility, soil type, and land use are also important (Farrar *et al*, 1994). The analysis in this study did not consider all participating variables and mechanisms. This is typical of vegetation studies which tend to focus on particular aspects of land surface processes without accounting for coupling among the different parameters (Bounoua *et al.*, 2000). This is necessitated by the complexity of the feedback mechanism especially considering the several spatio-temporal scales involved and the many 'difficult-to-measure' surface parameters.

The flux data obtained from the NCEP data servers are model-derived and may have inherent model biases giving limitations in the interpretation of results. For example, satellite derived observations of latent heat are not readily available for the period of climatological record. However, the co-location of intraseasonal modes of variability for rainfall and vegetation with those for boundary layer fluxes provides some confidence in the data.

The determination of boundary layer height is a subjective process which may influence the research output. Studies define the height according to some surface forcing such as turbulence, evapotranspiration and heat transfer and they often differ significantly. Models using turbulence fail under conditions of stable and calm weather. NCEP reanalysis specific humidity was used as proxies for boundary layer height.

Data gaps still exist over much of the subcontinent particularly upper air information. Too few stations report upper air data consistently largely due to the high cost of radiosondes and soundings and this problem is not unique to the poor regions. Some national weather services such as the South African Weather Service are using Aircraft Meteorological Data Relay (AMDAR) data for ascents/descents profiles. AMDAR data are the future and give good value for the cost.

The limitations discussed here do not pose significant drawbacks on the major conclusions of this study.

7.4 Implications and future research

The objectives of this study have been considerably achieved. While some results have confirmed the findings of earlier studies, this study contributes new input to climate research over southern Africa.

Questions remain over the variable influence and preferred location of the 20-day ISO. Relationships between the PC modes, zonal wind and the propagation of the intraseasonal oscillations are also crucial in the understanding of rainfall variability over southern Africa. PCA for rainfall and latent heat flux ISOs has shown more seasonality for terrestrial modes of variability than marine modes which continue throughout the year.

A major contribution to the scientific literature by this thesis is the examination of vegetation dynamics in southern Africa in time and space at an intra-seasonal time scale using the decadal NDVI data over almost 20 years. A clear distinction is that this study used a long time series of dekadal NDVI with a much higher temporal resolution than the shorter series of monthly maximum NDVI used by earlier studies (e.g. Anyamba *et al.*, 2002; Gondwe and Jury, 1997). Intraseasonal oscillations of vegetation have been determined over southern Africa although their influence on rainfall events is still not conclusive and requires further research. This is an artifact of the complexity of the feedback mechanism.

The study has established the region along the eastern edge of the Kalahari as a distinct mode of variability for vegetation and meteorological parameters. This has been linked to tropical-temperate troughs and attendant cloud bands. However, the contribution of vegetation (apart from the tropical-temperate

troughs) to the cloud band requires further investigation. More work is thus needed to establish sensitivity of the NW cloud band (hence rainfall) to vegetation at intraseasonal time scales.

As suggested by Drew (2004), dynamic vegetation components need to be incorporated in Regional Climate Models in order for vegetation to respond to climate change projections and hence feedback to the boundary layer. It is intended to expand this work to include numerical modelling to PhD level. Sensitivity analyses will be made of the regional atmosphere to changes in land use and local surface forcing with the external forcings fixed at the lateral boundaries.

Kanamitsu and Mo (2003) determined that the vertical flux of moisture can be a result of moisture convergence, surface evapotranspiration, or convection, which are all influenced by soil moisture. The influence of soil moisture and soil type on vegetation response patterns to rainfall needs further examination. Since vegetation has no direct response to rainfall but to soil moisture (Malo and Nicholson, 1990), time lags for vegetation response to rainfall vary depending on environmental factors such as soil type (Richard and Poccard, 1998). Davenport and Nicholson (1993) also determined that NDVI reflects soil moisture better than rainfall. Vegetation (biosphere) models need to incorporate these differences in order to simulate more realistic responses. However, soil moisture data has largely been obtained from model reanalyses than from observed field values (Wang *et al.*, 2003).

An increased understanding of land-biosphere-atmosphere interactions could enhance predictability using NDVI data and hence better agricultural management in southern Africa, especially given the high correlation between the maize yield and co-located NDVI data ($r = +0.82$; Jury *et al.*, 1997). The NDVI data may also be used to determine climatic impacts on societal systems and livelihoods. While agriculture remains the mainstay of livelihoods over the

study area, malaria remains one of the major killer diseases affecting communities. With careful evaluation, vegetation anomalies may be a useful predictor of crop yield and malaria incidence and also environmental management can thus be improved by adopting policies guided by scientific argument.

REFERENCES

Aldrian, E. and R.D. Susanto, 2003. Indonesian rainfall and sea surface temperature. *Int. J. Climatol., 23, 1435-1452*

Anyamba, A., 1992. Some properties of a 20-30 day oscillation in tropical convection. *J. Afr. Met. Soc., 1, 1-19*

Anyamba, A. and J.R. Eastman, 1996. Interannual variability of NDVI over Africa and its relation to El Nino/Southern Oscillation. *Int. J. Remote Sens., 17, 2533-2548*

Anyamba, A., Tucker, C.J. and R. Mahoney, 2002. From El Nino to La Nina: vegetation response patterns over east and southern Africa during the 1997-2000 period. *J. Climate, 15, 3096-3103*

Bartman, A.G., Landman, W.A. and C.J. de W. Rautenbach, 2003. Recalibration of General Circulation Model output to austral summer rainfall over southern Africa. *Int. J. Climatol., 23, 1407-1420*

Bounoua, L., Collatz, G.J., Los, S.O., Sellers, P.J., Dazlich, D.A., Tucker, C.J. and D.A. Randall, 2000. Sensitivity of Climate to Changes in NDVI. *J. Climate, 13, 2277-2292*

Carleton, A., Travis, D., Arnold, D., Brineger, R., Jelinski, D.E. and D.R. Easterling, 1994. Climate-scale vegetation-cloud interactions during drought using satellite data. *Int. J. Climatol., 14, 593-623*

Chahine, M.T., 1992. The hydrologic cycle and its influence on the climate. *Nature, 359, 373-380*

Charney, J.G., 1975. Dynamics of deserts and drought in the Sahel. *Quart. J. Royal Meteor. Soc., 101, 193-202*

Choudhury, B.J., 1993. Reflectivities of selected land surface types at 19 and 37 GHz from SSMI observations. *Remote Sens. Environ., 46, 1-17*

Cihlar, J., St Laurent, L. and J.A. Dyer, 1991. Relation between the normalised difference vegetation index and ecological variables. *Remote Sens. Environ., 35, 279-298*

Claussen, M., 1997. Modeling bio-geophysical feedback in the African and Indian monsoon region. *Climate Dynamics, 13, 247-257*

Crimp, S.J., Lutjeharms, J.R.E. and S.J. Mason, 1998. Sensitivity of a tropical-temperate trough to sea-surface temperature anomalies in the Agulhas retroflection region. *Water SA, 24, 93-100*

D'Abreton, P.C. and J.A. Lindesay, 1993. Water vapour transport over southern Africa during wet and dry early and late summer months. *Int. J. Climatol., 13, 237-256*

Davenport, M.L. and S.E. Nicholson, 1993. On the relation between rainfall and the Normalized Difference Vegetation Index for diverse vegetation types in East Africa. *Int. J. Remote Sens., 14, 2369-2389*

Delire, C., Foley, J.A. and S. Thompson, 2003. Evaluating the carbon cycle of a coupled atmosphere-biosphere model. *Global Biogeochem. Cycles, 17, 1012, doi:10.1029/2002GB001870*

Dickinson, R.E.,1992. Changes in land use. *In Trenberth, K.E. (ed),* Climate system modeling. *Cambridge University Press, Cambridge, pp 698-700*

Douville, H., Chauvin, F. and H. Broqua, 2001. Influence of soil moisture on the Asian and African Monsoons. Part I: Mean Monsoon and daily precipitation. *J. Climate, 14, 2381-2403*

Drew, G.H., 2004. Modelling vegetation dynamics and their feedbacks over southern Africa in response to climate change forcing. *Unpublished PhD. Thesis, Univ. Cape Town*

Dube, L.T., 2002. Climate of Southern Africa. *S. Afr. Geog. J., 84(1), 125-138*

Entin, A., Robock, A., Vinnikov, K.Y., Qiu, S., Zabeli, V., Liu, S., Namkhai, A., and Ts. Adyasuren, 1999. Evaluation of Global soil Wetness Project soil moisture simulations. *J. Meteor. Soc., Japan, 77, 183-198*

Farrar, T.J., Nicholson, S.E. and A.R. Lare, 1994. The influence of soil type on the relationships between NDVI, rainfall, and soil moisture in semiarid

Botswana. II NDVI response to soil moisture. *Remote Sens. Environ., 50, 121-133*

Ghil, M. and K. Mo, 1991. Intraseasonal oscillations in the global atmosphere, Part II: Southern Hemisphere. *J. Atmos. Sci., 48, 780-790*

Gondwe, M.P. and M.R. Jury, 1997. Sensitivity of vegetation (NDVI) to climate over southern Africa: Relationships with summer rainfall and OLR. *S. Afr. Geogr. J., 79 (1), 52-60*

Gray, T.I. and B.D. Tapley, 1985. Vegetation health: nature's climate monitor. *Adv. Space Res., 5(6), 371-377*

Grimsdell, A.W. and W.M. Angevine, 1998. Convective Boundary Layer height measurement with wind profilers and comparison to cloud base. *J. Atmos. Oceanic Tech., 15, 1331-1338*

Gutmann, G.G., 1990. Towards monitoring drought from space. *J. Climate*, 3, 282-295

Hahmann, A.N. and R.E. Dickinson, 1997. RCCM2-BATS model over tropical South America: Applications to tropical deforestation. *J. Climate, 10, 1944-1964*

Harrison, 1984. A generalized classification of South African summer rain-bearing synoptic systems. *J. Climatol., 4, 547-560*

Hastenrath, S., Greischar, L. and J. van Heeden, 1995. Prediction of summer rainfall over South Africa. *J. Climate, 8, 1511-1518*

Hoffman, W.A. and R.B. Jackson, 2000. Vegetation climate feedbacks in the conversion of tropical savanna to grassland. *J. Climate, 13, 1593-1602*

Hulme, M. (ed), Arntzen, J., Downing, T., Leemans, R., Malcom, J., Reynard, N., Ringrose, S. and D. Rogers, 1996. Climate change and southern Africa: an exploration of some potential impacts and implications in the SADC region. *Tech. Rept WWF Intl. Norwich, UK, 104pp*

IPCC, 2001. Climate Change 2001: Working Group I: The scientific basis.

Janowiak, J.E., 1988. An investigation of interannual rainfall variability in Africa. *J. Climate, 1, 240 -255*

Jury, M.R., 1999. Intra-seasonal convective variability over southern Africa: Principal component analysis of pentad outgoing-longwave radiation departures 1976-1994. *Theor. Appl. Climatol., 62, 133-146*

Jury, M.R. and C. Reason, 1989. Extreme subsidence in the Agulhas-Benguela air mass transition. *Boundary-Layer Meteorology, 46, 35-51*

Jury, M.R. and B.M.R. Pathack, 1991. A study of climate and weather variability over the tropical southwest Indian Ocean. *Meteor. Atmos. Phys., 47, 37-48*

Jury, M.R., Pathack, B.M.R. and B.J. Sohn, 1992. Spatial structure and interannual variability of summer convection over southern Africa and the SW Indian Ocean. *S. Afr. J. Sci., 88, 275-280*

Jury, M.R. and K.M. Levey, 1993. The climatology and characteristics of drought in the eastern Cape of South Africa. *Int. J. Climatol., 13, 629-641*

Jury, M.R., Valentine, H.R. and J.R.E. Lutjeharms, 1993. Influence of the Agulhas current on summer rainfall along the southeast coast of South Africa. *J. Appl. Meterol., 32, 1282-1287*

Jury, M.R., McQueen, C., and K. Levey, 1994. SOI and QBO signals in the African region. *Theor. Appl. Climatol., 50, 103-115*

Jury, M.R., Levey, K.M. and A. Makarau, 1996. Mechanisms of short term rainfall variability over southern Africa. *WRC Report No 436/1/96, Oceanography Dept., Univ. Cape Town*

Jury, M.R. and K.M. Levey, 1997. Vertical structure of the atmosphere during wet spells over southern Africa. *Water SA 23(1): 51-55.*

Jury, M.R., Weeks, S. and M.P. Gondwe, 1997a. Satellite-observed vegetation as an indicator of climate variability over southern Africa. *S. Afri. J. Sci., 93, 34-38*

Jury, M.R., Rouault, M., Weeks, S. and M. Schormann, 1997b. Atmospheric boundary-layer fluxes and structure across a land-sea transition zone in south-eastern Africa. *Boundary-Layer Meteorology 83:311-330.*

Jury, M.R. and S.E. Nkosi, 2000. Easterly flow in the tropical Indian Ocean and climate variability over south-east Africa. *Water SA, 26(2), 147-152*

Jury, M.R., White, W.B. and C.J.C. Reason, 2004. Modelling the dominant climate signals around Southern Africa. *Climate Dynamics, (accepted)*

Justice, C.O., Holben, B.N. and M.D. Gwyne, 1986. Monitoring east African vegetation using AVHRR data. *Int. J. Remote Sens., 7, 1453-1474*

Justice, C.O, T.Eck, D.Tanr,, and B.N.Holben, 1991. The effect of water vapor on the normalized difference vegetation index derived for the Sahelian region from NOAA AVHRR data. *Int. J. Remote Sensing, 12, 1165-1187.*

Kalnay, E., Kanamitsu, M., Kistler, R., Collins, W., Deaven, D., Gandlin, L., Iredell, M., Saha, S., White, G., Woollen, J., Zhu, Y., Chelliah, M., Ebisuzaki, W., Higgins, W., Janowiak, J., Mo, K.C., Ropelwiski, C., Wang, J., Leetma, A., Reynolds, R., Jenne, R. and D. Joseph, 1996. The NCEP/NCAR 40-Year Reanalysis Project. *Bull. Amer. Met. Soc., 77, 437-470*

Kanamitsu, M. and K.C. Mo, 2003. Dynamical effect of land surface processes on summer precipitation over the southwestern United States. *J. Climate, 16, 496-509*

Landman, W.A. and W.J. Tennant, 2000. Statistical downscaling of monthly forecasts. *Int. J. Climatol., 20, 1521-1532*

Levey, K.M., 1993. Intra-seasonal oscillations of convection over southern Africa. *Unpublished MSc thesis, Oceanography Dept., Univ. Cape Town.*

Levey, K.M. and M.R. Jury, 1996. Composite intraseasonal oscillations of convection over southern Africa. *J. Climate, 9, 1910-1920*

Levis, S., Foley, J.A., Brovkin, V. and D. Pollard, 1999. On the stability of the high-latitude climate-vegetation system in a coupled atmosphere-biosphere model. *Global Ecol. Biogeogr., 8, 489-500*

Lutjeharms, J.R.E. and R.C. van Ballegooyen, 1988. The retroflection of the Agulhas Current. *J. Phys. Oceanogr., 18, 1570-1583*

Lyons, S.W., 1991. Origins of convective variability over equatorial southern Africa during the austral summer. *J. Climate, 4, 23-39.*

Majodina, M. and M.R. Jury, 1996. Composite winter cyclones south of Africa: Evolution during eastward transit over the Agulhas warm pool. *S. Afr. J. Mar. Sci., 241-252*

Makarau, A., 1995. Intra-seasonal oscillatory modes of the southern Africa summer circulation. *Unpublished PhD thesis, Oceanography Dept., Univ. Cape Town.*

Makarau, A. and M.R. Jury, 1997. Predictability of Zimbabwe summer rainfall. *Int. J. Climatol., 17, 1421-1232*

Malo, A. and S.E. Nicholson, 1990. A study of rainfall and vegetation dynamics in the African Sahel using Normalised Difference Vegetation Index. *J. Arid Env., 19, 1-24*

Martyn, D., 1992. Climates of the world. *Developments in Atmospheric Science 18, Polish Scientific Publishers, Warsaw.*

Mason, S.J., 1995. Sea surface temperature-South African rainfall associations, 1910-1989. *Int. J. Climatol., 15, 119-135*

Mason, S. J., 1996: Climatic change over the Lowveld of South Africa. *Climatic Change, 32, 35-54*

Mason, S.J., Lindesay, J.A. and P.D. Tyson, 1994. Simulating drought in Southern Africa using sea surface temperature variations. *Water SA, 20, 15-22*

Mason, S.J. and M.R. Jury, 1997. Climate variability and change over southern Africa: A reflection on underlying processes. *Progress in Physical Geography, 21, 23-50*

Matarira, C.H., 1990. Drought over Zimbabwe in a Regional and Global Context. *Int. J. Climatol., 10, 609-625*

Mestas-Nuñez, A.M., 2000. Orthogonality properties of rotated empirical modes. *Int. J. Climatol., 20, 1509-1516*

Myneni, R.B., Hall, F.G., Sellers, P.J. and A.K. Marshak, 1995. The interpretation ofspectral vegetation indexes. *IEEE Transactions Geoscience and Remote Sensing, 33, 481-486*

Mozambique National News Agency, 2000. Government reports on flood damage and reconstruction. *AIM Reports, Issue No. 194, 6 November 2000. Mozambique National News Agency*

Mulenga, H.M., 1998. Southern African Climatic anomalies, Summer rainfall and the Angola Low. *Unpublished PhD thesis, Oceanography Dept., Univ. Cape Town*

Nicholson, S.E., 1993. An overview of African rainfall fluctuations of the last decade. *J. Climate, 6, 1463-1466.*

Nicholson, S.E. and D. Entekhabi, 1987. Rainfall variability in equatorial and Southern Africa: relationships with sea surface temperatures along the southwestern coast of Africa. *J. Climate Appl. Meteor., 26, 561-578*

Nicholson, S.E., Davenport, M.L. and A.R. Malo, 1990. A comparison of vegetation response to rainfall in the Sahel and east Africa using the NDVI from NOAA AVHRR. *Climate Change, 17, 209-241*

Nicholson, S.E. and T.J. Farrar, 1994. The influence of soil type on the relationships between NDVI, rainfall, and soil moisture in semiarid Botswana. I NDVI response to soil moisture. *Remote Sens. Environ., 50, 107-120*

Ogallo, L.J., 1988. Relationship between seasonal rainfall in east Africa and the Southern Oscillation. *J. Climatology, 8, 31-43*

Oke, T.R., 1987. Boundary Layer Climates. *University Press, Cambridge, 435 pp*

Palmer, T.N. and D.L.T. Anderson, 1994. The prospects of seasonal forecasting - a review paper. *Quart. J. Royal Meteor. Soc., 120, 755-793*

Pan, Z., Arritt, R.W., Gutowski, Jr., W.J., and E.S. Tackle, 1999. Soil moisture in a regional climate model: simulation and projection. Geophys. Res. Lett., 0, 0-0

Pitman, A.J., Durbridge, T.B., Henderson-Sellers, A. and K. McGuffie, 1993. Assessing climate model sensitivity to prescribed deforested landscapes. *Int. J. Climatol., 13, 879-898*

Poolman, E.P. and D. Terblanche, 1984. Tropiese siklone Demonia en Imboa. *S. Afr. Wea. Bur. News Lett., 420, 37-45*

Preston-Whyte R.A. and P.D. Tyson, 1988. The amosphere and weather of southern Africa. *Oxford University Press, Cape Town, 374 pp*

Reason, C.J.C., 2001. Evidence for the influence of the Agulhas current on regional atmospheric circulation patterns. *J. Climate, 14, 2769-2778*

Reason, C.J.C. and J.R.E. Lutjeharms, 1998. Variability of the south Indian ocean and implications for southern African rainfall. *S. Afri. J. Sci., 94, 115-123*

Richard, Y. and I. Poccard, 1990. A statistical study of NDVI sensitivity to seasonal and interannual rainfall variation in southern Africa. *Int. J. Remote Sens., 19, 2907-2920*

Rouault, M., Reason, C.J.C., Lutjeharms, J.R.E. and A.C.M. Beljaars, 2003. Underestimation of latent and sensible heat fluxes above the Agulhas Current in NCEP and ECMWF Analyses. *J. Climate, 16, 776-782*

Rocha, A. and I. Simmonds, 1997. Interannual variability of southern Africa summer rainfall, 1: Relationships with air-sea interaction processes. *Int. J. Climatol., 17, 235-265*

Roderick, M.L. and G.D. Farquhar, 2004. Changes in Australian pan evaporation from 1970 to 2002. *Int. J. Climatol., 24, 1077-1090*

Rogers, R. R., 1979. A short course in cloud physics 2nd edition. *Pergamon Press, Oxford, 235 pp.*

Ropelewski, C.F. and M.S. Halpert, 1987. Global- and regional-scale precipitation patterns associated with El Nino/Southern Oscillation. *Mon. Wea. Rev., 115, 1606 - 1626*

Rutherford, M.C. and R.H. Westfall, 1986. The biomes of southern Africa - an objective categorization. *Memoirs Botanical Soc. S. Afr., 54, 1-98*

Shinoda, M. and R. Kawamura, 1996. Relationships between rainfall over semi-arid southern Africa and geopotential heights and sea surface temperatures. *J. Met. Soc. Japan, 74, 21- 36*

Shuttleworth, W.J., 1993. Evaporation. In *D.R. Maidment (ed.)*, Handbook of Hydrology, *Mcgraw-Hill*

Szilagyi, J., Rundquist, D.C., Gosselin, D.C. and M.B. Parlange, 1998. NDVI relationship to monthly evaporation. *Geosphys. Res. Lett., 25, 1753 -1756*

Taylor, C. M., Lambian, E.F., Stephenne, N., Harding, R.J. and R.L.H. Essery, 2002. The influence of land use change on climate in the Sahel. *J. Climate, 15, 3615 - 3629*

Tazalika, L., 2003. Satellite derived rainfall over tropical Africa. Its pattern, variability and calibration. *Unpublished MSc. Thesis, Geography Dept., Univ. Zululand*

Tennant, W.J. and B.C. Hewitson, 2002. Intra-seasonal rainfall characteristics and their importance to the seasonal prediction problem. *Int. J. Climatol., 22, 1033-1048*

Tinley, K.L.,1982. The influence of soil moisture balance on ecosystem patterns in southern Africa. In *Ecology of Tropical Savannas,* eds. B.J. Huntley and B.H. Walker, *Springer-Verlag, New York*

Tsai, T.H., O'brien, J.J. and M.E. Luther, 1992. The 26-day oscillation observed in the satellite seas surface temperature measurements in the equatorial western Indian Ocean. *J. Geophys. Res., 97, 9605-9618*

Tucker, C.J., 1979. Red and photographic infrared linear combinations for monitoring vegetation. *Remote Sens. Environ., 8, 127-150.*

Tucker, C.J. and P.J. Sellers, 1986. Satellite remote sensing of primary production. *Int. J. Remote Sens., 7, 1395-1416*

Tucker, C.J., Newcomb, W.W., Los, S.O. and S.D. Prince, 1991. Mean and inter-year variation of growing-season normalized difference vegetation index for the Sahel 1981-1989. *Int. J. Remote Sens.,12,1113-1115.*

Tucker, C.J. and S.E. Nicholson, 1999. Variation in the size of the Sahara Desert from 1980 to 1997. *Ambio, 28, 587-591*

Tucker, C.J., Brown, M.E., Pinzon, J.E., Slayback, D.A., Mahoeny, R., Saleous, N.E. and E.N. Vermote, 2005. An extended AVHRR 8-km NDVI dataset comparable with MODIS and SPOT vegetation NDVI data. *Int. J. Remote Sens., (in press)*

Tyson, P.D., 1981. Atmospheric circulation variations and the occurrence of extended wet and dry spells over South Africa. *J. Climatol., 1, 115-130*

Tyson, P.D., 1986. Climate change and variability over southern Africa. *Oxford University Press: Cape Town.* 220 pp

Tyson, P.D. and R.A. Preston-Whyte, 2000. The weather and climate of southern Africa. *Oxford University Press: Cape Town, 396 pp*

Tyson, P.D., Cooper, G.R.J. and T.S. McCarthy, 2002. Millenial to multi-decadal variability in the climate of southern Africa. *Int. J. Climatol., 22, 1105-1117*

Unganai, L.S. and S.J. Mason, 2001. Spatial characterization of Zimbabwe summer rainfall during the period 1920-1996. *S. Afr. J. Sci., 97, 425-431*

Vogel, C., 2000. Climate and climatic change: causes and consequences. In R. Fox and K. Rowntree (ed), The geography of South Africa in a changing world. *Oxford University Press, Cape Town, 509 pp*

Walker, N.D., 1990. Links between South African summer rainfall and temperature variability of the Agulhas and Benguela currents systems. *J. Geophys. Res., 95, 3297-3319*

Walker, N.D., and R.D. Mey, 1988. Ocean/atmosphere heat fluxes within the Agulhas retroflection region. *J. Geophys. Res., 93, 15473-15483*

Wang, G., 2004. A conceptual modeling study on biosphere-atmosphere interactions for physically based climate modeling. *J. Climate, 17, 2572-2583*

Wang, J., Price, K.P. and P.M. Rich, 2001. Spatial patterns of NDVI in response to precipitation and temperature in the central Great Plains. *Int. J. Remote Sens., 22, 3827-3844*

Wang, J., Rich, P.M. and K.P. Price, 2003. Temporal responses of NDVI to precipitation and temperature in the central Great Plains, USA. *Int. J. Remote Sens., 24, 2345-2364*

Woodward, F.I., 1987. Climate and plant distribution. *Cambridge University Press, 174 pp.*

Yin, B. and B.A. Albrecht, 2000. Spatial variability of Atmospheric boundary layer structure over the eastern equatorial Pacific. *J. Climate, 13, 1574-1592*

Young, S.S. and A. Anyamba, 1999. Comparison NOAA/NASA PAL and NOAA GVI data for vegetation change studies over China. *Photogr. Eng. Rem. Sens., 65, 679-688*

Zeng, N., Needlin, J.D., Lau, K.-M. and C.J. Tucker, 1999. Enhancement of climate variability in the Sahel by vegetation interaction. *Science, 286, 1537-1540*

Zeng, N. and D.J. Neelin, 2000. The Role of vegetation-climate interaction and interannual variability in shaping the African Savanna. *J. Climate, 13, 2665-2670*

Zeng, N., Hales, K. and J.D. Neelin, 2002. Nonlinear dynamics in a coupled vegetation-atmosphere system and implications for Desert-Forest Gradient. *J. Climate, 15, 3474-3487*

Zhou, L., Kaufmann, R.K., Tian, Y., Myneni, R.B. and C.J. Tucker, 2003. Relation between interannual variations in satellite measures of northern forest greenness and climate between 1982 and 1999. *J. Geophys. Res., 108, (D1) 4004, doi: 10.1029/2002JD002510*